UNIVERSITÀ DEGLI STUDI DI MILANO
Department of Medical Biotechnology and Translational Medicine
PhD Course in Experimental Medicine and Medical Biotechnologies
Curriculum: Neuroscience and Neuropathology
(XXXIII cohort)

Role of LSD1 in aging- and stress- dependent epigenetic drift leading to depression and anxiety disorders

PhD thesis of:
Chiara FORASTIERI
R12097

Tutor: Prof. Elena BATTAGLIOLI
Supervisor: Dr. Francesco RUSCONI
PhD Coordinator: Prof. Massimo LOCATI

Academic Year 2019/2020

ABSTRACT

The current understanding of the pathophysiologic processes underlying neuropsychiatric disorders remains dramatically limited, despite their epidemic diffusion and tremendous impact on patients' health and society. Mounting evidence suggests that the disruption of stress-coping mechanisms might be coupled to maladaptive forms of plasticity underlying stress-vulnerability, fostering mood disorders such as anxiety and major depressive disorder (MDD). The correct tuning of the relative ratio between the epigenetic enzyme Lysine-Specific Demethylase 1 (LSD1) and its neuronal-specific dominant negative isoform neuroLSD1 is crucial to guarantee homeostatic adaptive plasticity in response to environmental stimuli, in the frame of a stress-resiliency instrumental pathway. Another homeostatic regulator of excitatory neurons playing a fundamental part in environmental stress-response is the neuronal-enriched splicing factor RNA Binding Fox-1 Homolog 1 (RBFOX1) that is heavily implicated in the onset of several neurological disorders, such as autism and epilepsy, and has been recently listed among the few genetic loci associated to MDD.

During my PhD, I dissected a higher primates-restricted functional interaction between RBFOX1 and LSD1. Specifically, RBFOX1, thanks to a single nucleotide variation present only in higher primates and humans and generating a new acceptor splice site, acquires the ability to regulate splicing inclusion of a novel LSD1 cryptic exon, that we named exon E8b. This alternative spliced exon not only negatively regulates LSD1 levels by Nonsense-mediated mRNA decay, but also modulates brain-restricted expression of neuroLSD1, affecting LSD1 and neuroLSD1 ratio. Notably, we further demonstrated the involvement of LSD1/neuroLSD1 ratio modulation in physiological brain aging and psychiatric drift in humans. If on the one hand the evolution-driven acquisition of LSD1 as RBFOX1-regulated target could contribute to increase the complexity of stress response and environmental adaptation, on the other hand it likely represents a novel vulnerability harbor multiplying susceptibility substrates for stress-related neuropsychiatric disorder.

In parallel, always with the idea to identify neurobiological mechanisms associated with stress susceptibility, I evaluated the involvement of specific *LSD1* genetic variants able to set different levels of LSD1/neuroLSD1 ratio and potentially impacting stress susceptibility in humans.

INDEX

1 INTRODUCTION

1.1 STRESS: AN OVERVIEW

1.1.1 Physiological response to stress

All living organisms maintain a dynamic equilibrium of physiological and psychophysical parameters in the face of an ever-changing environment. This equilibrium, which is challenged by physical and psychological events known as stressors, is maintained through homeostatic mechanisms [1, 2]. As the brain represents the forefront organ in environmental sensing, it has to manage a wide variety of stimuli whose inherent strength, and circuital modification competence, must be counterbalanced to return to resting conditions once the stimulus ceases. Nature, intensity and duration of stressful stimuli, along with individual characteristics including age, gender and genetics that affect the efficacy of homeostatic mechanisms, determine the actual impact of stressful events on the individual, eliciting a highly subjective stress response [3]. In this light, stress can be defined as a subjective perception of a potential or manifested threat that leads to immediate and future changes in an individual's psychophysical equilibrium.

Short-term behavioral changes instrumental to stress coping are achieved through the release of stress response mediators. Neurotransmitters such as glutamate, noradrenaline and serotonin, hormonal peptides for example corticotropin-releasing hormone (CRH), and steroid hormones like cortisol, all modulate neuronal activity at specific neuroanatomical sites in the central nervous system in order to quickly respond to stress meanwhile engraving a protective memory trace of threatening experience. Different types of stressors require different responses and engage specific central loci. For instance, physical stressors, like blood loss and traumas, recruit the brainstem and hypothalamic regions. Instead, a psychological stressor such as deadlines, social embarrassment, bullying and the loss of a beloved person, recruits limbic brain structures, which include the hippocampus, amygdala and prefrontal cortex (PFC). These areas control learning, emotional responses and decision making, but also autonomic and hormonal responses [4, 5], being never completely segregated, as physical stressors often have psychological aspects and vice versa.

The stress response is characterized by two phases of physiological changes at a molecular and cellular level. The first phase, the so-called primary or "fight-or-flight" response, is fast-acting and is meant to maximizing survival chances in the face of the perceived threat. The secondary response promotes the termination of stress response and elicits homeostatic

mechanisms aimed at restraining excessive reactions reinstating a psychophysical equilibrium [6].

The main neuroendocrine pathways that are involved in both primary and secondary response activation are the autonomic nervous system (ANS) and the hypothalamic-pituitary-adrenal (HPA) axis (Figure 1). When a stressful event takes place a state of mild anxiety is established through the disinhibition of the amygdala. A physical or psychosocial stressor, in this way, antagonistically diminishes the normal action of the prefrontal cortex, a brain area involved in cognition but also in cognitive and emotional extinction of anxiety and fear through a complementary inhibitory effect on the amygdala, which promotes anxiety and fear [7]. Initial phases of stress response imply an attention focus on the threatening stimulus and temporary improvement of cognitive acuity and vigilance [2]. Another behavioral response elicited in the arousal phase is the anhedonia, aimed at minimizing distractions. During stress, indeed, PFC inhibition downregulates dopaminergic release from ventral tegmental area (VTA) towards the nucleus accumbens (NAc), reducing reward [8, 9]. At the same time, the PFC inhibition and amygdala disinhibition activate the HPA axis through corticotropin releasing hormone (CRH) release mediated by the paraventricular nucleus (PVN) of the hypothalamus. CRH stimulates the anterior lobe of the pituitary gland to secrete adrenocorticotropic hormone (ACTH), which in turn acts on the adrenal gland inducing cortisol release. Simultaneously, CRH-mediated activation of locus coeruleus leads to the engagement of sympathetic nervous system (SNS) in stress response. The principal mediators of SNS are norepinephrine and epinephrine released by adrenal medulla. Together, cortisol and catecholamine mediators concur in preparing the body to “fight-or-flight” reaction. ANS and HPA axis effects on multiple functions during stress response are reported in Figure 1. Some of them are i) increased glucose availability in blood flow, thanks to glycogenolysis and gluconeogenesis, with a concomitant enhanced blood flow in skeletal muscles and brain, ii) increased myocardial contractility along with heart and respiratory rate, bronchodilatation, iii) inhibition of digestive function, enhanced vigilance, attentive focus and pupils dilatation [10, 11].

In a physiological situation, different mechanisms of secondary response are adopted. Cortisol itself, indeed, establishes a negative feedback on the amygdala, hippocampus, hypothalamus and pituitary gland in order to terminate cognitive and autonomic stress responses thereby homeostatically restoring the psychophysical equilibrium [12]. Interestingly, cortisol binds to glucocorticoid receptors (GRs) in the hippocampus that largely contribute in stress response termination by the inhibition of the HPA axis [13]. Convergently, ANS actively promotes “rest

and digest" response through the activation of parasympathetic nervous system (PSNS) [10, 11].

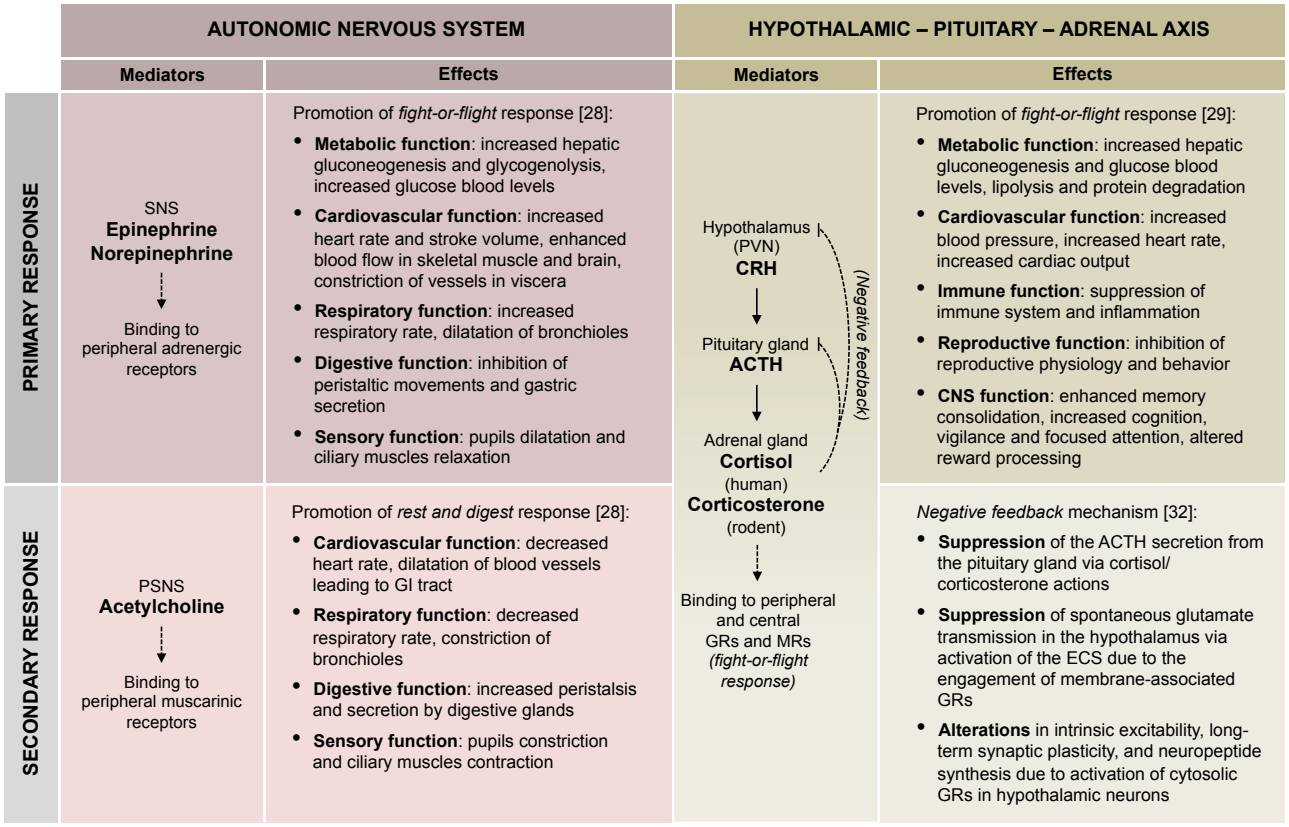

Figure 1. Primary and secondary stress response. The table resumes the molecular mediators and the main effects of primary and secondary stress response of the ANS and HPA axis [14]. SNS = sympathetic nervous system; PSNS = parasympathetic nervous system; PVN = paraventricular nucleus; CRH = corticotropin releasing hormone; ACTH = adrenocorticotropic hormone; GRs = glucocorticoid receptors; MRs = mineralocorticoid receptors; CNS = central nervous system; ECS = endocannabinoid system.

In the brain, acute stressful events elicit molecular modifications at transcriptional, structural and circuitry levels [15]. Stimulus-evoked increase in glutamate release promotes neuroplasticity in the hippocampus, in terms of increasing neuronal dendrites complexity and number of dendritic spines, fostering memory formation and processing of new threat-related information with an adaptive meaning. Such information indeed can be used to accelerate appropriate responses against similar threatening situations [2], establishing for instance protective behavioral processes of avoidance. This is promoted through a fundamental feature of glutamate signal transduction in excitatory neurons, i.e. the transactivation of plasticity-related genes, including the immediate-early genes (IEGs). In line, the molecular mechanisms, engaged during the secondary, homeostatic phase of stress response, also contribute to cope with stress through a fine-tuning of glutamate molecular responses, thus guaranteeing a limited and transient wave of neuroplasticity-related genes activation, hence a

timely rescue of psychophysical equilibrium [16]. All together these mechanisms promote adaptation via *allostasis*. The outcome of stress transduction is indeed the achievement of a *novel* steady-state, which represent a new equilibrium that is somehow different from the original one rather than exactly the same. One of these differences, with respect for instance to environmental stress allostasis, is represented by the acquired layer of stress learning and the cognitive trace of stress circumstances. This information will change the individual's behavior in response to similar threatening conditions, making the resting setting substantially novel than before. In other words, if a subsequent similar stressful stimulus takes place, the molecular landscape and the psychophysical responses are *primed* to react differently guaranteeing adaptation and habituation. [17].

1.1.2 Maladaptive response and stress-related neuropsychiatric disorders

Depression, mood and eating disorders, post-traumatic stress disorders, schizophrenia and addiction are only some examples of brain disorders referred to as neuropsychiatric conditions. Their prevalence has grown over the last decades and today 10 to 20% of the general population suffers from these pathologies, strongly affecting the quality of life of patients and their families and representing a burden for healthcare national systems and society [14].

Neuropsychiatric disorders display high degree of genetic heritability, despite no single gene mutations with a strong effect and high penetrance have been indicated as thoroughly responsible for stress vulnerability. The most important risk factors for depression but also, more in general, for stress-related neuropsychiatric disorders are environmental negative contingencies, in particular if chronically reiterated and perceived [18, 19]. Indeed, if acute stress triggers rapid neurotransmission, neuronal activation and hormones release, followed by a rapid return to stable levels although this can ultimately lead to adaptive changes in subsequent neuronal responses, chronic stress can elicit maladaptive neuronal responses in susceptible individuals [20-22]. As said, depending on the stress nature, intensity and duration, but most of all innate or acquired individual susceptibility, in terms genetic or epigenetic predisposition, the homeostatic mechanisms can be overloaded. This overload entails maladaptive molecular and structural alterations [6, 23, 24] that ultimately impact on behavior and psychological health eventually leading to stress-related neuropsychiatric disorders [17, 22]. As a matter of fact, acute stress paradigm performed in mice or rats barely elicits, if characterized by mild intensity, long-term behavioral changes. On the contrary, when

the same stress is chronically repeated, also in rodent models it might cause maladaptive stress responses eliciting, in a subset of animals, vulnerable phenotypes in term of long-lasting cognitive and emotional abnormalities [20, 25]. Stable increase of fear and anxiety, and impaired spatial and working memory are the phenotypical manifestation of maladaptive structural remodeling in neuronal networks in the hippocampus, prefrontal cortex and amygdala, upon chronic stress (Figure 2A) [22, 26].

In the hippocampus, a brain area responsible for declarative memory formation in higher primates and spatial memories in rodents [27, 28], different paradigms of reiterated stress, performed both in mice and rats, negatively impact synaptic plasticity. These alterations involve the shrinkage of dendrites of hippocampal CA3 and dentate gyrus neurons and loss of spines in CA1 neurons [26, 29], and impair long-term potentiation (LTP) while enhance long-term depression (LTD) [13], leading to reduced hippocampal function and ultimately cognitive impairments.

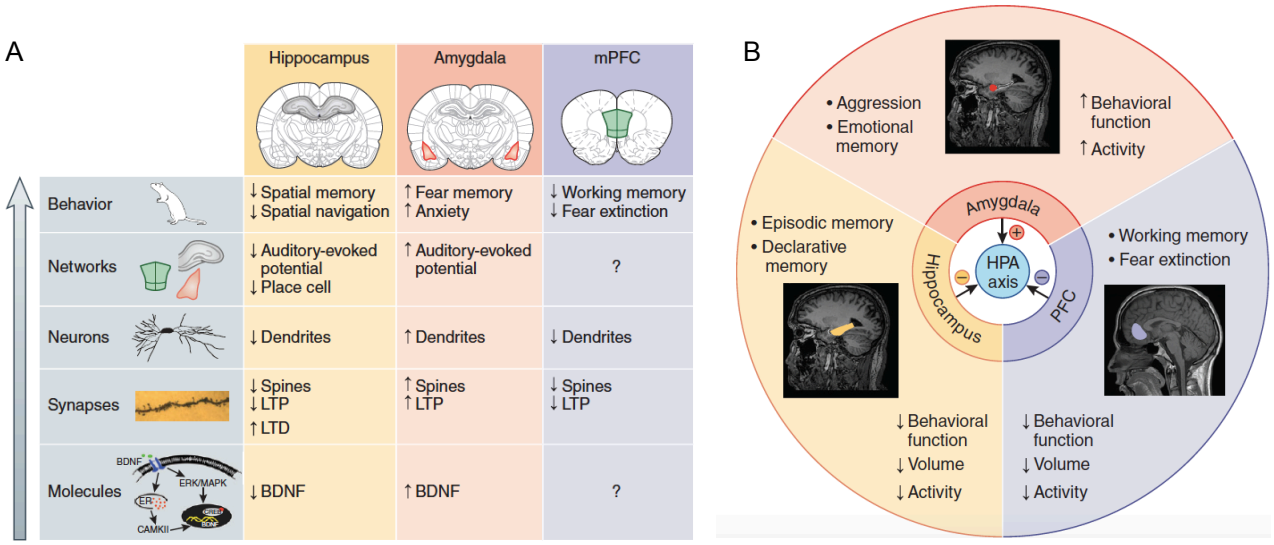

Figure 2. The hippocampus, amygdala and prefrontal cortex undergo contrasting structural and functional changes in stress disorders. (A) Molecular, cellular, circuitry and behavioral alterations in hippocampus, amygdala and medial PFC upon chronic stress in rodents. (B) Chronic stress induces structural and functional alterations in the hippocampus, amygdala and PFC in individuals suffering of stress-related disorders. Adapted from [22].

In addition to the hippocampus, also the PFC exerts a negative feedback function on stress response. Interestingly, upon chronic restrain stress but also corticosterone injections, the medial PFC undergoes similar morphological modification in the infralimbic region with loss of dendrites and spines and simplification of dendritic branching along with impaired LTP [30-32].

On the contrary, increased neuroplasticity in the amygdala plays a key role in anxiety arousal and the activation of HPA axis. Such an increased excitability upon chronic stress reiterations

is responsible for emotional symptoms of stress disorders. Surprisingly, the same chronic stress paradigms that induce dendritic atrophy in the hippocampus and PFC, enhance spine density and dendritic arborization in the basolateral complex of the amygdala (BLA) [33, 34] and correlate with enduring increased anxiety.

Similar effects of chronic stress can be observed in humans, where clinical and neuroimaging studies have shown that individuals with stress-related neuropsychiatric disorders display contrasting functional and structural modifications in the hippocampus, prefrontal cortex and amygdala (Figure 2B) [22].

1.1.3 Epigenetic stress-response

Neuronal circuits adaptation in response to environmental stressful stimuli is achieved at least in part through epigenetic mechanisms. Stress experiences that occur either during early-life or adulthood have deep consequences on neurons epigenome, strongly suggesting the existence of an epigenetic component in the onset of neuropsychiatric disorders [19, 35, 36]. Epigenetic stress-induced modifications are plausible mechanisms to explain, in terms of risk and resiliency, how everyday life psychosocial stressful events can lead to long-lasting behavioral alteration and eventually to neuropsychiatric disorders [16].

A series of epigenetic mechanisms are engaged during acute stress response with the homeostatic valence to avoid excessive transduction of glutamatergic-signaling and restrain neuroplasticity. One of epigenetic delayed responses to acute stress is the global increase of trimethylated lysine 9 of histone H3 (H3K9me3), a histone mark associated with transcriptional-silencing and heterochromatin formation. Interestingly, this putative allostatic mechanism is disrupted by chronic stress upon which no modifications of H3K9me3 levels are observed [37, 38]. In the hippocampus of stressed mice that undergo foot shock stress paradigm, increased lysine 4 methylation of histone H3 (H3K4me3), associated with active transcription, is observed at the level of the IEG *egr1* gene, coherently with IEGs transactivation that occurs upon stress, representing this epigenetic modification instrumental to fear memory formation [39]. However, an increase in repressive histone modification H3K9me2 is triggered during the following secondary stress response together with a concomitant increase of DNA methylation of *egr1* promoter region, which represses transcription of the same gene [39]. Increased DNA methylation at the level of IEGs *c-fos* and *egr1* promoter region due to overexpression of the DNA demethylase enzyme DNA methyl transferase 3a (Dnmt3a) is similarly responsible for the constrain of IEGs transcription in the hippocampus after forced swim stress paradigm [40]. Another example of epigenetic

modification elicited by acute stress involves the chromatin modifier Lysine-Specific Demethylase 1 (LSD1), a transcriptional corepressor responsible for demethylation of histone H3K4me1/2 [41]. It has been reported that in the hippocampus, in response to an acute psychosocial stress paradigm, LSD1 repressive potential is increased through a splicing-based transient reduction of its dominant negative isoform neuroLSD1, which is unable to repress transcription [42-44].

The functional outcome of these and others epigenetic modulations, referred to as epigenetic stress response (ESR), is the buffering of plasticity genes transactivation as well as an increase of their transcriptional activation threshold for a limited time window, likely participating in stress habituation in resilient individuals. On the other hand, in susceptible individuals the disruption of epigenetic stress-coping responses upon chronic stress could entail maladaptive neuroplastic modifications favoring the onset of stress-related neuropsychiatric disorders [16]. As a matter of fact, differential IEGs expression in the hippocampus is correlated to susceptible and resilient phenotype upon chronic social defeat stress in mice. In particular, resilient animals display a reduced expression of IEGs, among which *egr1* and *arc*, while in susceptible mice IEGs result upregulated with respect to controls implying excessive neuroplasticity and representing a possible molecular mechanism of stress vulnerability [45].

1.2 THE EPIGENETIC ENZYME LYSINE-SPECIFIC DEMETHYLASE 1 (LSD1)

1.2.1 LSD1 structure and functions

Lysine-Specific Demethylase 1 (LSD1) is a highly specific flavin-dependent demethylase conserved from the yeast Saccharomyces pombe to Homo sapiens [46, 47]. The epigenetic enzyme LSD1 specifically removes methyl groups on lysine 4 on histone H3 (H3K4) when it is mono- or dimethylated (H3K4me1/2) [41, 48, 49]. Human LSD1 protein is an ubiquitously expressed 852 amino acid-long protein with a molecular weight of 116KDa. LSD1 protein structure is well described in [50] and consists in three main domains (Figure 3). The N-terminal SWIRM (Swi3p, Rsc8p and Moira) domain, which is usually present in many chromatin-remodeling proteins [51], is responsible for the interaction with protein complexes. The Amine Oxidase Domain (AOD) contains the enzyme active site, located between a substrate-binding region that interacts with histone H3 tail and a flavin adenine

dinucleotide (FAD)-binding one. The Tower domain consists of a pair of antiparallel α-helices and is involved in the interaction with a α-helix domain of corepressor of REST (CoREST) [50].

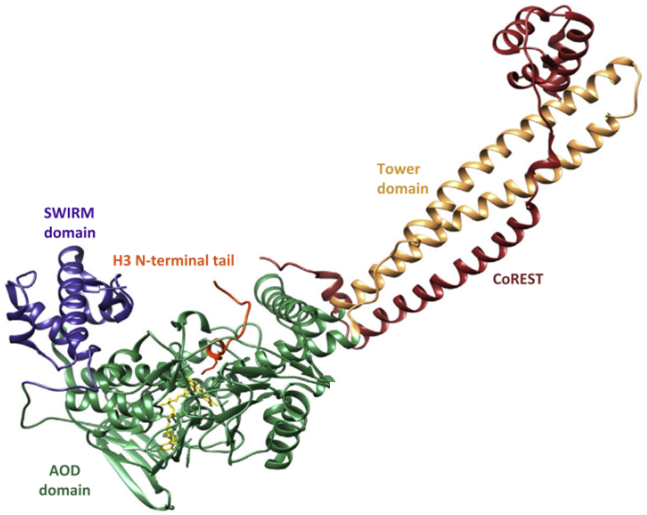

Figure 3. LSD1 structure. Ribbon drawing shows the three LSD1 domains interacting with CoREST and histone H3 tail. SWIRM domain is indicated in purple, the amine oxidase domain (AOD) in green and the Tower domain in yellow. CoREST α-helix (in dark red) encircles the two α-helices of LSD1 Tower domain. The AOD binds histone H3 N-terminal tail (in orange) and FAD cofactor (in yellow). Adapted from [52].

During the enzymatic reaction catalyzed by LSD1 (Figure 4) the N-terminal histone tail interacts with LSD1 AOD catalytic pocket and the methylated lysine is oxidized by FAD cofactor, generating an imine intermediate product that is non-enzymatically hydrolyzed producing formaldehyde (HCHO) and the demethylated residue [53].

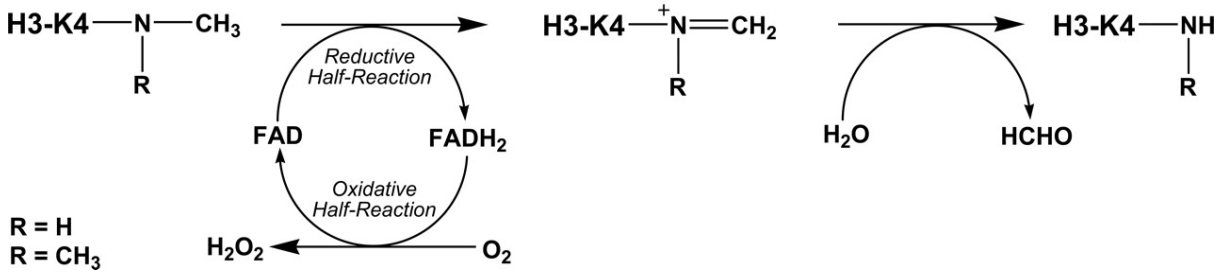

Figure 4. FAD-dependent H3K4 demethylation reaction catalyzed by LSD1. Mono- or dimethylated K4 of H3 (H3K4me1/2) interacts with AOD of LSD1 and is oxidized by FAD cofactor generating an imine intermediate product that is hydrolyzed producing formaldehyde (HCHO) and the demethylated residue [53].

LSD1 works within a protein complex, including CoREST and Histone Deacetylase 1 and 2 (HDAC1/2) [41, 49, 54]. LSD1-Corest-HDAC1/2 protein complex erases histone marks that are associated with active transcription [55, 56]. Specifically, this corepressor complex exerts transcriptional repression through deacetylation of Lys 9 and 14 of histone H3 (H3K9/K14ac) operated by HDAC1 and 2, and the demethylation of H3K4me1/2 catalyzed by LSD1. The interaction with CoREST and HDAC1/2 is essential for LSD1 catalytic activity. In this regard, it

has been demonstrated that the detachment of LSD1 from the repressor complex causes the loss of its transcriptional repression activity [57]. As a matter of fact, SANT2 domain of CoREST directly binds to DNA facilitating the corepressor complex to associate with chromatin [58]. Moreover, since histone H3 tail binds LSD1 catalytic domain through an interaction that involves at least 21 amino acids, LSD1 ability to catalyze demethylation reaction is affected by the presence of other histone modifications on the same histone H3 substrate. More in detail, it has been shown that the phosphorylation of serine 10 alters LSD1-H3 tail bond in a unproductive way while the acetylation of lysine 9 reduces LSD1 enzymatic activity, demonstrating that this epigenetic enzyme is also able to read the histone code [49].

The first described transcription factor able to recruit LSD1 corepressor complex on target genes is RE1 Silencing Transcription factor (REST), thanks to the interaction with CoREST. REST is a master regulator of neuronal development, indeed it inhibits neuronal genes transcription in non-neuronal cells by binding to Repressor Element 1 (RE1) [41, 53, 59, 60]. Consequently, the initial functional studies deciphering LSD1 role in regulating gene expression correlate demethylation of H3K4 with the silencing of neuronal gene targets and phenotypical traits in non-neuronal cells. On the contrary, in neuronal stem cells, where LSD1 is essential for proliferation [61], LSD1 downregulation [62] and the disassembly of the corepressor complex from neuronal-specific genes are required for the differentiation into mature neurons [60, 63]. Notably, LSD1 activity is not restricted to REST-regulated neuronal genes. Indeed, LSD1 is involved in several epigenetically driven biological functions through the interaction with different protein complexes [64] and lncRNAs [65, 66] as well as through the demethylation of Lys residues of non-histone proteins [67-70]. Moreover, within a protein complex involving the androgen receptor (AR) and the estrogen receptor (ER), LSD1 has been also proposed to act as transcriptional co-activator gaining the ability to demethylate mono- and dimethylated lysine 9 of histone H3 (H3K9me1/2) [71, 72].

Among its widespread functions, LSD1 has been reported to regulate multi-lineage hematopoiesis [73], endocrine cells differentiation [74], oocytes function [75] and circadian cycle [76]. Moreover it is involved in DNA damage response [77] and the regulation of retrotransposable elements [78], mitochondrial metabolism [79] and telomere length [66]. Interestingly, LSD1 is known to be an epigenetic regulator of gene expression in embryonic stem cells playing a crucial role in pluripotency maintenance. Consistently, reduction of LSD1 levels is observed during physiological differentiation to tissue-committed cells [74, 80-82]. As expected, LSD1 is overexpressed in several cancer types and has been demonstrated to be

involved in dedifferentiation of tumor cells and cancer progression [83, 84]. In line with these roles, the inhibition of LSD1 activity has been proposed as a candidate cancer therapy [85-90].

1.2.2 Neuron-specific alternative splicing isoform of LSD1: neuroLSD1

Human *LSD1* gene (GeneBank accession number NM_015013), also known as *AOF2* (Amine Oxidase Flavin-containing Domain 2) and *KDM1A* (Lysine Demethylase 1A), maps on the short arm of chromosome 1 (1p36.12) and contains 19 highly conserved exons that encode the ubiquitously expressed 852 amino acid-long LSD1 protein. However, LSD1 transcript can be subjected to alternative splicing processes that give rise to different LSD1 isoforms. Specifically, it is possible to identify two alternative spliced exons. Because of their position into *LSD1* gene they are indicated as exon E2a and exon E8a: the first one maps between exon E2 and exon E3 being indicated as exon E2a, the second one is located between exon E8 and exon E9, being referred to as exon E8a [91].

Exon E2a is 60bp-long while exon E8a is a microexon of 12 base pairs. Exons E2a and E8a can be combinatorially included in mature LSD1 transcripts, generating 4 different LSD1 isoforms: LSD1, LSD1-E2a, LSD1-E8a and LSD1-E2a/E8a. Importantly, their inclusion does not alter LSD1 open reading frame, allowing the generation of functional proteins. Exon E2a is ubiquitously included into LSD1 transcripts. Differently, the inclusion of microexon E8a is the result of a neural-specific splicing process. Given its neural-restricted expression, all LSD1 isoforms that contain exon E8a (LSD1-E8a and LSD1-E2a/E8a) are referred to as neuroLSD1 (Figure 5). Interestingly, neuroLSD1 isoform can be found only in mammals, and only in humans alternative splicing of microexon E8a is also present in testis [91].

Neurospecific splicing isoform neuroLSD1 differs from ubiquitously expressed LSD1 isoform only for the presence of the tetra-peptide Asp-Thr-Val-Lys, coded by the 12 nucleotides long microexon E8a. As already said, the inclusion of exon E8a does not alter LSD1 open reading frame and results in a small loop protruding in the vicinity of the catalytic pocket, immediately before the CoREST-binding Tower domain [91] (Figure 6).

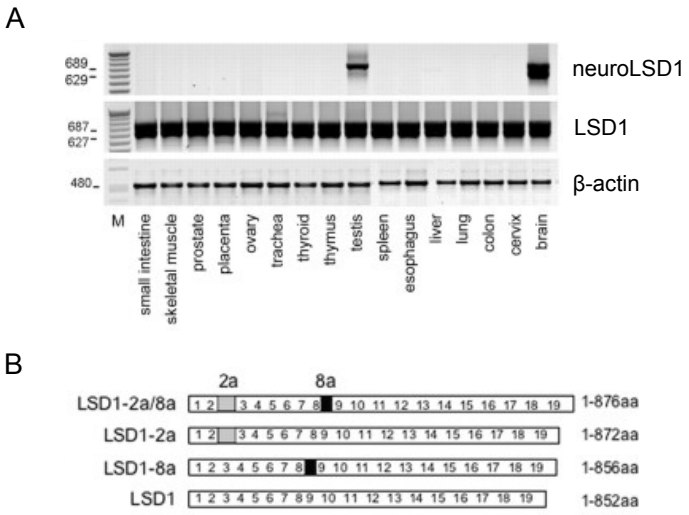

Figure 5. In mammals, single or double inclusion of two alternatively spliced LSD1 exons, exon E2a and exon E8a, generates four different LSD1 splicing isoforms. (A) Expression of LSD1 isoforms in human tissues. Exon E2a is ubiquitously spliced in human tissues, while neuroLSD1 isoforms (LSD1-E8a and LSD1-E2a/E8a) is restricted to brain and testis. (B) Schematic representation of the four possible LSD1 isoforms: LSD1, LSD1-E2a, LSD1-E8a and LSD1-E2a/E8a. Adapted from [91].

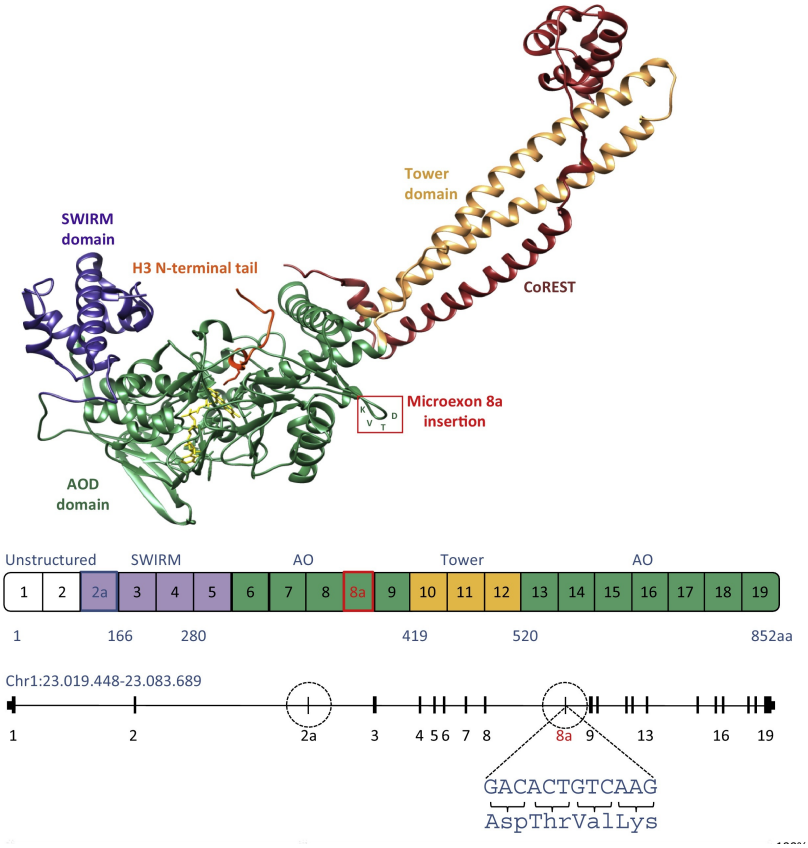

Figure 6. Structure of neuroLSD1 protein. Ribbon drawing shows the tetra-peptide Asp-Thr-Val-Lys coded by microexon E8a generating a small protruding loop proximal to the catalytic site, immediately before the CoREST-binding Tower domain. The lower panel shows the exons composing each domain and the localization of the two LSD1 alternative exons E2a and E8a. Amino acids are reported [52].

The presence of exon E8a encoded tetra-peptide does not affect *per se* the demethylase activity of the enzyme. However it has been shown that phosphorylation of the neuroLSD1 threonine 369b residue prevents it from binding CoREST and HDAC1/2 [92]. Thus, differently from ubiquitous LSD1 isoform, which acts as a transcriptional corepressor through its H3K4me1/2 demethylase activity, neuroLSD1 is unable to repress transcription probably because the enzymatic activities coexisting within the LSD1/CoREST/HDAC1/2 corepressor complex allow each other [93]. Since LSD1 and neuroLSD1 share the same target genes but mediate an opposite effect on their transcription, neuroLSD1 can be considered as a dominant negative isoform of LSD1. NeuroLSD1 transcript relative percentage shows a marked brain area specificity ranging from 40% to 65% of total LSD1 transcript. The balance between LSD1 and neuroLSD1 determines the chromatin landscape of their target genes towards a more repressive or more permissive layout through a splicing-based mechanism [91]. As a consequence, the modulation of exon microexon E8a splicing represents a mechanism for fine-tuning the transcription of selected targets.

In 2016, Rusconi and colleagues discovered that also the transcription factor Serum Response Factor (SRF), similarly to REST, can recruit LSD1 corepressor complex in the brain [44]. SRF binds to the Serum Response Element (SRE) sequence of peculiar plasticity-related genes, namely the immediate early genes (IEGs). They include *egr1*, *c-fos* and *arc* and represent a particular class of genes that undergo rapid and transient transactivation in response to stimuli independently on de novo protein synthesis. A variety of protein complexes resides at the level of IEGs promoters guaranteeing their activity-dependent rapid transcription. Even in absence of an activity-dependent stimulus, the IEGs promoters are already bound by the RNA polymerase II complex and by their activity-dependent transcription factors CREB (cAMP Responsive Element Binding protein) and SRF [94, 95]. Furthermore, nucleosomes at IEGs promoters already carry chromatin modifications that are permissive for transcription, including trimethylated lysine 4 of histone H3 (H3K4me3) [96]. However, in basal conditions IEGs are held in a repressed state by the presence of a series of transcriptional corepressor complexes (among which LSD1/CoREST/HDAC1/2 complex) recruited by SRF and CREB. When an environmental stimulus is perceived, the activation of calcium-dependent signaling pathways culminates with detachment of repressor complexes and recruitment of activators, allowing RNA polymerase II to start transcription [97]. Madabhushi and colleagues provided an additional insight into this mechanism indicating that neuronal activity elicits the formation of DNA double strand breaks that, resolving local topological constraints, favor IEGs rapid transcription [98]. IEGs experience-induced transcription is widely recognized as

fundamental to neuronal plasticity and circuitry modification underlying complex brain functions, such as memory formation and emotional behavior [97, 99]. In the central nervous system, SRF represents a versatile transcription factor that promotes transcriptional repression in resting conditions and transcriptional activation upon stimuli [95]. The activity of SRF, likewise LSD1, is regulated by alternative splicing through the generation of SRFΔ5 isoform, a variant lacking the transactivation domain and acting as dominant negative [100, 101]. SRF and SRFΔ5, together with LSD1 and neuroLSD1, contribute in setting the chromatin state of IEGs. Importantly, the relative amount of pro-repression LSD1 and pro-transcription neuroLSD1 isoforms, defining the precise chromatin landscape of their target genes, sets the intensity of the plasticity-related genes transcriptional wave in response to circuital activity to shape neuronal plasticity (Figure 7) [42, 43, 92].

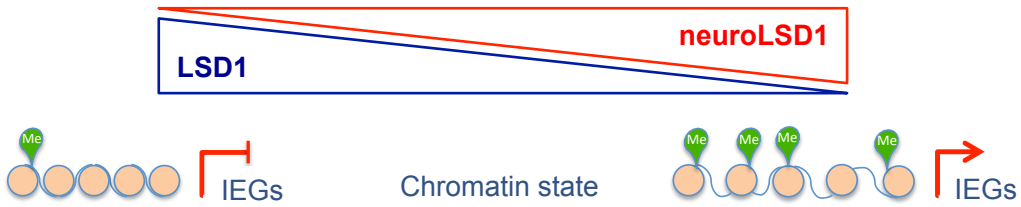

Figure 7. The efficiency of IEGs transactivation depends on the relative amount of LSD1 and neuroLSD1. NeuroLSD1 positively modulates activity-dependent transcription of immediate early genes (IEGs) through a chromatin-based mechanism. Adapted from [52].

1.2.3 Involvement of neuroLSD1 in complex brain functions

NeuroLSD1 expression is finely regulated during neuronal developmental phases. Indeed, within the perinatal window, neuroLSD1 undergoes a significant increase with a concomitant decrease of LSD1 in rat and mice cortical tissues. This preponderance of neuroLSD1 isoform is maintained until postnatal day 7 (P7). Subsequently, LSD1 isoforms stabilize to values found in adult cortical neurons [91]. On the contrary, E2a-containing LSD1 transcript expression remains stable (Figure 8). As the peak of neuroLSD1 expression corresponds to a stage of neuronal development characterized by increased neuroplasticity and synaptogenesis, a picture emerges supporting neuroLSD1 functional role in promoting neuronal differentiation, maturation and morphogenesis.

In line, in vitro experiments performed on rat primary cortical neurons support neuroLSD1 involvement in neuronal development, reflecting in vivo physiological modulation of LSD1 isoforms [91]. Moreover, short hairpin RNA-mediated neuroLSD1 knockdown leads to impairment in neurites morphogenesis in terms of dendritic arborization, neurite thickness and length. The other way around, neuroLSD1 overexpression promotes neuronal maturation

[91]. NeuroLSD1 has been also described to regulate neuronal differentiation through a different molecular mechanism that does not account on the inhibition of H3K4me1/2 demethylation as LSD1 dominant negative isoform. Indeed, when associated to Supervillin (SVIL) neuroLSD1 has been proposed to gain the ability to remove methyl group from dimethylated lysine 9 residue of histone H3 (H3K9me2). Interestingly, when this interaction is inhibited, neurons fail to differentiate [102].

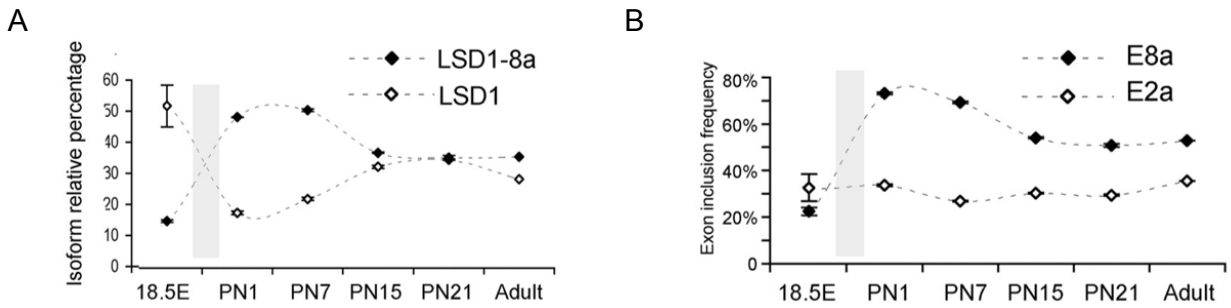

Figure 8. NeuroLSD1 isoforms are dynamically regulated during development in rat cortical tissues. (A) neuroLSD1 increase with a concomitant decrease of LSD1 during the perinatal window, in rat cortical tissues. (B) LSD1-E2a isoform expression is not modulated during development. Adapted from [43].

The generation of a neuroLSD1^{KO} mouse strain [43] shed light on neuroLSD1 involvement in molecular processes underlying complex brain functions such as neuronal excitability [43], memory formation [42, 103], and emotional behavior [44]. The neuroLSD1^{KO} mouse model was generated by genetically removing the exon E8a. It is important to underline that in neuroLSD1^{KO} mice E8a removal does not affect LSD1 expression. As a result, given that in neuronal tissues neuroLSD1 cannot be generated, all LSD1 transcripts will encode LSD1 protein, which is why neuroLSD1^{KO} mice represent a model of LSD1 overexpression in the brain [43].

An important aspect that emerged from the phenotypical characterization of neuroLSD1^{KO} mice is that they are hypoexcitable and protected against epilepsy (Figure 9). In fact, neuroLSD1^{KO} mouse shows a higher excitability threshold and decreased seizure susceptibility, evidenced by a reduced responsiveness to pilocarpine, a well-known chemoconvulsant agent. On the contrary, in the murine model of Rett Syndrome (Mecp2$^{Y/-}$), which is characterized by an increased susceptibility to seizures, neuroLSD1 is overexpressed in several brain areas [43]. These data suggest a tight connection between neuroLSD1 and circuitry of hyperexcitability underlying epileptogenesis.

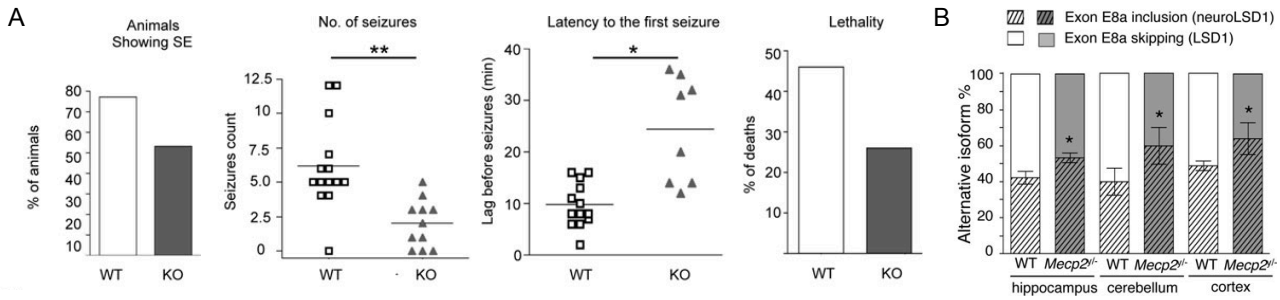

Figure 9. NeuroLSD1 is involved in circuitry of hyperexcitability underlying epileptogenesis. (A) Upon pilocarpine induced status epilepticus (PISE), neuroLSD1^{KO} mice are hypoexcitable compared to wild type ones in terms of presence of seizures, number of seizures, latency to first seizure and lethality. (B) Higher levels of neuroLSD1 are observed in different brain areas in the mouse model of Rett Syndrome (Mecp2$^{Y/-}$). Adapted from [43].

Direct evidence supporting the idea that LSD1 and neuroLSD1 regulate the transcriptional substrates of memory and cognition comes from the observation that neuroLSD1^{KO} mice show significant memory deficits in Novel Object Recognition test [42, 103]. This behavioral phenotype is also associated to reduced structural plasticity at the level of the hippocampus as shown by diminished number of dendritic spines measured through Golgi Staining technique [42, 103] (Figure 10).

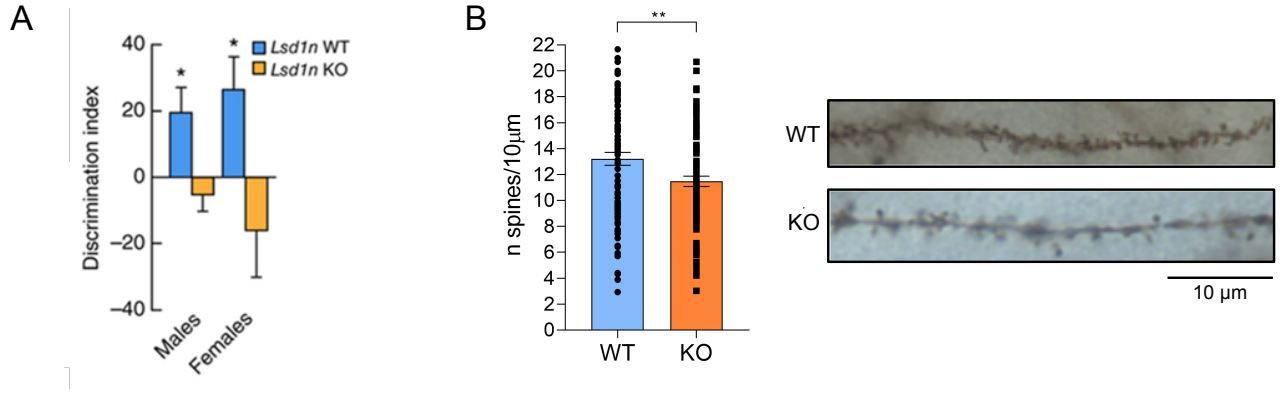

Figure 10. NeuroLSD1^{KO} mice show long-term memory deficits. (A) Discrimination index in Novel Object Recognition reveals memory impairment in neuroLSD1^{KO} mice compared to wild type (adapted from [42]). (B) Golgi-Cox staining of secondary dendritic segments of mouse hippocampal neurons (CA1) and quantification of spine density in neuroLSD1^{KO} mice compared to wild type (adapted from [103]).

Moreover, behavioral assays performed in our laboratory linked neuroLSD1 with emotional behavior. Indeed neuroLSD1^{KO} mice display a reduced anxiety-like phenotype measured with the Elevated Plus maze assay, the Marble Burying test and the Novelty Suppressed Feeding paradigm (Figure 11). This behavioral outcome is associated to a deficient stress-driven transactivation of IEGs in the hippocampus, implying a role for neuroLSD1 in transducing stressful stimuli into proper anxiety-related plasticity [44].

Remarkably, LSD1 repressive activity against plasticity-related genes can be pharmacologically targeted through systemic administration with SAHA, a pan-histone HDAC inhibitor, able to restrain the repressive function of the whole LSD1/HDAC2/CoREST epigenetic complex. Interestingly, SAHA treatment is sufficient to restore memory deficits and to revert low anxiety-like behavior of neuroLSD1^{KO} mice [44].

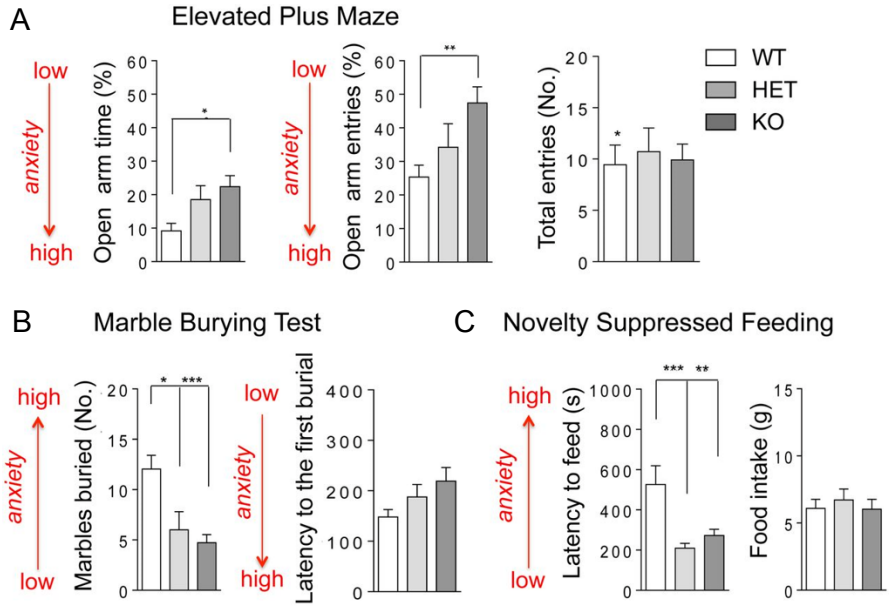

Figure 11. NeuroLSD1^{KO} mice show a low anxiety-like phenotype. Evaluation of anxiety in neuroLSD1^{KO} mice compared to wild type and heterozygous mice based on different parameters of (A) Elevated Plus Maze, (B) Marble Burying and (C) Novelty Suppressed Feeding test [44].

1.2.4 LSD1/neuroLSD1 dynamic ratio

Three molecular mechanisms have been shown to modulate exon E8a inclusion into LSD1 transcripts and their role has been largely investigated by carrying out minigene splicing assays [43]. In detail, two *trans*-acting splicing factors, NOVA1 and nSR100, have been described to positively regulate microexon E8a inclusion in LSD1 mature transcripts. The neurospecific splicing factor nSR100 is necessary and sufficient to regulate E8a splicing, conferring neuronal specificity, while NOVA1 requires nSR100 presence to positively influence E8a inclusion. A third molecular mechanism of E8a splicing modulation is represented by the negative *cis*-acting regulation of a palindromic sequence located about 300bp downstream E8a sequence. This sequence is a 21bp-long element complementary reverse to E8a and it anneals to the microexon and its surrounding regulatory elements preventing its splicing through the formation of a double-stranded RNA structure (Figure 12). The palindromic region acts ubiquitously fostering exon E8a skipping in non-neuronal contexts, where no positive mechanisms are present [43].

Figure 12. The palindromic sequence in action. The 21bp-long palindromic element acts in *cis*- as a negative regulator preventing microexon E8a inclusion in LSD1 mature transcripts through the formation of a double-stranded RNA structure that provokes exon skipping. Adapted from [103].

I already showed how neuroLSD1 is dynamically modulated during neuronal development contributing to neuronal differentiation and maturation. Moreover, neuroLSD1 expression is regulated also during aging in the mouse brain. Indeed, in aged mouse brain, increased LSD1 and decreased neuroLSD1 relative mRNA levels are detectable (Figure 13) [42].

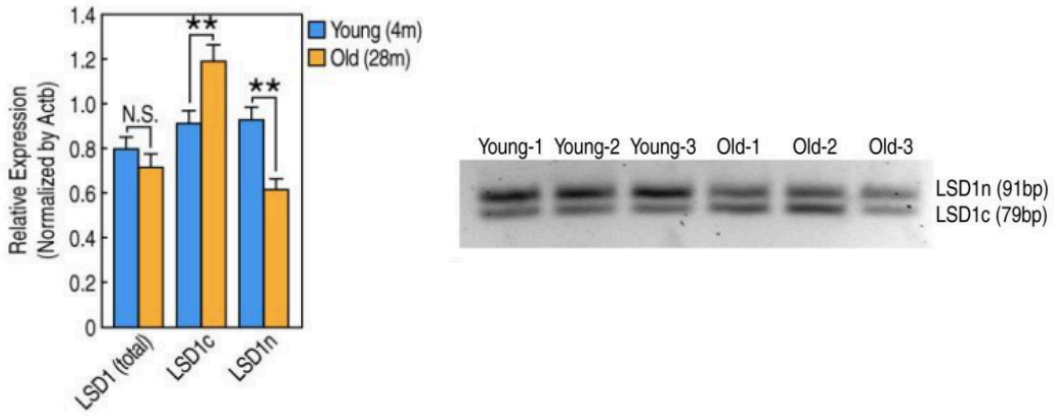

Figure 13. Increased LSD1 and decreased neuroLSD1 mRNA levels are detectable in aged mouse brain. On the left, qRT-PCR showing LSD1 decrease and neuroLSD1 increase in 28-month-old mice (Old) compared to 4-month-old mice (Young). On the right, LSD1 transcript isoforms modulation in old mice compared to young controls. Adapted from [42].

The modulation of exon E8a splicing regulators is certainly involved in LSD1 and neuroLSD1 dynamic changes during brain development and aging. However, although within adulthood the ratio between LSD1 and neuroLSD1 stabilizes to a steady-state balance, different paradigms of neuronal activation are able to perturb this equilibrium inducing a dynamic neuroLSD1 levels modulation also in the adult brain [43, 44] (Figure 14). Consistently, it has been published that NOVA1 and nSR100 are dynamically modulated in response to neuronal activation. More in detail, neuronal activation affects nSR100 activity by influencing its expression [104], while NOVA1 is regulated through a shuttle mechanism that modifies its cellular localization from nucleus to cytoplasm [105]. Their modification could be crucial in

dynamically modulating neuroLSD1 expression in response to environmental stimuli in the adulthood.

Our laboratory published that LSD1 and neuroLSD1 balance is modified upon a pharmacological paradigm of neuronal activation, the Pilocarpine-induced Status Epilepticus (PISE) (Figure 14A). In the mouse hippocampus, PISE induces neuroLSD1 downregulation with a concomitant increase of LSD1 isoform. This modulation is transient indeed after 24 hours LSD1/neuroLSD1 ratio returns to the levels observed in adult hippocampal samples [43].

A similar splicing modulation can be observed upon a paradigm of psychosocial stress, the Acute Social Defeat Stress (ASDS). In this paradigm, an experimental mouse is defeated within a direct interaction with an aggressor CD1 mouse. After that, psychological phase that lasts seven hours lets the stress continue in an olfactory and visual contact. As it happens in PISE, neuroLSD1 relative levels are downregulated after seven hours of psychosocial stress and a recovery to basal levels can be scored after a resting phase (Figure 14B) [44].

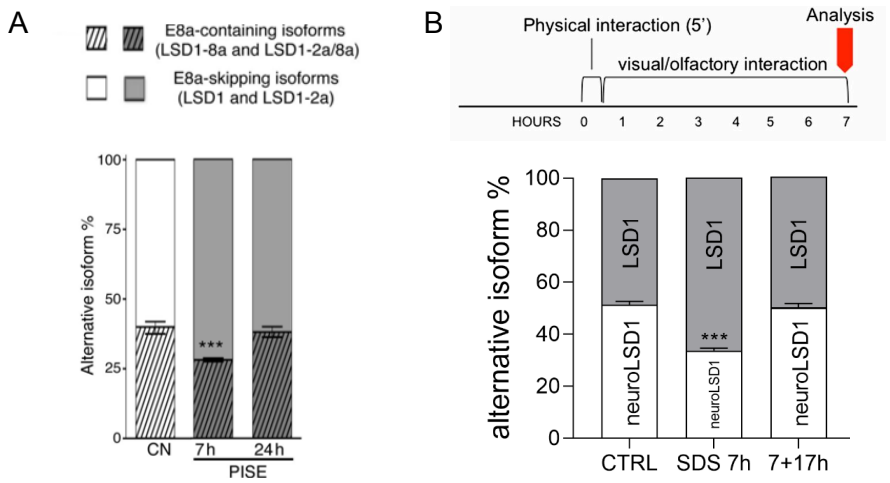

Figure 14. In vivo paradigms of neuronal activation are able to transiently modify LSD1/neuroLSD1 splicing ratio in the mouse hippocampus. Histograms show alternative isoform percentage in (A) PISE and (B) ASDS paradigm. In both paradigms neuroLSD1 downregulation can be observed 7 hours after PISE or 7 hours of ASDS. Note that neuroLSD1 modulation is transient. Adapted from [43] and [44].

1.2.5 Role of LSD1 and neuroLSD1 in homeostatic response to stress

The homeostatic mechanisms that are engaged during the secondary phase of stress response contribute to cope with stress through a fine-tuning of glutamate response maintaining IEGs transactivation within an adaptive range. At the neuronal level, restrain of excessive glutamatergic signaling and its transduction is achieved through complex homeostatic

responses involving also the endocannabinoid system (ECS) [106-110] and different epigenetic modifications ultimately aimed at diminishing IEGs transcription [16].

As previously stated, LSD1 and neuroLSD1 are recruited at the IEGs promoter thanks to SRF and contribute to set their chromatin structure. Relative LSD1 and neuroLSD1 amount impacts the strength of corepressor assembly controlling the transcriptional responsiveness of their target genes [42, 43, 92]. According to this, molecular analyses performed on the hippocampus of defeated wild type and neuroLSD1 heterozygous mice (a genetic model of neuroLSD1 haploinsufficiency, neuroLSD1^{HET}) show a decreased ability to activate IEGs transcription upon acute stress. As expected, a single session of psychosocial stress induces the transactivation of c-fos and egr1 IEGs in wild-type mice hippocampus. However, in neuroLSD1^{HET} mice, although IEGs basal expression levels were almost comparable to wild-type ones, c-fos and egr1 stress-induced transcriptional activation is defective with respect to wild-type animals (Figure 15) [44]. NeuroLSD1^{HET} impaired response to stressful events suggests that LSD1/neuroLSD1 optimal balance is needed for a proper transcriptional response to stimuli and a ratio shifted towards low levels of neuroLSD1 isoform reduces IEGs transactivation.

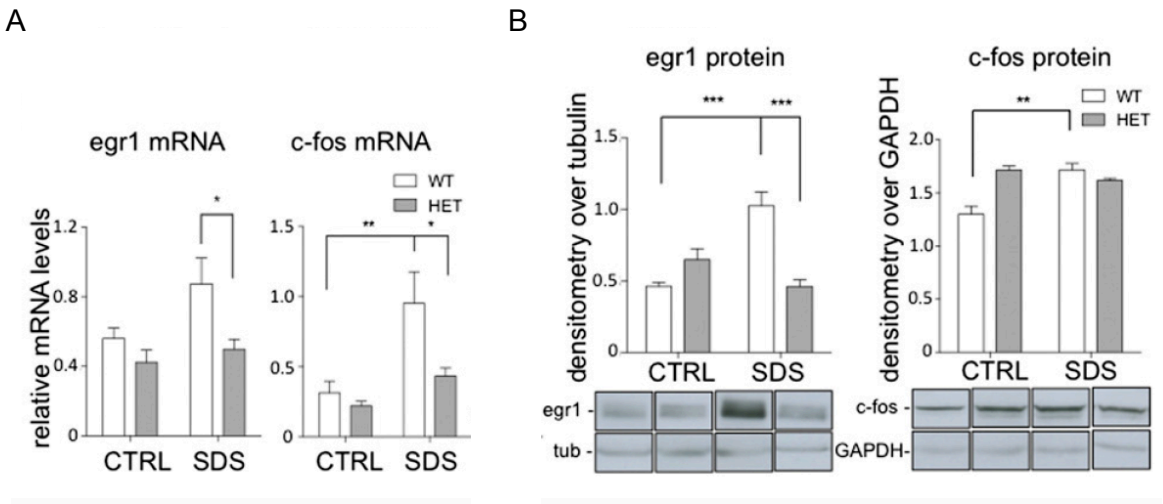

Figure 15. Reduced levels of neuroLSD1 impair IEGs transactivation upon acute stress. (A) NeuroLSD1^{HET} mice display an impaired transactivation of egr1 and c-fos upon ASDS compared to wild-type, both at (A) transcript and (B) protein levels. Adapted from [44].

Considering that a reduced neuroLSD1 amount due to genetic removal of exon E8a in one allele implicates a deficient transactivation of target genes, neuroLSD1 transient downregulation upon acute stress could represent a splicing-based homeostatic mechanism taking part into the previously described epigenetic stress-coping responses. In fact, stress-induced LSD1 and neuroLSD1 splicing modulation shifts LSD1 isoforms splicing balance

towards a more repressive layout through the increase of LSD1-mediated H3K4me1/2 demethylation concurring in restraining IEGs transcription in the hippocampus [16].

At the behavioral level, we must consider neuroLSD1^{KO} mice phenotype of reduced anxiety and impaired memory formation. Stress-evoked IEGs transcription in the hippocampus is fundamental to promote the behavioral effects of stress and a short-term cognitive enhancement aimed at memorizing the threatening stimulus, providing the ability to engage in protective responses against subsequent similar threatful conditions. This memorization process, however, should not elicit excessive anxiety and fear. In this regard, stress-induced increase of LSD1 repressive activity on IEGs could suppress excessive anxiety arousal also avoiding long-term behavioral changes by buffering excessive consolidation of stress plasticity [52]. Moreover, in vitro and in vivo experiments performed in our lab indicate that glutamate-induced neuroLSD1 downregulation might in turn have a role in restraining glutamatergic signaling and its transduction by controlling transcriptional mechanisms of synapse potentiation. This homeostatic mechanism, being part of an adaptive stress-coping process, ultimately aims at limiting memorization of traumatic experiences [103].

Finally, LSD1 and neuroLSD1 system is also involved in endocannabinoid system (ECS)-mediated homeostatic response to stress [109]. ECS contributes to stress response termination through the presynaptic inhibition of glutamate release, mediated by increased levels of endocannabinoid (eCB) 2-arachidonyl glycerol (2-AG) acting on cannabinoid 1 (CB1) receptor in the presynaptic compartment. 2-AG increased concentration upon acute stress is obtained through transcriptional repression of α/β-hydrolase domain containing 6 (ABHD6) and monoacylglycerol lipase (MAGL), enzymes involved in 2-AG degradation [106, 110]. We proposed a synapse-to-nucleus cross-talk mechanism in which LSD1 directly interacts with ABHD6 and MAGL promoters thanks to REST-mediated tethering. By repressing their transcription, LSD1 sustains 2-AG-induced synaptic inhibition. Interestingly, such negative control is disrupted upon chronic stress impairing LSD1- and ECS-mediated synaptic modulation on glutamate transmission [109].

All together these observations support LSD1 and neuroLSD1 role as epigenetic modifiers of homeostatic control of stress-response aimed at limiting the toxic effect of stress. Accordingly, an aberrant regulation of this buffering-oriented stress-response mechanism could concur to maladaptive forms of plasticity associated to stress-vulnerability, eventually promoting the onset of neuropsychiatric disorder such as depression and mood disorders.

1.2.6 Disease-associated mutations in *LSD1* gene

LSD1 gene is highly conserved from yeast to humans, suggesting the functional relevance of this epigenetic enzyme. In addition to interspecies conservation, *LSD1* gene also displays high intraspecies constraint belonging to the top 2% of the less polymorphic human genes [111]. Marked LSD1-associated low rate of genetic variants, especially in coding regions, underlines intolerance to functional variations. Although constrained genes are often associated to dominant Mendelian phenotypes, *LSD1* mutations had never been linked to a human disease-associated phenotype until 2012 when a *de novo* mutation in *LSD1* gene (c.1739A>G encoding p.Asp580Gly, D580G) predicted to affect LSD1 function, was identified among many other gene mutations in an exome sequencing study on severe non-syndromic sporadic intellectual disability [112]. LSD1 D580G was not characterized further. In 2014, Tunovic and colleagues described another *de novo LSD1* mutation (c.2353T>C encoding for p.Tyr758His, Y785H) in a male child affected by a Kabuki-like syndrome [113]. Two years later, another family was found via social networking having a child with a similar phenotype and a third *de novo LSD1* mutation (c.1207G>A encoding for p.Glu403Lys, E403K) [114]. Interestingly, all these three children carried dominant missense point mutations in the *LSD1* gene showing similar clinical findings which gave the opportunity to describe a new genetic disorder showing some pathological traits with the Kabuki syndrome along with typical facial features, hypotonia, skeletal anomalies, global developmental delay and cognitive impairment [114].

The functional effects of these pathological mutations in term of LSD1 activity modulation have been analyzed in [115]. Notably, all the mutations localized within the amine oxidase catalytic domain, in proximity to H3 substrate binding site (Figure 16).

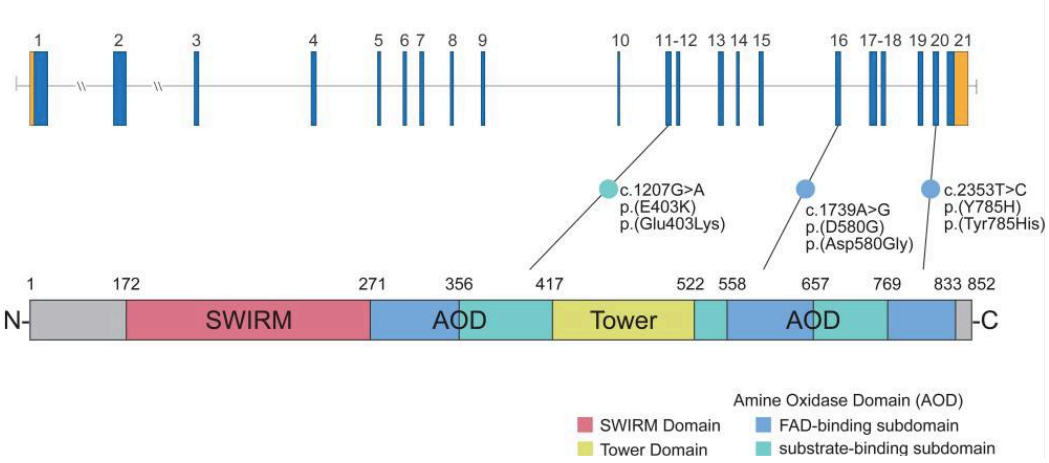

Figure 16. Localization of the three identified *LSD1* mutations within *LSD1* gene and LSD1 protein. Genomic structure of *LSD1* gene, predicted LSD1 protein and spectrum of mutations that cause cognitive impairment. Adapted from [114].

The researchers showed how the quantitative effect of *LSD1* mutations on protein activity was mutation-specific. In detail, all three mutations did not alter LSD1 ability to bind to CoREST and HDAC1/2, properly assembling the corepressor complex. Consistently mutated LSD1 maintained the transcriptional repressive activity evaluated on a reporter gene. However, although not displaying folding instability, mutant protein half-life was significantly reduced compared to wild-type LSD1. D580G and Y785H displayed a binding affinity to H3 substrate similar to wild-type LSD1 protein while E403K strongly impaired substrate binding. Due to sterical and electrostatical alteration of the active site, LSD1 demethylase activity was strongly reduced by D580G and Y785H mutations and barely detectable in E403K. Regarding the ability of LSD1 mutant isoforms to bind the Snail Family Transcriptional Repressor 1 (SNAIL1), a transcription factor that orchestrates key embryonic developmental programs in association with LSD1, D580G mutant showed little impairment while Y785H and E403K mutations almost completely abolished this interaction [115].

The embryonic development of homozygous $LSD1^{KO}$ mice is strongly compromised, with no viable embryos after embryonic day E7.5 [74]. Data obtained from LSD1 mutants analyses [115] indicate that LSD1 catalytic features are fundamental for proper organism development and that even slight perturbations of LSD1 activity cause developmental delay and cognitive impairment [113-115]. However, as mutant human LSD1 isoforms retain the ability to assemble a functional corepressor complex, it seems that preservation of LSD1 scaffolding activity likely concurs to its biological relevance, suggesting a hint to understand life compatibility of annotated LSD1 human mutations.

1.3 OVERVIEW OF ALTERNATIVE SPLICING

Alternative splicing (AS) is a biological mechanism that allows the formation of a set of functionally different transcripts starting from a single gene, enhancing proteome complexity without the need of an increased number of genes [116, 117]. Nearly all intron-containing human genes have been shown to undergo alternative splicing, having at least one alternative spliced exon [118]. Interestingly, the average number of spliced isoforms per gene is higher in vertebrates, implying that alternative splicing contributes to the increasing evolutionary complexity. In other words, alternative splicing represents a potent regulatory mechanism of protein functions, being indeed the major contributor to protein diversity in metazoan organisms [119, 120].

The mRNA splicing machinery requires the presence of specific consensus sequences to interact with the pre-mRNA. These *cis*-acting elements are the 5' acceptor splice site and the 3' donor splice site, located at the boundaries between introns and alternative exons, the branch site and the polypyrimidine tract [121]. However, splicing sites are not sufficient *per se* to guarantee the proper splice site selection and to correctly regulate splicing events. Indeed, a variety of auxiliary *cis*-acting elements and *trans*-acting factors are needed for the regulation alternative but also constitutive exons. In this regard, exonic or intronic splicing enhancers and silencers (ESE-ESS and ISE-ISS) RNA motifs are required to bind and recruit *trans*-acting splicing factors on target pre-mRNAs that positively or negatively regulate the splicing process [122].

Most splicing factors that regulate alternative and constitutive splicing processes are ubiquitously expressed across tissues. Nevertheless, a large number of splicing factors are tissue-specific or display an enriched expression in few cell types, hence controlling alternative splicing events in tissue- or cell-type-dependent manners, contributing to provide cells with a further drive of identity specification [123-125]. Moreover, many alternative splicing events are controlled in a developmental stage-specific way [126]. Consequently, dysregulation of splicing process often results in different pathologies such as developmental disorders, hereditary diseases or cancer [127].

1.3.1 Alternative splicing coupled to Nonsense-mediated decay (AS-NMD)

LSD1 and dominant negative neuroLSD1 represent an example of how alternative splicing leads to the generation of different proteins having distinct, sometimes opposite functional roles. However, many alternative splicing events never result in alterative spliced functional proteins [128, 129]. The functional consequence of AS is in fact often related to transcript regulation. In some transcripts, alternative splicing results in the inclusion of exons containing an in-frame premature termination codon (PTC), the so-called "poison exons". Their name stems from the fact that when the exon is spliced into the mature transcript it "poisons" the host transcript with an early stop codon that triggers transcript degradation by the Nonsense-mediated decay (NMD) pathway. NMD is a cytoplasmic, translation-coupled [130, 131] surveillance system aimed at protecting cells from transcripts that contain nonsense mutations or splicing errors encoding truncated or dysfunctional proteins [132]. However, it is now clear that NMD represents also a RNA turnover mechanism involved in regulating the expression of physiological transcripts, finely controlling the unproductive splicing of poison exons [133]. Eukaryotic cells engage alternative splicing (AS) combined

with NMD to regulate the abundance of mRNA transcripts in a mechanism known as AS-NMD [134] or Regulated Unproductive Splicing and Translation, shortly termed RUST [135, 136]. This is a widespread mechanism, indeed one third of human protein coding genes has at least one NMD-targeted splicing isoform [137] and exhibits a high degree of evolutionary conservation [138]. RNA-binding proteins and particularly many splicing factors employ unproductive splicing on their own mRNA as a negative feedback to dynamically modulate their protein levels establishing a self-limiting range of protein expression to maintain cellular homeostasis [134, 139, 140].

NMD is a complex pathway involving numerous factors [133]. Some of these factors are involved in the "recognition phase" of NMD that establishes which transcripts are NMD targets. This recognition phase relies on NMD-inducing features all centered on the termination of mRNA translation (Figure 17). The recognition of PTCs from normal stop codons is established by the presence of a downstream acceptor site that characterizes exon-exon junctions. When the ribosome reaches a premature stop codon a NMD-promoting complex is assembled: eukaryotic release factors (eRFs) are recruited along with the exon junction complex (EJC), physically connected thanks to the protein UPF3B, and other recognition factors including the RNA helicase UPF1 and UPF2 [132, 141]. The formation of this complex leads to phosporylation and dephosporylation cycles of UPF1 [142] that trigger transcript degradation. This "decay phase" of NMD is driven by other factors, including SMG6 and endonucleases that cleave NMD target mRNAs [133, 141].

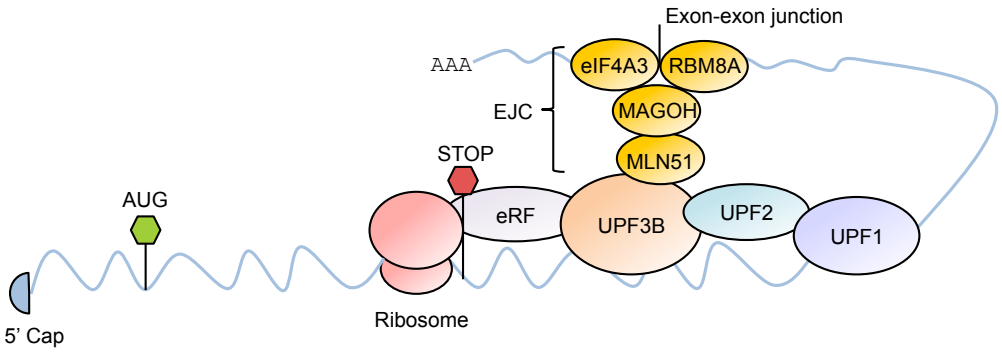

Figure 17. Schematic representation of NMD recognition phase. Transcripts with at least one exon–exon junction downstream of the stop codon terminating the main open reading frame (ORF) are degraded by nonsense-mediated decay (NMD) through the shown protein–protein interactions. Adapted from [141].

Coherently with the importance of NMD pathway in preserving cellular homeostasis, alterations of NMD surveillance and transcript abundance-tuning system lead to pathological conditions including neurological disorders, immune diseases and cancers. Different neurological disorders, such as mental retardation and intellectual disabilities [143-145] and

neurodevelopmental disorders i.e. Autism Spectrum Disorders [144, 146] and Schizophrenia [147, 148], have been linked to genetic mutations or dysregulation of NMD factors.

1.3.2 Alternative splicing relevance in the brain

It is well known that neurospecific transcripts undergo alternative splicing with a significantly increased frequency compared to those populating the other cell types. As a matter of fact, alternative splicing events are particularly frequent in the nervous system [149, 150] where they allow a fine regulation of fundamental neuronal processes like synapse formation and axons sprouting [151-154]. Moreover, it is thought that such high alternative splicing prevalence in neuronal tissues might concur to the establishment of complex brain functions [155], such as learning and memory formation [156].

Splicing of the so-called "microexons", namely 3 to 27 nucleotide-long exons, seems to be particularly important for neuronal functions. In neurons, microexons sequence and their flanking intronic regions are more conserved than longer ones [157]. Similarly to the switch-like regulation of microexon E8a inclusion in neuroLSD1 transcripts, the majority of neuronal microexons display a significant increase in their inclusion levels during the terminal stage of neuronal differentiation [157]. Accordingly, different studies have shown that microexons participate in both neurogenesis and adult neuron physiology [158]. Neurospecific splicing of these microexons often displays a functional role at the protein level. Indeed, they provide new regulatory platforms for protein-protein interactions or binding site for post-translational modification [155], as it happens for microexon E8a encoded tetra-peptide in LSD1 protein [92].

Interestingly, the splicing factor nSR100 (which positively regulates microexon E8a inclusion into mature LSD1 transcripts) regulates more than a half of neurospecific microexons inclusions [157]. As a matter of fact, nSR100 is characterized by the presence of an Enhancer of Microexons domain (eMIC) that has been discovered as far back as into a bilaterian ancestor where neuronal microexons programs appeared for the first time. The eMIC domain originated in the pan-eukaryotic *Srrm2/SRm300* gene through an alternative splicing process and then became fixed in the vertebrate nSR100 protein driving the evolution of neuronal microexons. The eMIC domain is necessary and sufficient to promote microexons splicing, and its appearance led to an evolution in splicing programs that likely contributed to the increase of bilaterians neuronal complexity [159].

1.3.3 Single nucleotide variations affect alternative splicing

Ubiquitous or tissue-specific expression of splicing factors along with gene body chromatin organization directly impact alternative splicing [160]. Likewise, pre-mRNA secondary structure strongly affect AS, as it happens for microexon E8a in LSD1 transcript that is trapped by the palindromic sequence into a hairpin structure, negatively affecting its inclusion in mature transcript. Along with these regulatory mechanisms, also single nucleotide variations can entail changes in alternative splicing process, a phenomenon known as genetically modulated alternative splicing (GMAS) [161].

Splicing mutations occur both in introns and exons sequence and, depending on which regulatory element is affected, they can promote or inhibit the splicing of alternative exons.

The most common splicing mutations are those that alter 5' and 3' splice sites. Indeed, this highly conserved splice sites define intron-exon boundaries, being recognized by the splicing machinery to allow exon recognition. Any variation in 5' AG or 3' GT dinucleotide disrupts the existing splice site typically leading to exon skipping. Furthermore, mutations in the nucleotides immediately upstream 5' or downstream 3' splice site have a similar effect [162, 163]. For instance, G to A mutation (1525-1G>A) in the acceptor site of exon 10 of Cystic Fibrosis Transmembrane Conductance Regulator (*CFTR*) gene causes the skipping of E10 and the usage of alternative acceptor sites within exon 10 or intron 10 sequence [164].

Single nucleotide variations at the branch point, a short element located around 20 nucleotides upstream the polypyrimidine tract containing a hyper-conserved adenosine, are very rare. This is also due to the fact that branch point is a degenerate motif, YUNAY in humans, difficult to predict [165]. In NPC Intracellular Cholesterol Transporter 1 (*NPC1*) gene, associated to Niemann-Pick disease type 1, the mutation of branch point adenosine c.882-28A>G in intron 6 causes the skipping of exon 7 [166]. However alterations of the splicing process can be due to branch point mutation that does not involve the adenosine. For example, in Fibrillin 2 (*FBN2*) gene, a rare single nucleotide mutation from T to G inside intron 30, located many nucleotides upstream the predicted branch point sequence, entails a partial skipping of exon 31 [167].

Similarly to branch point, mutations in polypyrimidine tract are very uncommon. One example is the mutation c.937-11 C>G of Lamin A/C (LMNA) gene whose outcome is the retention of 40 nucleotides of intron 5 during exon 6 splicing [168].

Deep intronic variations are instead more frequent among GMAS. Typically, they consist in mutations within long introns that create new splice sites or activate cryptic exons, resulting in the inclusion of a new exon in the mature transcript. Another possible outcome of deep

intronic mutations is the generation of novel consensus motifs that are recognized by *trans*-acting splicing factors [162, 169]. A well-known example is c.3718-2477C>T mutation inside intron 19 of *CFTR* gene that generates of a new donor site leading to the inclusion of a cryptic exon with an in-frame premature stop codon translated into a truncated inactive protein [170].

Mutations can disrupt splicing enhancer or silencer through modifications of the consensus sequence that could not be recognized by *trans*-acting splicing factors, or alter the secondary structure of transcripts preventing or facilitating the interaction with spliceosome machinery [161].

It has been estimated that mutations disrupting the splicing process account for 15-60% of all human mutations associated to diseases. However, population-scale transcriptome analyses have disclosed that also single nucleotide polymorphisms (SNPs), obviously more frequent in the human population compared to disease-associated mutations, could have a functional impact on alternative splicing regulation [171]. They of course would not result in drastic changes in the expression of alternative isoforms, contributing instead in fine-tuning splicing processes and concurring to generate phenotypic variability and diversity between individuals but also different levels of disease susceptibility.

1.3.4 The splicing factor RBFOX1

RNA Binding Fox-1 Homolog 1 (RBFOX1), also known as Ataxin 2-Binding Protein 1 (A2BP1), is a neuronal-enriched *trans*-acting splicing factor. RBFOX1 belongs to a protein family of RNA binding proteins, the RBFOX family. In mammals, two related splicing factors, RBFOX2 and RBFOX3, belong to the same family [172].

All three RBFOX proteins exert their function as splicing factors by recognizing the highly specific conserved consensus motif UGCAUG within introns, thanks to a single RNA-recognition motif (RRM). RBFOX genes sequence, along with the consensus sequence that they bind, is conserved from worms to mammals [173], highlighting their importance in splicing regulation. RBFOX consensus motifs can be localized both downstream and upstream the alternative spliced target exon. Depending on the localization of their binding sequences, RBFOX proteins either promote or repress the splicing of target alternative exons (Figure 18). More in detail, if the consensus motif is in the downstream intronic region, RBFOX splicing factors promote exon inclusion in the mature transcript. On the contrary, when RBFOX

proteins bind to consensus elements mapping in the upstream intron, they usually lead to exon skipping [172, 174-177].

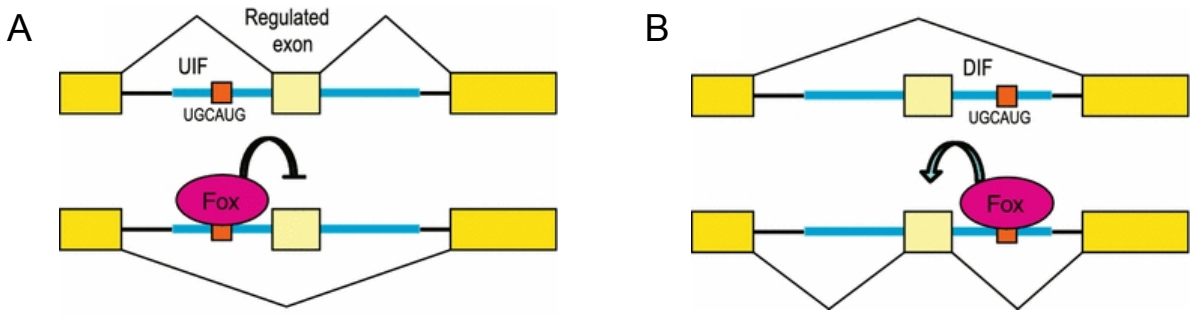

Figure 18. RBFOX proteins either promote or repress the splicing of target alternative exons. Schematic representation of alternative splicing regulation by RBFOX proteins. (A) When RBFOX factor binds to a consensus motif in upstream intronic flanking (UIF) region represses exon inclusion. On the contrary, (B) RBFOX protein promotes exon inclusion by binding the consensus element in downstream intronic flankin (DIF) region. Adapted from [172].

In mammals, RBFOX factors display different expression patterns. RBFOX1 is expressed in the brain, muscle and heart. RBFOX3 expression is restricted to neuronal tissues, while RBFOX2 is ubiquitously expressed. Consequently, considering that they all bind the same UGCAUG sequence, the function of these splicing factors is partially redundant especially in the brain where all the three RBFOX proteins are present and all of them regulate alternative splicing of important neurospecific transcripts [172].

Human *RBFOX1* gene (GenBank accession number NM_001142334) maps on the short arms of chromosome 16 (16p13.3) and encodes several protein isoforms, summarized in Figure 19, with different localization and interaction with regulatory proteins. As a matter of fact, *RBFOX1* is one of the longest genes in the human genome with a size of almost 1.7Mb. Its outstanding size is due to an extra-long 5' region containing multiple transcription start sites that allow *RBFOX1* gene to be transcribed through alternative promoters, generating several transcripts with alternative first exons [178-180]. Moreover, alternative splicing of the downstream coding sequence generates multiple isoforms with functional or non-functional RRM domain, brain- or muscle-restricted isoforms and alternative C-terminal domains that affect RBFOX1 protein localization [175, 176, 178]. RBFOX1 and RBFOX2 activity undergoes auto-regulation through the generation of a dominant negative isoform that, due to skipping of a 93bp-long exon in the RRM domain regulated itself by UGCAUG RBFOX proteins consensus motif, is not able to bind DNA [179]. In addition, RBFOX2 regulates the levels of its own mRNA by controlling the inclusion of two poison exons inducing transcript degradation by NMD pathway [181].

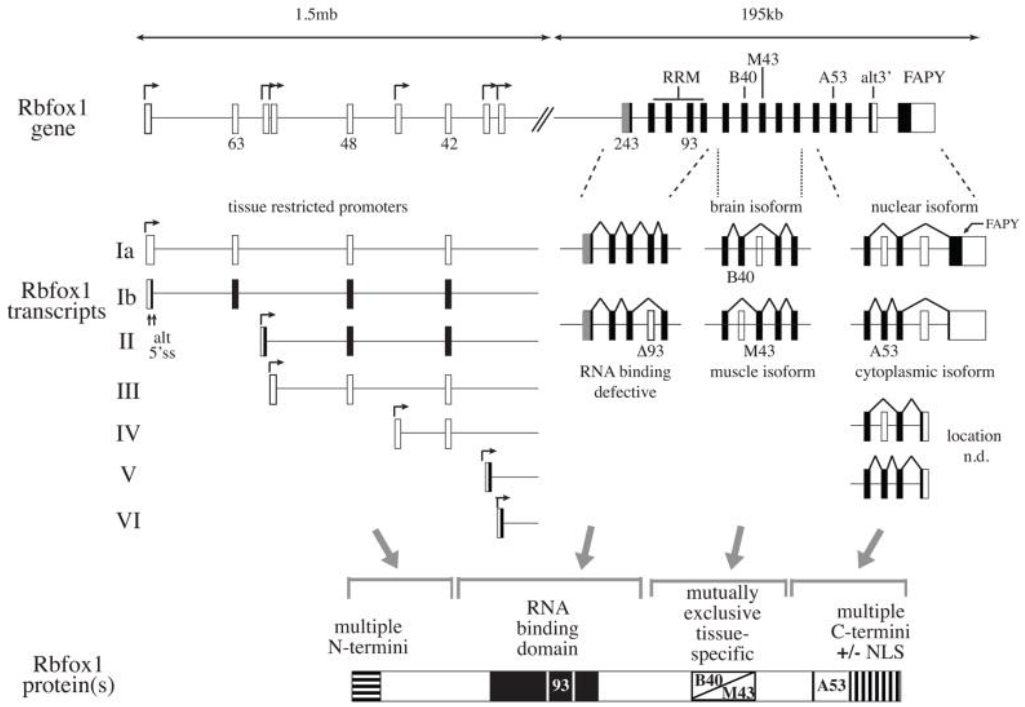

Figure 19. *RBFOX1* gene encodes different transcript and protein isoforms. The schematic representation display how RBFOX1 is transcriptionally and post-transcriptionally regulated to generate differential isoforms [179].

Featuring pronounced versatility, RBFOX1 proteins not only act as splicing factors. Indeed, all together, RBFOX1 isoforms control alternative splicing of neurospecific exons and microexons, mRNA stability and microRNA processing, ultimately regulating important neuronal processes such as neuronal development, maturation and differentiation, neuronal migration, axon and dendrite development, neuronal morphology and synaptic activity [182-189]. RBFOX1 is absent in mouse and human neural progenitors increasing its expression along with neuronal commitment [185]. Accordingly, RBFOX1 knockdown in neuronal progenitors during mouse embryos development leads to neuronal migration and axon growth defects [189]. Neuronal-restricted RBFOX1^{KO} mice display increased seizure susceptibility [182], suggesting that RBFOX1 activity is not restricted to brain development but also involves the regulation of complex neuronal function in the adult brain.

Particularly interesting is the cytoplasmic RBFOX1 isoform. It is generated by a frame-shift in 3' end of Rbfox1 transcript, due to the inclusion of the 53-bp long alternative spliced exon E19, indicated also as exon A53 because of its length (Figure 20). Nuclear RBFOX1 isoforms terminate with the nuclear localization signal (NLS) sequence, which encode for the tetrapeptide FAPY, and works as a splicing factor. The alternative C-terminal domain of the cytoplasmic RBFOX1 protein terminates with the peptide TALVP. Cytoplasmic RBFOX1 is

involved in the regulation of post-transcriptional gene expression by binding the consensus motif in 3'UTR of cytoplasmic mature transcripts and controlling mRNA stability and translation efficiency [175, 176], both positively and negatively regulating transcripts abundance [188].

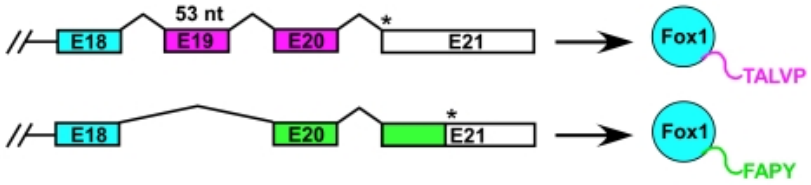

Figure 20. The inclusion of E19 generates a cytoplasmic RBFOX1 isoform. Schematic representation of RBFOX1 alternative splicing that generates nuclear (FAPY) and cytoplasmic (TALVP) isoforms (adapted from [190].

Interestingly, the balance between nuclear and cytoplasmic RBFOX1 isoforms is dynamic. Indeed, nuclear/cytoplasmic ratio can be regulated by neuronal activity through a splicing based mechanism. In vitro experiments carried out in neuronal-differentiated mouse P19 embryonal carcinoma cells show that upon chronic neuronal activation with KCl, RBFOX1 alternative splicing switches towards the repression of E19 inclusion favoring the production of nuclear RBFOX1 isoform and when depolarizing media is removed, cytoplasmic/nuclear ratio return to basal levels [190]. This environmentally responsive alternative splicing modulation seems to be part of an adaptive response ultimately aimed at recovering depolarization-evoked splicing changes [191, 192]. One of these events is the inclusion of *GRIN1* exon 5 in transcripts that encodes NMDA receptor subunit GluN1. Upon depolarization, exon 5 is skipped generating a GluN1 subunit without N1 cassette. Subsequently, as soon as the nuclear RBFOX1 isoform is synthesized, it homeostatically restores exon 5 inclusion [190]. Recently, it has been published that N1 cassette-containing GluN1 subunit negatively controls the extent of hippocampal Long Term Potentiation (LTP) and consequently learning and memory formation in mice [193]. Interestingly, GluN1 transcripts containing N1 cassette have been found to be reduced in the brain of individuals with autism spectrum disorder (ASD) [194]. In this light, homeostatic RBFOX1 increase at the level of excitatory neuronal nuclei, reinstating N1 cassette inclusion in GluN1, could be interpreted as a buffering mechanism that concurs to keeping LTP at adaptive levels upon neuronal activation.

Adopting a global neurophysiological view, it is worth noting how RBFOX1 also plays a role in the multisystem homeostatic adaptation to environmental stressful stimuli, being involved in molecular pathways downstream the homeodomain protein Orthopedia (Otp) [195]. In brief, stress-induced transcriptional activation of corticotropin releasing hormone (CRH) in PVN neurons of the hypothalamus requires the activation of the G_S protein-coupled receptor PAC1

bound to its ligand, the pituitary adenylate cyclase-activating polypeptide (PACAP) [196, 197]. The consequent increase of cAMP allows the recruitment of the phosphorylated form of cAMP Responsive Element Binding protein (pCREB) at the *crh* promoter [198, 199] in a complex with Otp [195]. Restraint stress paradigm in mice (and osmotic stress in zebrafish) showed that Opt is also present on *RBFOX1* promoter in a stress-dependent manner, promoting a rapid increase in RBFOX1 transcript levels upon stress [195]. RBFOX1 transcriptional activation has been proposed to be involved in the termination of CRH synthesis through the modulation of an alternative splicing-based mechanism involving PAC1 isoforms. In fact, RBFOX1 regulates the activity-dependent inclusion of alternative exon 14 in PAC1 mature transcripts [177, 190, 195], generating a longer PAC1 splice variant containing the "hop cassette" within the third intracellular loop (PAC1-hop) unable to transduce PACAP signals. The increase of RBFOX1-induced PAC1-hop isoform upon stress allows CRH levels to return to basal condition terminating HPA axis activation [195].

Coherently with its broad spectrum of functions and mutant mice phenotype, disruption in RBFOX1 regulatory network has been associated with different human pathologies. Indeed, RBFOX1 is implicated in several neurodevelopmental and neuropsychiatric disorders including autism spectrum disorder (ASD) [194], mental retardation [200], epilepsy [182], attention-deficit and hyperactivity disorder (ADHD) [201], bipolar disorder and schizophrenia [202]. Remarkably, RBFOX1 has been recently identified as one of the few genetic loci strongly associated to Major Depression Disorder (MDD) [203]. Last but not least, RBFOX2 has been found altered in several oncological conditions [204-208].

2 RATIONALE AND AIM OF THE PROJECT

Environmental stressful stimuli elicit a primary fast-acting stress response aimed at preparing the body to face the perceived threat and to foster the consolidation of stress-related memories with an adaptive valence. Engraving of stress-related memory traces requires glutamate release in different brain areas and the transactivation of plasticity-instrumental neuronal genes. In the secondary, slow-acting stress response, *homeostatic* mechanisms are engaged to restrain excessive reactions and to reinstate a psychophysical equilibrium. The epigenetic enzyme Lysine-Specific Demethylase 1 (LSD1) and its neuronal-specific dominant negative isoform neuroLSD1 play an important role in the homeostatic stress-response. Indeed, LSD1 transcriptional co-repressive activity temporarily increases through a splicing-based mechanism, which is directly aimed at buffering the wave of neuroplasticity-related genes activation and also contributes in the inhibition of glutamate release through the positive regulation of another homeostasis-directed mechanism orchestrated by the endocannabinoid system. Mounting evidence suggests that a disruption of stress-coping mechanisms, including LSD1 aberrant regulation, and endocannabinoid desensitization, might be coupled to maladaptive forms of plasticity underlying stress-vulnerability. Increased stress vulnerability fosters neuropsychiatric disorders such as anxiety and major depressive disorder. Long-term cognitive and emotional behavioral changes in response to reiterated environmental challenges arise in an individual-specific manner according to life experiences and to genetic predisposition. As a matter of fact, a spectrum of human responses to stress can be identified in the general population. Most individuals (resilient) are able to cope with threatening or socially stressful situation maintaining adaptive physiological and psychological functioning. However, individual responses can be variably active or passive, braver or fearful within adaptive thresholds. On the contrary, a minority of individuals (vulnerable) engages in maladaptive behavioral abnormalities developing sometimes stress-related neuropsychiatric disorders. Although neuropsychiatric disorders genetic heritability is a matter of fact, genetic underpinnings of stress vulnerability remain elusive. Major findings supporting the genetic basis of stress-susceptibility come from case-control association studies, allowing the identification of genetic variants associated to neuropsychiatric diseases. However, if little is known about how many nondeterministic genetic risk variants are involved in mental illness, even less has ever been clarified about how they exert their molecular effects.

The first aim of my PhD project was to deepen the role of LSD1 and neuroLSD1 in stress vulnerability through LSD1- and non-LSD1-related genetic evidence. Genome wide association studies showed the splicing factor RBFOX1 as one of the few genetic loci of major depressive disorder (MDD). We propose that one of the pathological mechanisms that justify RBFOX1 correlation with MDD may be related to its stress-homeostatic implication via regulation of LSD1 function. As a matter of fact, MDD is a pathological condition characterized by an altered response to environmental stimuli that, in turn, could be one of the main consequences of an aberrant regulation of homeostatic stress-response through LSD1 and neuroLSD1 splicing ratio. The first aim of my work was to provide evidence of a functional relationship between RBFOX1 and LSD1. In particular, I worked to functionally correlate RBFOX1 splicing activity to the sophisticated control mechanism that regulates LSD1/neuroLSD1 isoform ratio.

On the other hand, the genetic basis of stress resiliency or vulnerability could directly involve LSD1 gene. Thus, the second aim of my thesis work was to establish a strategy to genetically characterize *LSD1* gene, to verify the existence of human genetic variants that could affect the relative ratio between LSD1 and its dominant negative isoform neuroLSD1. My goal was to provide a proof of principle that LSD1 variants might predispose or protect from stress-related disorders. My in vitro identification of functionally different *LSD1* alleles, will allow to investigate *LSD1* contribution in disease onset within defined cohorts of patients including, but not limited to mood disorders and other stress-related psychopathologies.

The last part of my work was dedicated to investigate LSD1/neuroLSD1 relevance in the human brain. Up to now there was indeed no evidence of its possible implication in physiological or pathological human conditions. Notably, the characterization of LSD1 and neuroLSD1 transcriptional profile in human post-mortem brain samples represented a unique opportunity to implicate LSD1 isoforms in human brain physiology and pathology. In particular, we proved LSD1 involvement in physiological brain aging and psychiatric drift.

The study of LSD1- and non-LSD1-related genetic bases of human neuropsychiatric disorders along with LSD1/neuroLSD1 relevance, represents a chance to widen the knowledge related to splicing-based adaptive mechanism of stress-coping, already proposed as divergence point between engaging resiliency or vulnerability paths in mammals.

3 MATERIALS AND METHODS

3.1 Cell lines and cell culture conditions

In our experiments we used the following cell lines: SH-SY5Y and SK-N-BE human neuroblastoma cell lines, COV434 human ovarian granulosa tumour cell line, Neuro2A mouse neuroblastoma cell line, EFU1 and LCA1 lemur fibroblast cell lines and MMU macaca mulatta linfoblast cell line. They were cultured at 37°C in a humidified atmosphere of 5% CO_2 and 95% air according to standard procedures. SH-SY5Y was grown in EMEM (ECB2071L, Euroclone) and Ham's F12 (ECB7502L, Euroclone) 1:1 supplemented with 15% FBS (ECS0180L, Euroclone), 1% penicillin-streptomicin solution (ECB3001D, Euroclone), 1% GlutaMAX Supplement (35050-038, Gibco) and 1% Non-essential amino acids (ECB3054D, Euroclone). SK-N-BE, EFU1, LCA1 and MMU cell lines were cultured in RPMI (ECB9006L, Euroclone) supplemented with 15% FBS, 1% penicillin and streptomicin solution and 1% GlutaMAX Supplement. SK-N-BE, EFU1 and LCA1 grows in adhesion culture whereas MMU in suspension culture. Neuro2A and COV434 cell lines were cultured in DMEM high glucose (ECB7501L, Euroclone) supplemented with 10% FBS, 1% penicillin-streptomicin and 1% GlutaMAX Supplement.

3.2 Transfection

Cells were transfected using Lipofectamine LTX and PLUS Reagent (15338, Invitrogen). In addition to lipofectamine, the kit provides PLUS Reagent that favors liposomes formation. One day before transfection cells were seeded to be 70-90% confluent at the time of transfection. Specifically, we seeded $1x10^6$ cells/well in 6-well plates. The day after, cells were transfected using 1.25µg of DNA, 4µl of Lipofectamine LTX and 4µl of PLUS in serum-free culture medium in 250µl of final transfection volume. Transfection medium is replaced after 4 hours with complete medium. 24-48 hours after transfection cells were washed with PBS (ECB4053L, Euroclone) and collected for RNA or protein extraction.

We used the following expression plasmids: pCDNA3.1-Flag-nSR100 that contains the human full-length *nSR100* cDNA cloned into pCDNA3.1+ vector (V79020, Invitrogen) from the lentiviral pLDPuro-hsnSR100N (35172, Addgene); pCGN-HA-RBFOX1 that carries the human full-length *RBFOX1* cDNA of its nuclear isoform cloned into pCGN vector (53395, Addgene) from pENTR-A2BP1 (16176, Addgene). Control samples were transfected with the proper empty vector.

3.3 NMD inhibition

Nonsense-mediate decay (NMD) is a cytoplasmatic surveillance system that selectively degrades premature stop codon containing mRNA aimed at preventing formation of truncated and regulating the expression of physiological transcripts as RNA turnover mechanism. Common strategies to inhibit NMD take advantage of the fact that NMD is a translation-dependent mechanism. Indeed when ribosome reaches a premature stop codon it promotes the assembly of NMD machinery and transcript degradation. Cycloheximide (CHX) is a compound that inhibits eukaryotic protein synthesis by interfering with the translocation step. Consequently, CHX is used also as inhibitor of NMD pathway [209-211]. We inhibited NMD by CHX treatment as in [211]. Cells were plated at a density of $2x10^5$ cells/well in 6-well plates. After 72 hours, they were treated for 6 hours, unless differently specified, with CHX 100μg/ml. Untreated samples were incubated with the drug solvent (H_2O).

We also exploited a different strategy to inhibit NMD using an indole compound, NMDI-1 [212] that does not interfere with protein synthesis. NMDI-1 inhibits NMD avoiding the interaction between UPF1 and SMG5 (see section 4.1.1.3.1 for details). NMDI-1 issued from the Institute Curie–Centre National de la Recherche Scientifique compound library. We treated SH-SY5Y cells with 5μM NMDI-1 for 24 hours, according to literature procedures [212, 213]. Untreated samples were incubated with the drug solvent (DMSO).

After NMD inhibition treatments, cells were rinsed twice with PBS and total RNA extracted.

3.4 Inducible stable SH-SY5Y cell line generation

In order to analyze RBFOX1 role in regulating exon E8b inclusion into LSD1 mature transcript, we generated an inducible stable SH-SY5Y cell line that expresses RBFOX1 only in presence of doxycycline. To this aim we exploited the Tet-On system, a method of inducible gene expression where transcription is turned on only in the presence of the antibiotic tetracycline or one of its derivatives such as doxycycline. In Tet-On system, a tetracycline transactivator protein (tTA) binds to tetracycline responsive element (TRE) on DNA only in presence of tetracycline/doxycycline and in doing so it activates transcription.

To generate SH-SY5Y inducible stable cell line, we used the following plasmids kindly donated by Professor Roberta Benfante of the University of Milan: (1) pTet-On (K1621-A, Clontech), carrying TetR gene coding for tTA protein and NeoR gene to confer resistance to G418; (2) pTRE2hyg-Luc vector carrying TRE motif upstream Luciferase cDNA sequence and HygR gene to confer resistance to hygromycin; (3) pTRE2hyg vector (6255-1, Clontech) used to clone

human HA-*RBFOX1* cDNA sequence downstream TRE motif and CMV promoter and generate pTRE2hyg-HA-RBFOX1 plasmid.

We produced pTRE2hyg-HA-RBFOX1 by cloning HA-RBFOX1 sequence, obtained through high fidelity PCR from pCGN-HA-RBFOX1, into pTRE2hyg vector using PvuII (R0151T, New England BioLabs) and SalI (R3138S, New England BioLabs) restriction enzymes. The resulting plasmid was sequenced to exclude random mutations and digested with proper restriction enzymes to verify the correct orientation of the insert.

In order to generate an inducible stable SH-SY5Y cell line that expresses RBFOX1 only in presence of doxycycline, it is necessary to integrate into SHSY5Y genome both TetR and TRE followed by HA-*RBFOX1* sequence. To this aim, we firstly generated a SH-SY5Y cell line stably transfected with pTet-On plasmid. SH-SY5Y cells were transfected with pTet-On. After 48 hours, transfected cells were split at lower concentrations in complete medium with tetracycline-free serum supplemented with 400 μg/ml G418, according to G418 toxicity curve performed previously, in order to select cells that had integrated exogenous DNA into their genome. SH-SY5Y pTet-ON clones were collected and expanded into separate wells. We used pTRE2hyg-Luc construct to select the tTA-expressing clone displaying the best response to doxycycline. Each clone transfected with pTRE2hyg-Luc and pRL-Renilla (E2241, Promega) and after 4 hours treated with 1μg/ml doxycycline. Transfected but untreated cells were used as control. 24 hours after transfection, cells were collected and underwent firefly/renilla luciferase assay using Dual-Luciferase Reporter (DLR) Assay System (E1910, Promega) performed according to manufacturer's protocol. Luminescent signal was quantified using GloMax Discover luminometer (Promega). Then, we performed a stable transfection of the chosen SH-SY5Y pTet-On clones with pTRE2hyg-HA-RBFOX1 construct. Cells were grown in complete medium with tetracycline-free serum supplemented with 400μg/ml G418 and 100μg/ml hygromycin, according to hygromycin toxicity curve. Each SH-SY5Y pTet-ON pTRE2hyg-HA-RBFOX1 clone was treated with 1μg/ml doxycycline for 24 hours and screened for HA-RBFOX1 expression by western blot analysis using a primary antibody against HA-tag. Untreated controls were incubated with the drug solvent (H_2O).

3.5 Total RNA extraction, RT-PCR and qRT-PCR

Total RNA extraction from cells and tissue samples was performed using TRIzol reagent (15596026; Invitrogen) according to manufacturer's protocol. Cells were collected and lysed directly in cold TRIzol reagent. Human and mouse tissue samples were homogenized in a glass-potter in cold TRIzol reagent. To measure RNA concentration and purity we used NanoDrop 1000 spectrophotometer (Thermo Scientific). In order to remove any residual DNA, RNA was treated with RNase-free DNase set contained in the reverse transcription reaction kit. 1μg of total RNA was reverse transcribed using Maxima H Minus cDNA Synthesis Master Mix with dsDNase kit (M1682; Thermo Scientific) in 20μl of cDNA.

RT-PCR was conducted on 1μl of cDNA using GoTaq G2 Flexi DNA Polymerase (M7805, Promega) following standard PCR protocol. PCR products were separated on 2% agarose gels. Since endogenous E8b-including LSD1 mRNA is present in a very low amount, we exploited touchdown PCR strategy in order to increase amplification specificity and sensitivity. Additionally, we run 50 cycles of amplification in order to detect it. E8b expression was quantified using UVITEC Gel Documentation System Essential V6 (Cambridge) and normalized over a proper housekeeping gene. Primer sequences used for RT-PCR experiments are reported in Table 1.

Quantitative RT-PCR (qRT-PCR) analysis was performed on QuantStudio 5 Real-Time PCR System (A28575, Thermo Fisher Scientific) using Power SYBR Green PCR Master Mix (A25742, Applied Biosystem). Gene expression levels were calculated based on the fold change method ($2^{-\Delta\Delta Ct}$). Target genes expression was normalized on the proper housekeeping gene chosen using the Microsoft Excel-based tool BestKeeper [214]. Primers used for qRT-PCR are indicated in Table 2.

Table 1. Primers for RT-PCR

Name	Sequence
LSD1 RT-PCR	
h/mmu/lemurLSD1_Ex2_Fw	GTGAGCCTGAAGAACCATCG
h/mmu/lemurLSD1_Ex9_Rev	CTACCATTTCATCTTTCTCTTTAGG
mLSD1_Ex2_Fw	AGTGAGCCGGAAGAGCCGTCTG
mLSD1_Ex9_Rev	CTACCATTTCATCTTTTTCTTTTGG
LSD1-E8b upstream RT-PCR	
h/mmuLSD1_E8b_Rev	CTGAGGACCTTCCAAGAATAAGG
h/mmu/mLSD1_E7_Fw	GCAAAGGAAACTATGTAGC
lemurLSD1_E8b_Rev	CTGAGGACCCTTCAGAGTAAGG
lemurLSD1_E7_Fw	GCAAGGGAAACTACGTAGC
mLSD1_E8b_Rev	GTTACCTGCTCAAGGATGA
LSD1-E8b downstream RT-PCR	
h/mmu/lemurLSD1_E8b_Fw	CTTTGAGGGGAAGCCAGATACC
h/mmu/lemur/mLSD1_E10_Rev	TCTTCCAATGTTCAATCTGCT
mLSD1_E8b_Fw	TCATCCTTGAGCAGGTAAC
other RT-PCR	
hβ-actin_Fw	CCTTCCTGGGCATGGAGTCC
hβ-actin_Rev	AATGCCAGGGTACATGGTGGG
hmrRPSA_Fw	CAACAACAAGGGAGCTCACTC
hmrRPSA_Rev	CTTCTCAGCAGCAGCTGCT
hABI1_Fw	TTCCCAGTATGGCACAATGA
hABI1_Rev	CCAAGCAGGATCCCCATCTGC
hNUMA1_Fw	GGAGCTGGAGGTGATGACTGC
hNUMA1_Rev	CTTCAGCTTCTGCTGCTGCAC
hRPLP0_real_Fw	CATTCTCGCTTCCTGGAG
hRPLP0_real_Rev	CTTGACCTTTTCAGCAAGTGG
hRbfox1_E17_Fw	TATCAAGAGCCTGTGTATGGC
hRbfox1_E20_Rev	AGCAAGTGCGTGGTGGTAGGG

Table 2. Primers used for qRT-PCR

Name	Sequence
hLSD1_E15_Fw	GCTAATGCCACACCTCTCTCA
hLSD1_E16_Rev	CCTGTCGCACTGCTGTATTCA
hmLSD1_E8a_real_Fw	AGCTGACACTGTCAAGGTTC
hLSD1_E8a_real_Fw	GACACTGTCAAGGTTCCTAAAG
hLSD1_w/oE8a_real_Fw	ACGGACAAGCTGTTCCTAAAG
hLSD1_Ex9_real_Rev	GGACACAGGCTTATTATTGAGG
hmr_nSR100_Fw	GGGGTGTAATCACTGGGTCG
hmr_nSR100_Rev	GAGCTGGTTTGCGTGGAGGG
hmrNOVA1_real_Fw	GCCGGACTCGCGGAAAAG
hmrNOVA1_real_Rev	TGAACAATTGTCTGTCCTCC
hmRBFOX1_real_Fw	AGCCCCAGACACAACCTTC
hmRBFOX1_real_Rev	ATTTCTCCCTCGCCCTGTC
hPRKCA_NMDsens_Fw	TCCCCTGTATTGCTAGTCTGC
hPRKCA_NMD_Rev	TGAACTTGTGCTTGCTCCTG
hmrRPSA_Fw	CAACAACAAGGGAGCTCACTC
hmrRPSA_Rev	CTTCTCAGCAGCAGCTGCT
hRPLP0_real_Fw	CATTCTCGCTTCCTGGAG
hRPLP0_real_Rev	CTTGACCTTTTCAGCAAGTGG
mGJA1_real_Fw	GAAGTACCCAACAGCAGCAG
mGJA1_real_Rev	CTCCGGCCGTGGAGTAGGCT
mLSD1_real_Fw	GCCTCAGCAGACACAGAAGG
mLSD1_real_Rev	TGTTGTAAGGCGCTTCCAGC
mHNRNPL_real_Fw	GGTCGCAGTGTATGTTTGATG
mHNRNPL_real_Rev	GGCGTTTGTTGGGGTTACT

3.6 Splicing analysis by rqfRT-PCR

We used relative quantity fluorescent PCR (rqfRT-PCR) to measure relative amount of each splicing isoform, as described in [91]. RqfRT-PCR is based on target transcripts amplification using a couple of primers able to amplify all the expected isoforms in a single reaction. Since it relies on a forward or reverse primer conjugated with a fluorochrome, it is a semi-quantitative method. In our splicing analysis we used forward primers conjugated with 6-Carboxyfluorescein (6-FAM) and a reverse unmodified one. PCR products were mix together

with GeneScan 500 ROX dye Size Standard (4310361, Applied Biosystems) and separated on the basis of their length by capillary electrophoresis under denaturing conditions. Capillary electrophoresis was performed using 3130xl Genetic Analyzer (Applied Biosystems). The amount of each amplified product was quantified using GeneMapper software. More in details, the final outcome consists in an electropherogram containing as many peaks of different length as the number of alternative spliced isoforms. The height of each peak represents the fluorescence unit level (relative fluorescence units, RFU) and it is directly proportional to the relative amount of the corresponding PCR product. Relative amount of each splicing isoform is reported as relative percentage with respect to the sum of all isoforms. The sequences of primers used for rqfRT-PCR are indicated in Table 3.

Table 3. Primers used for rqfRT-PCR

Name	Sequence
Minigene_A23_Fluo_Fw	[6-FAM]CAACTTCAAGCTCCTAAGCCACTGC
Minigene_Bra_Rev	CACCAGGAAGTTGGTTAAATCA
hLSD1_E7_fluo_Fw	[6-FAM]GCAAAGGAAACTATGTAGC
LSD1_E8b_Rev	CTGAGGACCTTCCAAGAATAAGG
hLSD1_Ex2_fluo_Fw	[6-FAM]GTGAGCCTGAAGAACCATCG
hLSD1_Ex9_Rev	CTACCATTTCATCTTTCTCTTTAGG

3.7 Minigene splicing assay

In order to study exon E8a and exon E8b splicing in LSD1 mature transcripts we exploit the minigene splicing report system [215]. It allows the identification of *cis*- and *trans*-acting regulatory elements that are involved in the modulation of alternative spliced exons. Minigene splicing assay is based on transfection of pBSplicing constructs, obtained by cloning a minigene cassette into pBlueScript II KS(+) vector. The minigene cassette is a hybrid construct containing exons from α-globin and fibronectin under the control of the α-globin promoter and SV40 enhancer sequences. A unique NdeI restriction site inside the intronic region between two fibronectin exons permits the cloning of a genomic region of interest containing one or more exons and their *cis*-acting regulatory elements. Inside the cell, the minigene cassette carrying the exon of interest is transcribed and spliced by cell machinery to generate a minigene chimeric transcript that may or may not contain the alternative exon

under analysis. Minigene-derived transcripts are not translated since translation start codon has been deleted [215].

Specifically, we generated the fragment of interest by PCR on human genomic DNA using primers carrying the selected restriction enzyme consensus sequence. We used Platinum Taq DNA Polymerase High Fidelity (11304, Invitrogen) in order to avoid random mutations. We cloned the genomic region of human or mouse LSD1 gene in pBSplicing plasmid using the unique NdeI restriction site located in the intron between fibronectin exons. Escherischia coli TOP10 competent cells were used for transformation by electroporation. After purification performed using Plasmid Midi kit (12143, QIAGEN), plasmid DNA were sequenced to exclude random mutations and digested with proper restriction enzymes to verify the correct orientation of the insert. Subsequently, we performed the splicing assay by transfecting minigene constructs in SH-SY5Y or Neuro2a cell lines. The minigenes were transfected, using Lipofectamine LTX as described previously. 48 hours after transfection, RNA was extracted and rqfRT-PCR was carried out using fluorescinated forward and unmodified reverse primers that anneal on minigene exons. We ran the PCR amplicons on capillary gel electrophoresis in order to discriminate different minigene splicing products thanks to their different length.

We generated the minigene constructs used in this thesis as follows:

- MG2700: The minigene construct used for the investigation of RBFOX1 role as *trans*-acting regulatory LSD1 alternative splicing was obtained by cloning the 2749 nucleotide-long human genomic region chr1:23,065,790-23,068,538 in pBSplicing plasmid. This region of interest contains exon E8a sequence and its upstream conserved intronic region of almost 400bp along with the full-length downstream intron including two identified RBFOX1 binding sites. Because this genomic region contains a NdeI restriction site we cloned it into pBSplicing NdeI site thanks to the compatibility between NdeI (R0111S, New England BioLabs) and AseI (R05265S, New England BioLabs).
- MG1300: To assess the relationship between neuroLSD1 splicing and three common SNPs identified in exon E8a flanking intronic region we generated MG1300 HAPLO1, carrying one of the four possible haplotypes. We cloned the 1393 nucleotide-long genomic region chr1:23,065,177-23,066,569 of human *LSD1* gene in pBSplicing plasmid using NdeI restriction sites. In order to obtain minigenes carrying the other haplotypes, exon E8a intronic regions cloned into the minigene cassette were mutagenized in SNP1 (MG1300 HAPLO2), SNP2 (MG1300 HAPLO3) or SNP3 (MG1300 HAPLO4) positions.

3.8 Sanger sequencing

Sanger sequencing was exploited in cloning experiments and E8b characterization. Before sequencing we purified PCR templates using Wizard SV Gel and PCR Clean-Up System (A9281, Promega). Sequencing analysis was conducted on 10ng of purified PCR products or 200ng of plasmid using BigDye Terminator v3.1 Cycle Sequencing Kit (4337455, Applied Biosystems). Sequencing reaction products were purified with Montage SEQ_{96} Sequencing Reaction Cleanup Kit (LSKS09624, Millipore) and underwent capillary electrophoresis on 3130xl Genetic Analyzer (Applied Biosystems). Electropherograms were visualized and analyzed with SeqMan Pro package of DNASTAR Lasergene (DNASTAR). Primer sequences used for E8b characterization are reported in Table 1. To exclude random mutations, pTRE2hyg-HA-RBFOX1, MG2700 and MG1300 (carrying the four haplotypes) plasmids were sequenced using forward and reverse primers annealing on vector sequence and within insert sequence (not reported).

3.9 Preparation of Protein Extracts and Western Blot Analyses

Total protein extracts from inducible stable SH-SY5Y cell line were obtained lysing the cells directly with electrophoresis sample buffer. Cells, seeded in 6-well plate, were washed in cold PBS and scraped from culture plate in 300μl of Laemmli's sample buffer 1X (62.5 mM Tris pH 6.8, 2% SDS, 10% Glycerol, 0.1% bromphenol blue) supplemented with 10% 2-mercaptoethanol (M6250, Sigma Aldrich) immediately before use. Cell lysate were stored at -80°C until use. For western blot analysis samples were boiled for 10 minutes and then sonicated with a Bandeline Electronic Sonicator. 30μl of protein extract were run on a SDS-9% polyacrylamide gel along with Color Prestained Protein Standard, Broad Range (11-245 kDa) (P7712S, Biolabs) and then transferred onto 0.45μm nitrocellulose membranes (1620115, Bio-Rad). Blots were blocked 1 hour at room temperature with 5% non-fat dry milk (M7409, Sigma Aldrich) in TBS-Tween buffer (50 mM Tris base, 150 mM NaCl adjusted to pH 7.6 with HCl and 0.3% Tween-20). Then, they were incubated over night at 4°C with antibodies against the proteins of interest and 1 hour at room temperature with the proper secondary antibody. Primary antibodies are reported in Table 4. Blots were incubated with ECL Select Western Blotting Detection Reagent (RPN2235, Amersham) and bands were detected and quantified with UVITEC Alliance Mini HD9 (Cambridge). GAPDH was used as control protein for normalization.

Table 4. Primary and secondary antibodies used for Western Blot analysis

Antibody	Dilution	Brand	RRID
HA-probe (F-7) mouse mAb	1:5000	Santa Cruz Biotechnology	RRID:AB_627809
LSD1 (C69G12) rabbit mAb	1:1000	Cell Signaling Technology	RRID:AB_2070132
GAPDH (D16H11) rabbit mAb	1:1000	Cell Signaling Technology	RRID:AB_10622025
Anti-Mouse IgGκ BP-HRP	1:2000	Santa Cruz Biotechnology	RRID:AB_2687626
Anti-Rabbit IgG, HRP-linked whole Ab	1:3500	GE Healthcare	RRID:AB_772206

3.10 Acute Social Defeat Stress

We performed Acute Social Defeat Stress (ASDS) as described in [44]. During ASDS, ex-breeder CD1 aggressor mice were used to defeat 2-month-old C57BL/6N wild-type mice in a two-phase psychosocial stress paradigm. Firstly, the experimental C57BL/6N mouse is forced in a direct interaction with an aggressor CD-1 mouse for 5 minutes. During the second phase, mice were divided through a perforated Plexiglas barrier and kept in visual and olfactory interaction for 7 hours to allow the psychological stress phase. Importantly, to ensure the success of the psychosocial stress paradigm, we performed an aggressive behavior screening of CD1 mice. Control mice were manipulated, housed in opposite sides of the Plexiglas divider and roomed in a different place to avoid conditioning. At the end of the psychosocial stress phase, control and experimental mice were sacrificed and tissues were collected for molecular analyses.

3.11 Chronic Social Defeat Stress

We employed a modified protocol of Chronic Social Defeat Stress (CSDS) [109], adapted from the one described in [20]. CD1 aggressor mice defeated 2-month-old C57BL/6N wild-type mice for 5 minutes a day over 10 consecutive days. Experimental mice were exposed to a novel CD1 aggressor each day in order to avoid habituation and reduce variability. After physical interaction, mice were kept in sensory interaction for 7 hours, separated by a perforated Plexiglas divider. Then, experimental mice were moved back to their home cage to allow recover. Control mice, roomed in a different place, were manipulated and housed in opposite sides of the Plexiglas divider for 10 days similarly to experimental ones. This paradigm of repeated psychosocial stress is validated to induce long-lasting depression-like behaviors as anxiety and social-avoidance. Tissues collection occurred the 10^{th} day, before and after the 7-hour long psychosocial phase. To discriminate between mice in which

neuroLSD1 modulation occurred from the ones in which did not (responders and non-responders respectively), we set a threshold: since no control mice had a neuroLSD1 relative percentage under 40% we decided that 40% would be the cut-off percentage to assess whether neuroLSD1 modulation had occurred.

3.12 Experimental animals

For our in vivo experiments we used 2-month-old male C57BL/6N (RRID:IMSR_CRL:027) and 3-month-old male CD1 (RRID:IMSR_CRL:22). Animals were housed in a specific pathogen-free animal facility, at controlled temperature (20–22°C) with free access to food and water in a 12-hr light/dark cycle. Mice were kept in an enriched environment and individually caged only during testing periods. Animals were killed (decapitation) without anesthetic drugs to limit molecular interference with the processes analyzed.

All experimental procedures involving animals followed the Italian Council on Animal Care guidelines (Legislative Decree no. 26, March 2014) and European regulations (2010/63/ UE) and were approved by Italian Ministry of Health (no. 275/2015 and 322/2018). Every effort was made to accomplish to the "3R" regulations, that is, Reduction of animal number, Refinement of experimental procedures, Replacement with simpler research models.

3.13 Human hippocampal samples

Postmortem hippocampal tissues from subjects of both genders and different age were collected during routine autopsy at Arcispedale Maria Nuova in Reggio Emilia, Italy, (University of Milan Ethic Committee protocol n. 40-18 and Territorial Ethic Committee AUSLRE protocol n. 2019/0004645) and stored at -80°C. Cerebral tissues from old and very old individuals were kindly donated by Professor Marco Venturin (University of Milan) and were obtained from MRC London Neurodegenerative Diseases Brain Bank, South West Dementia Brain Bank and Newcastle Brain Tissue Resource.

To date, we collected 9 female and 21 male hippocampal samples from 21- to 96-year-old subjects and 7 samples from individuals who committed suicide with ages ranging from 22 to 90 years old. Sex, age, cause of death, post-mortem delay (PMD) and clinical records were available for each donor. Since it is known that pre-mortem events impact on extracted RNA quality [216-219], we scored the agonal state of the donors using a three-point classification based on the cause of death, adapted from [220]. Agonal state is defined as agonal conditions that occur immediately before death, including coma, hypoxia, multiple organ failure and intoxication [217]. Considering agonal state definition, clinical records and the cause of death

we determined agonal state score as follows: (1) sudden death of apparently healthy individuals, such as accident and ischemic heart disease; (2) unexpected death of ill individuals, that could be classified neither rapid nor slow; (3) slow death due to a pathology with a long terminal phase, such as cancer, chronic pulmonary diseases, intoxication and sepsis. Regarding suicidal victims agonal state, we categorized them as 2 considering that they all died for asphyxiation, which is neither a sudden death nor a prolonged illness conditions.
Post mortem delay (PMD) never exceeded 80 hours, which is within the time window previously validated as a bona fide interval of RNA integrity in the brain [221].
Hippocampal sections were homogenized using a glass potter in cold and RNA was extracted with TRIzol and processed as described above. The quality of extracted RNA was assessed measuring RNA integrity number (RIN), using RNA 6000 Nano Chips on Agilent 2100 bioanalyzer. Not all human hippocampal samples were available for all the performed analyses. In qRT-PCR RPL13 was used as stable housekeeping gene, assessed using Microsoft Excel-based tool BestKeeper [214].

3.14 Statistical analyses

Statistical analyses were performed using PRISM 8.0 software (GraphPad) with unpaired Student's *t* test and one-way Anova Tukey *post hoc* test for single and multiple comparisons respectively. P value < 0.05 was considered statistically significant.

4 RESULTS

4.1 GENETIC BASIS TO IMPLICATE LSD1 IN STRESS-RELATED NEUROPSYCHIATRIC DISORDERS

It is now widely recognized that stress exposure is one of the major risk factor for neuropsychiatric disorders. However, behavioral outcome in response to environmental challenges varies in an individual-specific manner, accordingly not only to life experiences, but also to genetic predisposition in the frame of genotype x environment interactions (GxE) [222]. Rather than being determined by single gene mutations with a strong effect and high penetrance, genetic basis of stress-susceptibility is seemingly influenced by multiple hypomorphic genetic variants, involved in a complex functional interaction with one another that ultimately affects environmental risk factor sensitivity [223].

The splicing factor RBFOX1 has been recently identified as one of the few genetic loci significantly associated to major depressive disorder (MDD). In the following paragraphs, I will show how LSD1 activity is regulated by the splicing factor RBFOX1. Representing targets of a splicing factor genetically associated to MDD, we reasoned that LSD1 and neuroLSD1 modulation could play an important role in the establishment of stress resiliency or vulnerability.

On the other hand, another genetic source of stress resiliency or vulnerability could involve *LSD1* gene also independently on its functional interactions with RbFOX1. Indeed, *LSD1* high level of interspecies conservation and intraspecies constraint, together with the fact that few disease-associated LSD1 mutations exist [114, 115], would indicate that evolutionary forces act to preserve LSD1 and neuroLSD1 functions. In this frame, and being LSD1 alternative splicing modulation highly relevant to stress coping, single nucleotide variants within intronic regions, definitely better tolerated, could influence LSD1 transcripts regulation.

In the second part of this chapter, I will describe how we gained information on the specific effect played by human SNPs present at the level of exon E8a flanking intronic regions, on *LSD1* exon E8a splicing (and therefore neuroLSD1 expression). In particular, we explored the hypothesis that specific SNPs combinations might generate different *LSD1* alleles possibly predisposing to a higher (or lower) neuroLSD1 level in vitro. If human LSD1 genetic variants do contribute in setting different basal neuroLSD1 levels, a novel functional basis of resiliency

and vulnerability to stress-related neuropsychiatric diseases could be proposed, given the importance of LSD1/neuroLSD1 splicing regulation in environmental stress response.

4.1.1 RBFOX1-mediated exon E8b splicing triggers Nonsense-mediated decay: a new higher primate-restricted mechanism of LSD1 and neuroLSD1 regulation

4.1.1.1 RBFOX1 regulates LSD1 alternative splicing: exon E8b discovery

RNA binding protein Fox-1 homolog 1 (RBFOX1) is a neuronal-enriched splicing factor implicated in neuronal development and maturation and predicted to regulate neuronal splicing networks already clinically implicated in neurodevelopmental disease [194]. A GWA meta-analysis of almost 10 million SNPs in seven cohorts of major depressive disorder (MDD) compared to controls identified 44 independent genetic loci as risk variants strongly associated with MDD. Among them, two independent genetic associations pointed out RBFOX1 as a relevant gene for MDD susceptibility [203]. In the hippocampus, stress-induced intensification of LSD1 repressive activity through a splicing-based mechanism contributes to stress response termination [44, 109]. Being part of an epigenetic homeostatic process finally aimed at restraining long-lasting behavioral changes, one of the main consequences of an unbalance LSD1/neuroLSD1 splicing ratio modulation could be an altered response to environmental stimuli that, in turn, characterizes MDD pathological condition. Hence, we asked whether one of the possible mechanism through which RBFOX1 is involved in stress response and consequently in stress susceptibility may be related to neuroLSD1 alternative splicing regulation.

Processes underlining the control of neuroLSD1 alternative splicing have already been partially dissected: exon E8a inclusion is under the positive control exerted by two neurospecific splicing regulators, nSR100 and NOVA1 and under negative control of a *cis*-acting palindromic sequence. Nevertheless, we know from literature that at least 15% of NOVA1 targets may be under NOVA1 and RBFOX1 combinatorial control, suggesting a synergistic action on their shared target [224]. As a consequence, we decided to investigate whether neuroLSD1 splicing could be regulated also by RBFOX1 splicing factor.

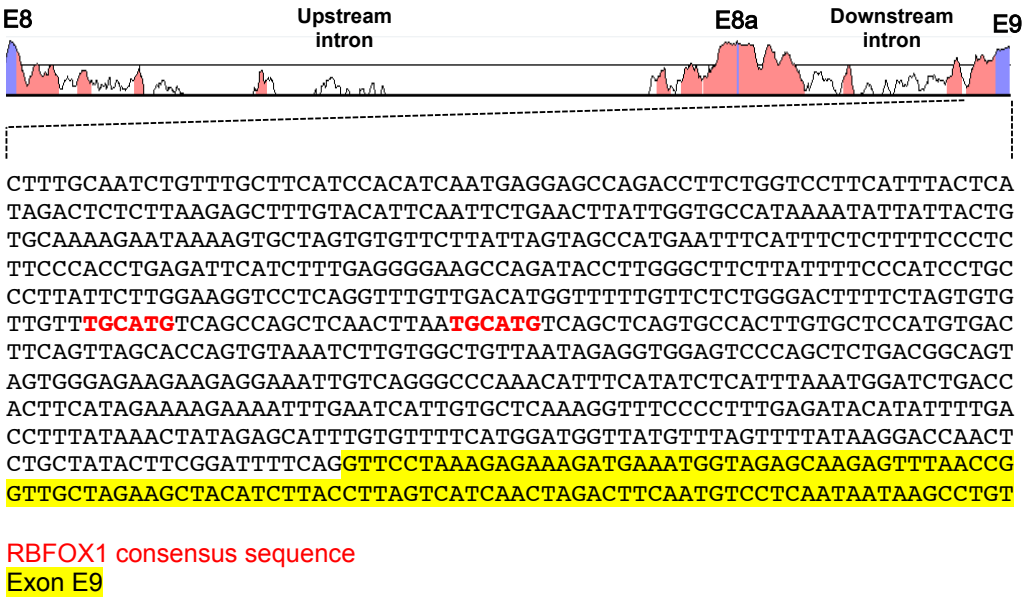

Figure 21. RBFOX1 consensus sequence localization in E8a downstream intronic region. The highly conserved region at the end of exon E8a downstream intron contains two RBFOX1 consensus sequences (in red). First 110 nucleotides of exon E9 are highlighted in yellow.

RBFOX1 exerts its function as alternative splicing factor by recognizing the conserved consensus motif (U)GCAUG within introns. We identified two RBFOX1 consensus sequence at the end of the highly conserved exon E8a downstream intronic region (Figure 21).

In order to assay RBFOX1 involvement in E8a splicing regulation we exploited the minigene report system. The final minigene construct used for this functional study was obtained cloning the 2749 nucleotide-long human genomic region showed in Figure 22 in pBSplicing plasmid. This region of interest contains exon E8a sequence and its upstream conserved intronic region along with the full length downstream intron including the two identified RBFOX1 binding sites (chr1:23,065,790-23,068,538). We called it MG2700.

Figure 22. MG2700 generation. VISTA conservation graph for human exon E8a flanking introns, showing high degree of conservation among mammalian species. LSD1 genomic region that was cloned into minigene cassette is indicated with a box (chr1:23,065,790-23,068,538).

We co-transfected MG2700 reporter plasmid with or without RBFOX1 and nSR100 expression plasmid, pCGN HA-RBFOX1 and pCDNA3.1 Flag-nSR100, in SH-SY5Y cell line. Control samples were transfected with minigene and the proper empty vector. 48 hours after transfection, RNA was extracted and rqfRT-PCR was carried out using fluorescinated forward and

unmodified reverse primers that anneal on minigene exons. We ran the PCR amplicons on capillary gel electrophoresis in order to discriminate E8a presence in minigene chimeric transcripts thanks to their different length. The results are reported in Figure 23, showing GeneMapper outcome of capillary gel electrophoresis. The electropherogram consists in one or more peaks of different length and different fluorescence intensity that is directly proportional to the quantity of each splicing product. The transfection of MG2700 alone revealed that E8a inclusion occurred and the exon E8a-containing minigene splicing product (MG+E8a, 258 bp) was detectable along with the constitutive one (MG, 246 bp) and accounted for 7% of total minigene-derived transcripts.

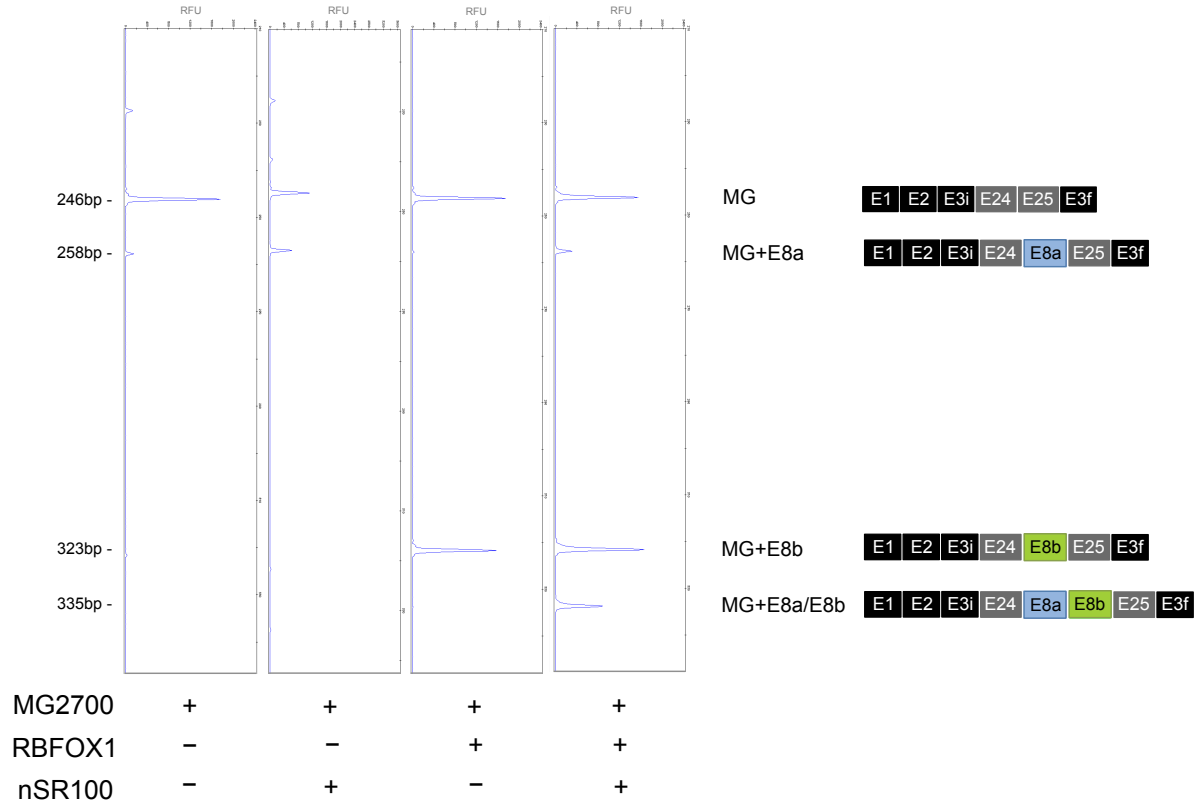

Figure 23. RBFOX1 regulates the inclusion of a new LSD1 cryptic exon. Minigene splicing assay performed in SH-SY5Y cell line transfected with MG2700 alone or together with nSR100 and/or RBFOX1 expression plasmid.

When nSR100, the main LSD1 E8a splicing positive regulator, is overexpressed in SH-SY5Y cells exon E8a inclusion increases to 30%. Interestingly, an unexpected result was obtained when MG2700 was co-transfected with pCGN HA-RBFOX1. We observed that RBFOX1 overexpression does not affect E8a inclusion while is able to induce the exonization of an intronic region of *LSD1* gene into minigene-derived transcripts, where an extra peak of 323 bp was identified. Specifically, the splicing factor RBFOX1 induced an unpredicted splicing event of a 77-bp long intronic portion of LSD1 located between exon E8a and E9. For this reason, we called it exon E8b. After RBFOX1 overexpression, in SH-SY5Y cells we observed an inclusion of

exon E8b (MG+E8b) in 47% of the mature minigene transcripts. Moreover, when both RBFOX1 and nSR100 are overexpressed together with MG2700 an additional splicing product, 335 bp-long, is detectable corresponding to the minigene transcript including both exon E8a and exon E8b (MG+E8a/E8b). Therefore, in a neuronal context, RBFOX1 regulates E8b inclusion in both E8a-containing and non-containing minigene transcripts. The inclusion frequency of E8b in minigene-derived transcripts with or without E8a depends on the amount of MG and MG+E8a. As I showed before, in SH-SY5Y cells MG and MG+E8a are not equally represented among minigine splicing products thus MG+E8a/E8b isoform amount is inevitably lower than MG+E8b.

In order to obtain exon E8b sequence and understand the exact location of this new cryptic LSD1 exon we directly sequenced the 335bp-long PCR fragment dissected from the agarose gel, using the forward primer on E8b-including amplicons. We identified exon E8b sequence in a highly conserved region at the end of the exon E8a downstream intron, upstream to the *cis*-acting RBFOX1-binding sequences that probably promote its inclusion in mature transcript (Figure 24).

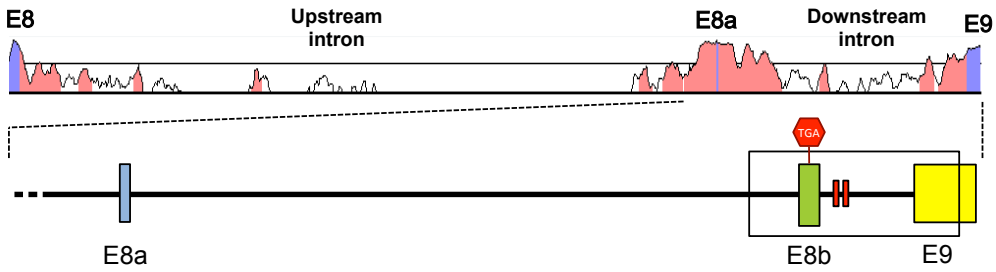

CTTTGCAATCTGTTTGCTTCATCCACATCAATGAGGAGCCAGACCTTCTGGTCCTTCATTTACTCA
TAGACTCTCTTAAGAGCTTTGTACATTCAATTCTGAACTTATTGGTGCCATAAAATATTATTACTG
TGCAAAAGAATAAAAGTGCTAGTGTGTTCTTATTAGTAGCCATGAATTTCATTTCTCTTTTCCCTC
TTCCCACCTG**AG**ATTCATCTT**TGA**GGGGAAGCCAGATACCTTGGGCTTCTTATTTTCCCATCCTG
CCCTTATTCTTGGAAGGTCCTCAG**GT**TTGTTGACATGGTTTTTGTTCTCTGGGACTTTTCTAGTGT
GTTGTT**TGCATG**TCAGCCAGCTCAACTTAA**TGCATG**TCAGCTCAGTGCCACTTGTGCTCCATGTGA
CTTCAGTTAGCACCAGTGTAAATCTTGTGGCTGTTAATAGAGGTGGAGTCCCAGCTCTGACGGCAG
TAGTGGGAGAAGAAGAGGAAATTGTCAGGGCCCAAACATTTCATATCTCATTTAAATGGATCTGAC
CACTTCATAGAAAAGAAAATTTGAATCATTGTGCTCAAAGGTTTCCCCTTTGAGATACATATTTTG
ACCTTTATAAACTATAGAGCATTTGTGTTTTCATGGATGGTTATGTTTAGTTTTATAAGGACCAAC
TCTGCTATACTTCGGATTTTCAGGTTCCTAAAGAGAAAGATGAAATGGTAGAGCAAGAGTTTAACC
GGTTGCTAGAAGCTACATCTTACCTTAGTCATCAACTAGACTTCAATGTCCTCAATAATAAGCCTG

Exon E8b
Exon E8b donor and acceptor splicing sites
STOP codon TGA
RBFOX1 consensus sequence
Exon E9

Figure 24. Exon E8b is a new 77-bp long exon carrying a premature STOP codon, located in the highly conserved region of E8a downstream flanking intron, nearby two RBFOX1 consensus elements. E8b nucleotide sequence, assessed by Sanger sequencing, is highlighted in green; donor and acceptor splicing sites are indicated in bold and STOP codon (TGA) in bold and highlighted in green; RBFOX1 consensus motifs are indicated in red. First 110 nucleotide of exon E9 are highlighted in yellow.

We identified the acceptor splice site AG upstream the 5' end of exon E8b sequence and the donor splice site GT downstream its 3' end, which usually identify an exon (Figure 24). Potentially they allow exon E8b to be spliced with exon E8 or E8a and with E9 in mature LSD1 transcripts. Notably, exon E8b sequence analysis uncovered the presence of an in-frame premature termination codon (PTC), the trinucleotide TGA, at the beginning of the exon (Figure 24). From literature we know that if a premature stop codon within a transcript is located more that 50bp from a downstream splice site, this mRNA can be considered as target of Nonsense-mediated Decay pathway (NMD) [225, 226]. Because E8b stop codon is 65 nucleotides upstream its downstream splice site, E8b could be a poison exon, defined as an exon that triggers NMD when included in the mature transcript. Thus, we can hypothesize that RBFOX1 binds to exon E8b acceptor splicing site in LSD1 pre-mRNA and leads to the inclusion of a poison exon causing its degradation by NMD.

4.1.1.2 Exon E8b characterization

The minigene splicing assay, aimed at identifying exon E8a *cis*- and *trans*-acting regulatory factors, allowed us to serendipitously discover the existence of a new LSD1 alternative exon, exon E8b. Indeed, E8b seems to be a true cryptic exon with acceptor and donor splicing sites that potentially can be spliced into mature LSD1 transcripts. Moreover, exon E8b carries an in frame premature termination codon potentially leading to the degradation of E8b-containing LSD1 transcripts by Nonsense-mediated decay. The identification of the exon E8b among MG2700 splicing products is not sufficient per se to prove E8b existence in the endogenous LSD1 mature transcripts. In order to verify if the 77-bp long exon that appears among minigene splicing products upon RBFOX1 overexpression really exists in endogenous LSD1 transcripts, we searched for E8b expression within LSD1 transcripts.

4.1.1.2.1 E8b is ubiquitously expressed in human tissues

The standard rqfRT-PCR strategy that we had always used to amplify LSD1 isoform had never showed the presence of a third alternative spliced exon in addition to exon E2a and exon E8a. This PCR strategy is based on LSD1 transcripts amplification using a fluorescinated forward primer that anneals to exon E2 and an unmodified reverse primer annealing to exon E9. The output has always been an electropherogram composed by different peaks corresponding to LSD1 isoforms that do not contain alternative exons (LSD1), containing only E2a (LSD1-E2a) and in neuronal contexts containing only E8a (LSD1-E8a) or both E2a and E8a (LSD1-

E2a/E8a) (Figure 25). Whatever the sample under analysis was, from human or murine cell lines to human or murine tissues, exon E8b had never been detected using this strategy.

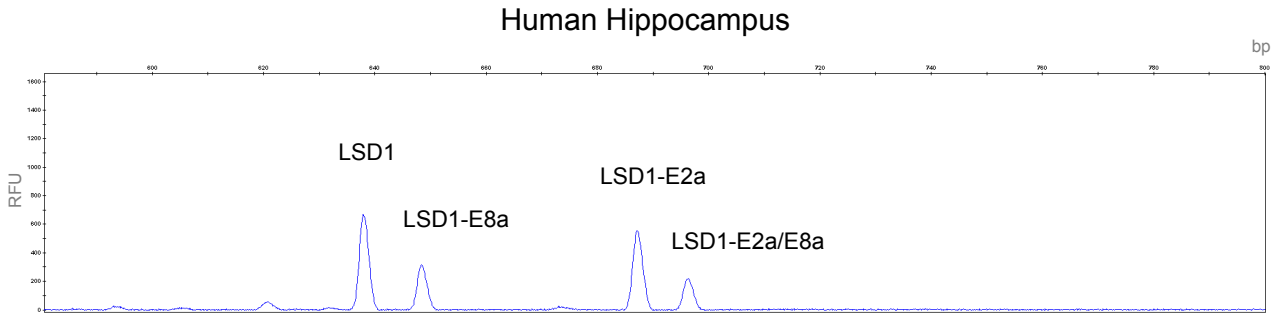

Figure 25. Example of the GeneMapper capillary gel electrophoresis output of rqfRT-PCR used to amplify LSD1 isoforms. The electropherogram obtained from rqfRT-PCR performed on human hippocampal samples shows 4 different peaks corresponding to LSD1 isoform that does not contain alternative exons (LSD1), containing only E8a (LSD1-E8a), only E2a (LSD1-E2a) and containing both E2a and E8a (LSD1-E2a/E8a).

The fact that exon E8b had never been observed in endogenous transcripts could be due to the fast degradation of E8b-containing LSD1 transcripts by NMD. Thus, we designed a specific RT-PCR strategy to detect only exon E8b-containing LSD1 transcripts. A schematic representation of E8b-specific RT-PCR is reported in Figure 26A. We set up a RT-PCR using a forward primer annealing to exon E8b sequence and a reverse primer on exon E10. This approach should amplify only LSD1 transcripts that contain exon E8b. Moreover, since the total amount of exon E8b-containing transcripts was supposed to be very low and considering that no results were obtained with a standard PCR protocol we performed a touchdown RT-PCR with 50 cycles of amplification to obtain visible PCR products. We performed E8b-specific RT-PCR on RNA deriving from different human tissues. We used FirstChoice Human Total RNA Survey Panel (AM6000, Ambion) consisting in total RNA deriving from normal human tissues. Each RNA sample is comprised of a pool of at least 3 tissue donors documented for age, sex and race. We carried out a RT-PCR to amplify LSD1 and β-actin, expressed in all human tissues, as positive controls.

From downstream E8b-specific RT-PCR we obtained an unexpected outcome: the estimated amplicon including E8b, E9 and E10 long 261bp was present only in the brain RNA but we obtained a 656-bp long product in all human tissues under analysis (Figure 26B). A 656-bp long amplicon is the exact length of a product that retains also the intron between E8b and E9. We cut out from the gel the 261 and 656-bp band and we carried out a sequencing reaction on them (data not shown). We observed that the lower band originated from the amplification of LSD1 transcripts that include only the 77-bp long E8b exon, while the upper band included also the 395-bp intron between exon E8b and exon E9. We hypothesized that exon E8b could

be preferentially exonized with its downstream intron resulting in a longer splicing isoform that we called exon E8b-long. RT-PCR reactions had always been performed after DNAse treatment. Anyway, we do not think that this finding could be a result of DNA contamination in RNA samples since 379-bp intron E9-E10 is not present in the obtained amplification product.

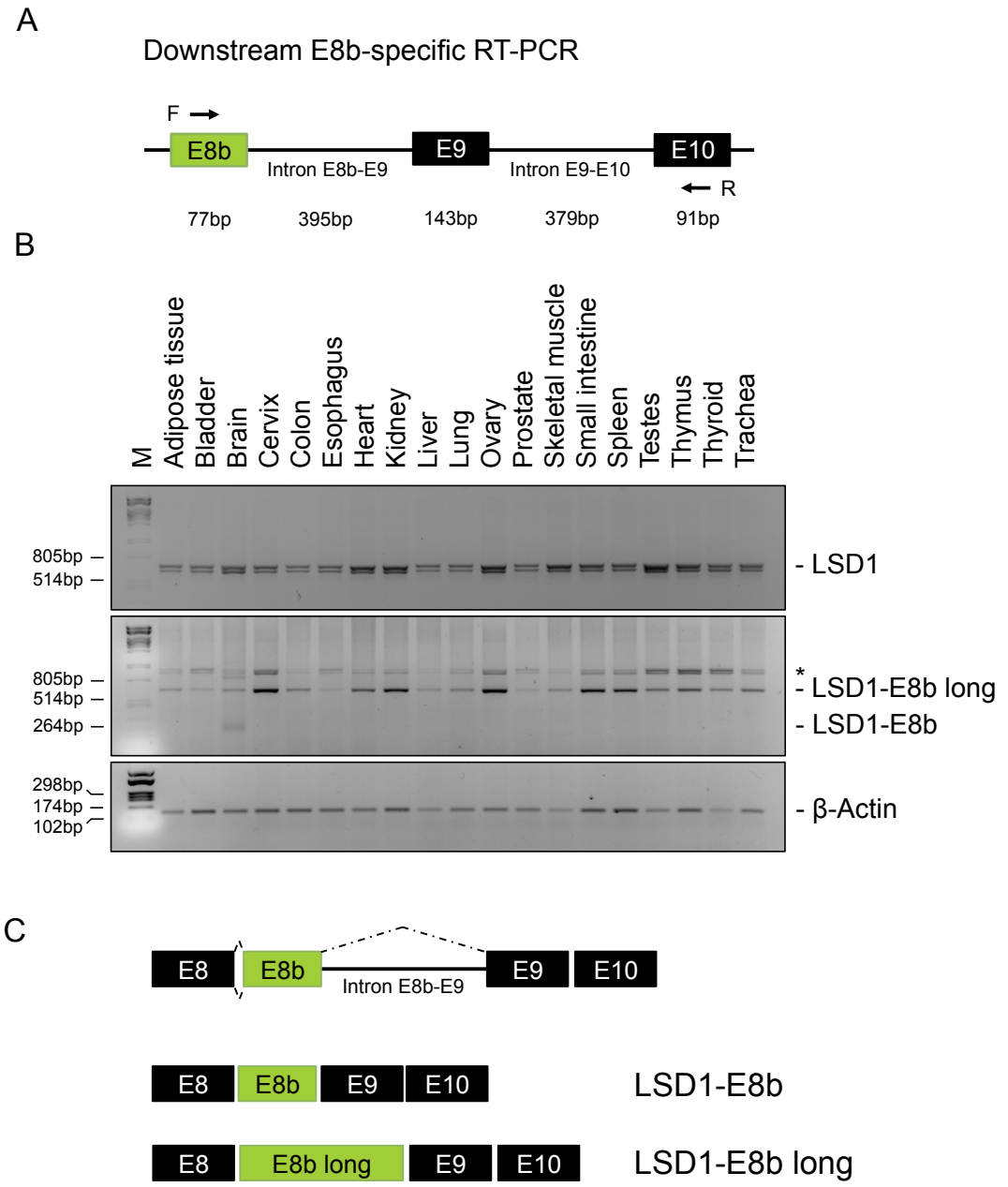

Figure 26. Exon E8b-containing LSD1 transcript is ubiquitously expressed in human tissues: (A) Schematic representation of E8b-specific RT-PCR strategy exploited to search for endogenous exon E8b-including LSD1 transcripts. We design forward primer on exon E8b and reverse on exon E10. Base pair length of each exon and intron is reported. The distance from forward primer and the end of E8b is 45 bp, from reverse primer and the beginning of exon E10 is 73 bp. The expected amplification product length is 261 bp. (B) Exon E8b-specific RT-PCR on human tissues (middle part of agarose gel). Aspecific bands are indicated with asterisk. LSD1 (upper part) and β-actin (lower part) RT-PCR are reported as positive controls. (C) Exon E8b can exist in two flavors: E8b short, 77 nt long, and E8b long including the first 77 nt and extending till the end of intron 8-9. E8b-long including transcripts can be found in all human tissues, while E8b-short is present only in the brain.

Therefore, we concluded that exon E8b truly exists in endogenous LSD1 transcripts and E8b-including LSD1 transcripts are ubiquitously expressed in human tissues. While in minigene experiments only the 77-bp exon including isoform was detected, in human tissues E8b-containing LSD1 transcript exists in two different forms (Figure 26C): the neurospecific LSD1-8b that includes only the 77-bp E8b and a ubiquitous longer one, LSD1-8b long, that retains the downstream intron. Because of the presence of a stop codon at the 5' end of exon E8b sequence, whatever exon E8b splicing isoforms is present in endogenous tissues, retaining or not E8b downstream intron, they both are supposed to trigger the degradation of all the exon E8b-containing transcripts by the NMD. Since from the functional point of view there is no difference between exon E8b-short and long, from now on we will only refer generally to exon E8b.

The ubiquitous expression of LSD1 isoforms including E8b could be explain by the fact that even if RBFOX1 is mainly neuronal, RBFOX family proteins are well represented in all human tissues and they all recognize the consensus sequence element (U)GCAUG within introns to act as splicing factors.

4.1.1.2.2 E8b is a novel primate-restricted LSD1 cryptic exon included both in LSD1 and neuroLSD1 transcripts

Exon E8b is located inside a highly conserved intronic region of human LSD1 gene (Figure 24). Thus, we decided to investigate whether this new LSD1 cryptic exon exists also in other mammals. We analyzed E8b sequence conservation among mammals using UCSC Genome Browser to perform a multiple alignment of human E8b sequence with the same genomic portion of different mammals. We compared human to higher or anthropoid primates, lower or prosimian primates and other mammals, including mouse. We noticed that exon E8b sequence is highly conserved among primates and less conserved among mammals. Interestingly, the AG acceptor splicing site upstream the 5' end of exon E8b is present only in human and higher primates, indeed lower primates and other mammals carry the dinucleotide AA instead of AG (Figure 27). On the contrary, GT donor splicing site downstream the 3' end is conserved among mammals (data not shown). TGA stop codon is conserved in all species under analysis. However, the absence of acceptor splicing site in prosimians and non-primate mammals indicates that exon E8b could not be recognized by cellular splicing machinery. This observation suggests that E8b inclusion might be a splicing event exclusively restricted to human and anthropoid primates.

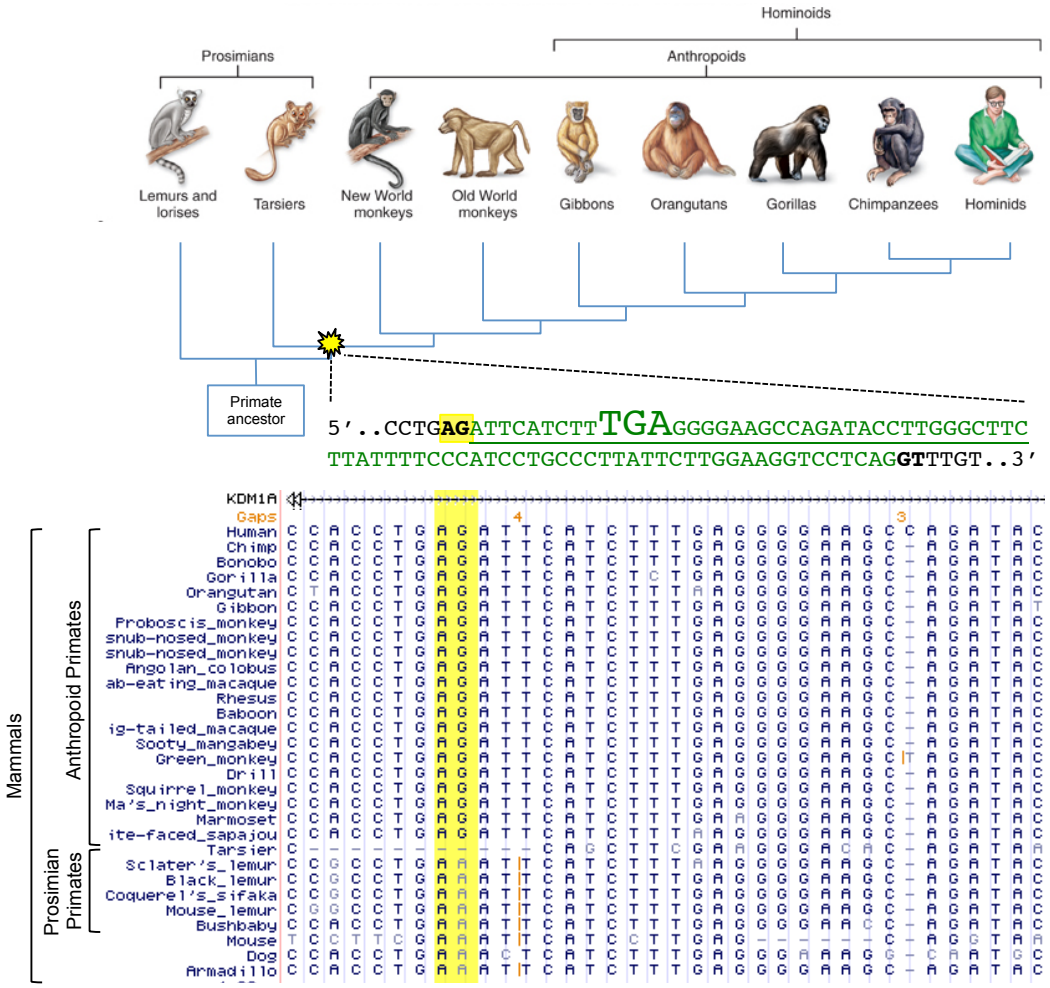

Figure 27. Exon E8b inclusion is a higher primate-restricted splicing event. UCSC Genome Browser multiple alignment of the 5' terminal end of human exon E8b and its intronic acceptor site in mammals. Note that AG acceptor splicing site (highlighted in yellow) is conserved only among anthropoid primates.

To confirm this hypothesis, we collected three cell lines deriving from non-human primates: two lemur fibroblast cell lines, Eulemur fulvus (EFU1) and Lemur catta (LCA1), and Macaca mulatta linfoblast cell line (MMU). We performed the E8b-specific RT-PCR described previously on RNA extracted from mouse hippocampus, lemur EFU1 and LCA1, Rhesus monkey MMU and human hippocampus. These samples are representative of non-primates, inferior primates and higher primates genera respectively. E8b-specific RT-PCR is capable of amplifying only LSD1 isoforms that contain exon E8b, because the forward primer anneals to exon E8b sequence. As a result, we expect amplification only in the species where exon E8b can actually be included into LSD1 mature transcript thanks to the presence of AG acceptor site. We conducted a RT-PCR to amplify LSD1, known to be expressed in all the species under analysis, as positive controls. The results are reported in Figure 29. As expected, all the analyzed species express LSD1. On the contrary, only higher primates (MMU cell line and human hippocampus) express LSD1 transcript including E8b, coherently with the presence of

the acceptor site in their genomes. This finding is in agreement with the lack of acceptor splicing site in lower primates and mouse genome.

A second different E8b-specific PCR was performed on these samples to confirm the results obtained in downstream E8b-specific RT-PCR (Figure 28). We set up an upstream E8b-specific touchdown RT-PCR using a forward primer annealing to exon E7 and a reverse primer to exon E8b. As downstream E8b-specific RT-PCR, this approach should amplify only LSD1 transcripts that contain exon E8b. In addition, since forward primer anneals to E7, this strategy permits to amplify LSD1 transcripts that either contains or do not contain exon E8a in neuronal samples. The expected amplicon including E7, E8 and E8b is 224-bp long and the one containing E7, E8, E8a and E8b is 236-bp long. We performed the upstream E8b-specific RT-PCR on the same samples and we obtained amplification of E8b-including LSD1 transcripts only in MMU and human hippocampus, as in downstream strategy (Figure 29).

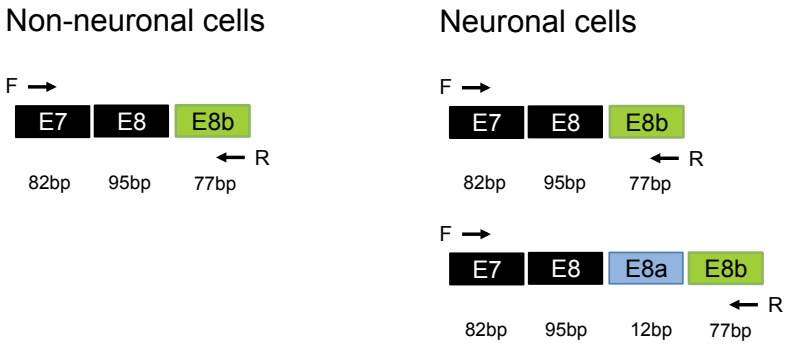

Figure 28. Schematic representation of upstream E8b-specific RT-PCR strategy exploited to verify for endogenous exon E8b-including neuroLSD1 transcripts. We design forward primer on exon E7 and reverse on exon E8b. Base pair length of each exon is reported. The distance from forward primer and the end of E7 is 52 bp, from reverse primer and the beginning of exon E8b is 77 bp. The expected amplification product length is 224 bp if it does not contain exon E8a and 236 if it contains exon E8a.

Notably, only in human hippocampus we detected two LSD1-E8b isoforms that either do or do not include exon E8a. Sanger sequencing confirmed the presence of two distinct bands, one including E8 and E8b and the second one containing also exon E8a between E8 and E8b. Indeed, two overlapping sequences could be appreciated in the electropherogram and they correspond to E8a and E8b sequence (Figure 30). This finding reflects exon E8a neuronal specific expression and indicates that exon E8b can be included both in LSD1 and neuroLSD1 mature mRNA, opening new possibilities for the regulation of LSD1/neuroLSD1 ratio by Nonsense-mediated decay preferential degradation.

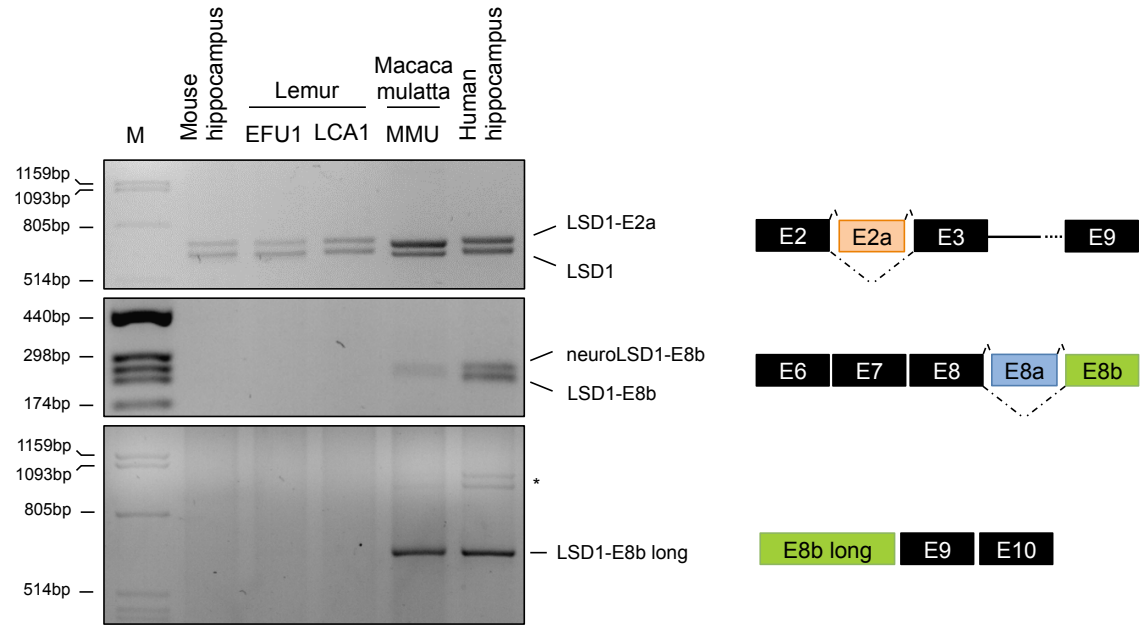

Figure 29. Exon E8b is an evolutionary acquisition of higher primates. Total LSD1 (upper part of the gel) and upstream (middle part) and downstream (lower part) E8b-specific RT-PCR on RNA extracted from mouse hippocampus, lemur EFU1 and LCA1 fibroblast cell lines, macaca mulatta MMU linfoblast cell line and human hippocampus. Aspecific bands are indicated with asterisk. Total LSD1 transcripts are detectable in all the species under analysis, while LSD1-E8b isoforms exist only in higher primates. Note that in the human hippocampus another also the isoform containing both exon E8b and exon E8a is detectable.

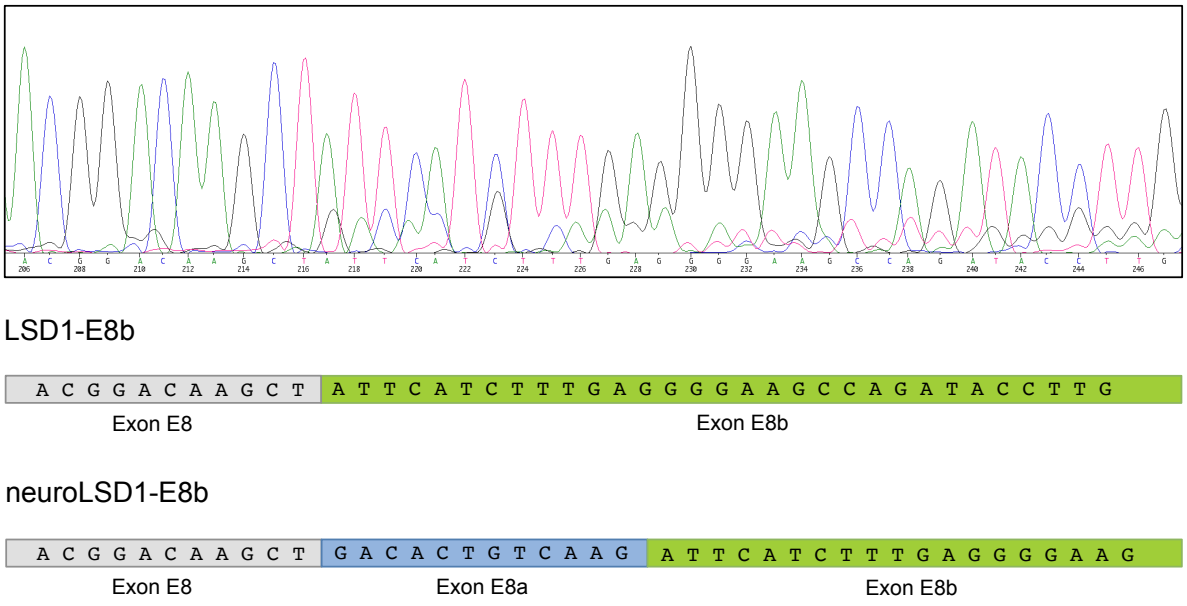

Figure 30. Exon E8b is included both in LSD1 and in neuroLSD1 isoforms. Electropherogram obtained by sequencing the product of upstream E8b-specific PCR performed on RNA extracted from human hippocampus. The presence of overlapping peaks corresponding to exon E8b and exon E8a sequences is the proof of principle of the combinatorial inclusion of exon E8b and exon E8a in LSD1 and neuroLSD1 mature transcripts. Exon E8a sequence is indicated in blue, exon E8b sequence in green.

These results confirm our hypothesis, based on acceptor splice site conservation, that exon E8b is a human and higher primates specific acquisition and E8b may be the result of evolutionary forces.

4.1.1.3 RBFOX1 modulates LSD1 levels by promoting exon E8b-mediated triggering of Nonsense-mediated decay

The presence of a premature stop codon at the 5' end of exon E8b suggests that its inclusion causes transcript degradation by the Nonsense-mediated decay (NMD). Alternative splicing coupled to NMD (AS-NMD), being a RNA turnover mechanism involved in regulating the expression level of physiological transcripts through the unproductive splicing of alternative poison exons, plays a key role in preserving cellular homeostasis [134, 139, 140]. Thus, we decided to set up different experiments to better understand exon E8b role in endogenous LSD1 transcripts regulation. If exon E8b would be really capable of mediating NMD, RBFOX1-mediated E8b inclusion in mature mRNA may represent an additional fine mechanism of LSD1 regulation present only in higher primates.

4.1.1.3.1 E8b-containing LSD1 transcripts are affected by Nonsense-mediated decay

In order to assess if exon E8b inclusion in LSD1 mature transcript really entails LSD1 transcript degradation by NMD we carried out NMD inhibition experiments in SH-SY5Y human cell line. Considering the translation-reliance of NMD pathway, we inhibited NMD by treatment with cycloheximide (CHX) that obstructs eukaryotic protein synthesis by interfering with the elongation step.

Cells were seeded at a density of $2x10^5$ cells/well in 6-well plates. After 72 hours of recovery, they were treated for 6 and 8 hours with CHX 100µg/ml. After the treatment, cells were harvested and total RNA extracted. We performed upstream E8b-specific RT-PCR as described previously. In order to quantify E8b expression, Ribosomal Protein SA (RPSA) was used as normalizer. RPSA stable expression during NMD inhibition in SH-SY5Y cells was previously assessed by qRT-PCR. Specifically, to quantify LSD1-E8b expression level, we used UVITEC Gel Documentation System Essential V6 (Cambridge) through which we quantified LSD1-E8b bands intensity on agarose gel, normalized over the intensity of the corresponding RPSA band. We expected that upon NMD inhibition the supposed E8b-containing LSD1 transcripts downregulation would be blocked with a consequent LSD1-8b transcripts increase.

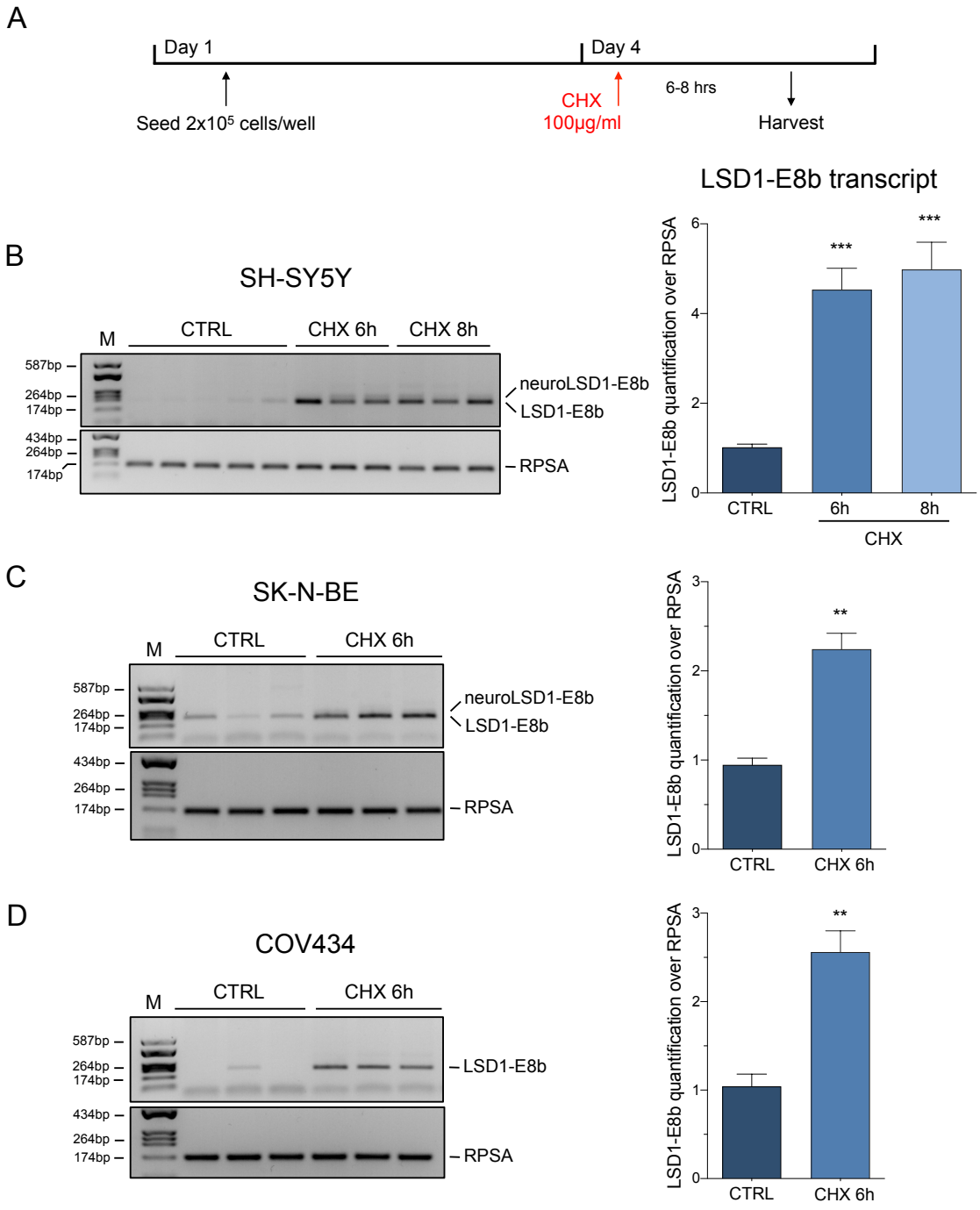

Figure 31. E8b-containing LSD1 transcripts increase after NMD inhibition in neuronal and non-neuronal human cell lines. (A) Schematic representation of adopted NMD inhibition assay based on CHX treatment, performed in SH-SY5Y, SK-N-DE and COV434 cell lines. E8b-specific RT-PCR and quantification after 6/8 hours of CHX treatment 100µg/ml on (B) SH-SY5Y, (C) SK-N-BE and (D) COV434. LSD1-E8b transcripts were normalized over RPSA. NMD inhibition induces an increase in LSD1-E8b transcripts in all analyzed human cell lines. Data are presented as means ± SEM. *** p<0.001, one way Anova Tukey *post hoc* test; **p<0.01, Student's *t* test.

Figure 31A and 31B show the obtained results: after 6 and 8 hours of NMD inhibition E8b-containing LSD1 transcript level, normalized over RPSA expression, is significantly increased with respect to untreated samples in SH-SY5Y cell line. Note that both LSD1-E8b and neuroLSD1-E8b are present. We confirmed the result obtained in SH-SY5Y cells by carrying

out the same NMD inhibition treatment in SK-N-BE human neuronal-like (Figure 31C) and COV434 human granulosa ovarian cancer derived (Figure 31D) cell line. We treated SK-N-BE and COV434 with CHX only for 6 hours since no relevant difference were detected between 6- and 8-hour treatments. These data suggest that LSD1 transcripts that include E8b are target of Nonsense-mediated decay. Proved that LSD1-8b is a target of NMD, we asked if the changes in LSD1-8b observed with NMD inhibition would be enough to elicit a significant increase in total LSD1 transcript amount. To verify E8b functional role in regulating LSD1 transcripts amount through NMD degradation, we measured total LSD1 expression level in CHX-treated SH-SY5Y samples compared to untreated ones. RPSA was used as housekeeping gene and A Protein Kinase C Alpha (PRKCA) transcript sensitive to NMD was used as positive control [211] for NMD inhibition with CHX treatment in SH-SY5Y cell lines (Figure 32B). Remarkably, a significant increase in total LSD1 transcript levels can be appreciated after 6 and 8 hours of NMD inhibition (Figure 32A). Data were confirmed again in SK-N-BE and COV434 (Figure 32C and 32D) cell lines, showing a trend towards increasing levels of total LSD1 mRNA.

A further evidence of E8b role in total LSD1 transcript level modulation came from CHX treatment of Neuro2a, a mouse neuroblastoma cell line. Since mouse genome does not contain E8b acceptor splicing site and considering that we demonstrated that LSD1-E8b is not expressed in mouse tissues, we did not expect any change in total LSD1 transcript levels after NMD inhibition. In fact, in mouse cell line no LSD1-E8b amplification by E8b-specific RT-PCR was observed either in untreated samples or in CHX-treated ones (data not shown) and no change in total LSD1 transcript levels was identified (Figure 32E). LSD1 expression was assessed by qRT-PCR using Gap Junction protein Alpha 1 (GJA1) as housekeeping gene and Heterogeneous Nuclear Ribonucleoprotein L (HNRNPL) as positive control [227] (Figure 32F).

From these results, we concluded that E8b splicing provides LSD1 with a new regulatory mechanism restricted to human and higher primates based on degradation of E8b-containing LSD1 transcripts through NMD.

In order to further strengthen these data, we performed NMD inhibition exploiting a different strategy described in [212], using indole compound NMDI-1 proved to inhibit NMD without interfering with translation process. Transcripts degradation through NMD pathway is dependent by sequential phosphorylation and dephosphorylation cycles of UPF1 [142] mediated by SMG1 kinase [228-230] and dephosphorylation complex composed of, among other proteins, SMG5 and PP2A [142, 231]. When phosphorylated, UPF1 localizes in P-bodies, cytoplasmic structures that contain untranslated transcripts and proteins involved in mRNA

decay [232]. It has been demonstrated that NMDI-1 avoids the interaction between UPF1 and SMG5 entailing the exclusion of dephosphorylation complex from P-bodies and the stabilization of the hyperphosphorylated UPF1 ultimately blocking NMD [212, 213]. The Institute Curie–Centre National de la Recherche Scientifique supplied NMDI-1 compound.

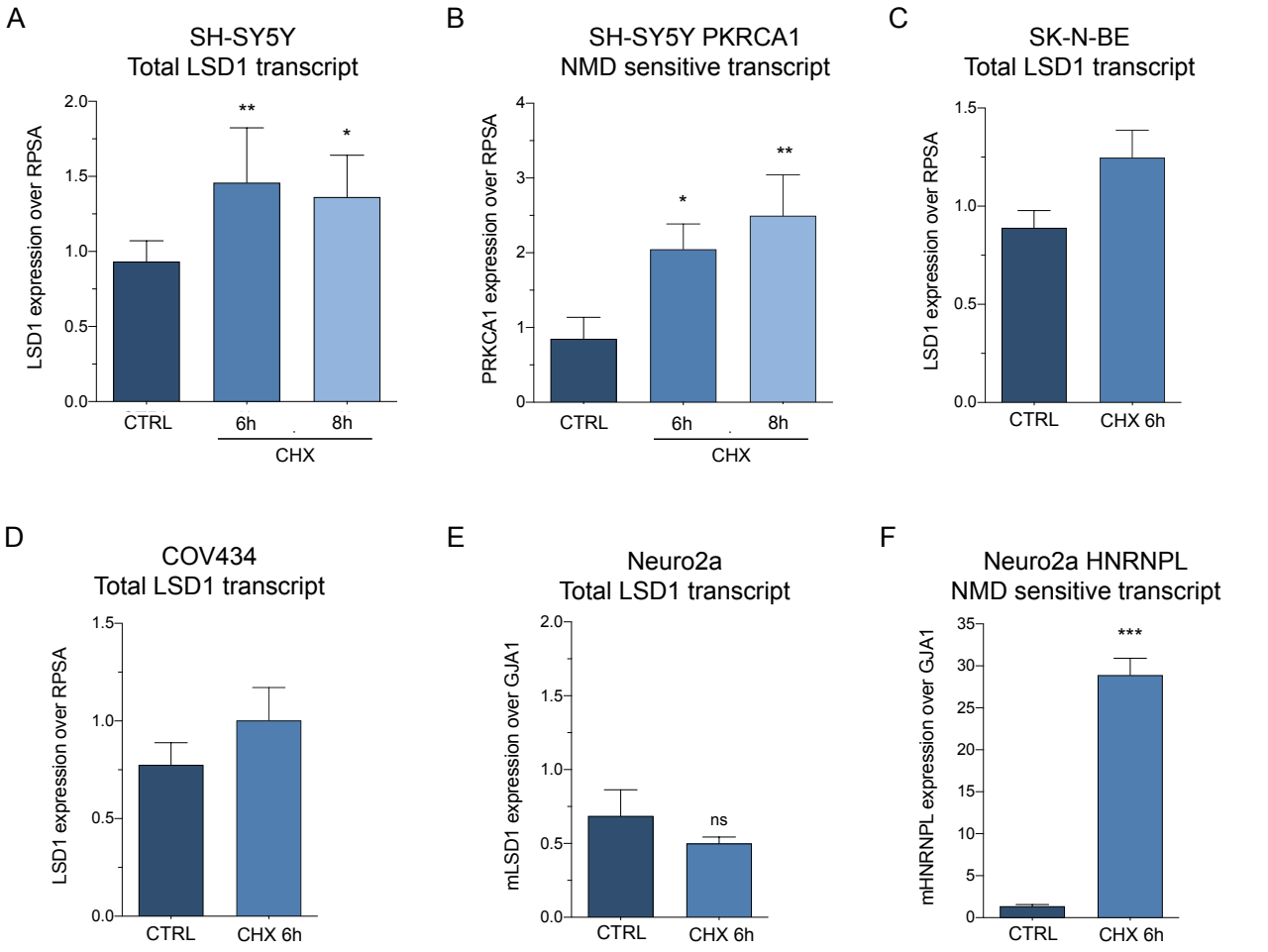

Figure 32. Exon E8b inclusion in mature transcript affects LSD1 transcript level by triggering NMD degradation in human cell lines. (A) Total LSD1 transcript level after 6/8 hours of CHX treatment 100μg/ml in SH-SY5Y, assessed by qRT-PCR. LSD1 expression was normalized over RPSA. (B) PRKCA1 was used as positive control for NMD inhibition. Data are presented as means ± SEM. * p<0.05, ** p<0.01, one way Anova Tukey *post hoc* test. Total LSD1 transcript level, normalized over RPSA, after CHX treatment after 6 hours of CHX treatment 100μg/ml in (C) SK-N-BE and (D) COV434, assessed by qRT-PCR. (E) Total LSD1 transcript level, normalized over GJA1, after 6 hours of CHX treatment 100μg/ml in Neuro2a cell line, assessed by qRT-PCR. (F) HNRNPL was used as positive control for NMD inhibition in mouse cell line. Data are presented as means ± SEM. *** p<0.0001, Student's *t* test.

We carried out NMDI-1 treatments to inhibit NMD in SH-SY5Y cell line. Cells were treated with 5μM NMDI-1 for 24 hours. We performed the same analyses described above for CHX treatment. Results are reported in Figure 33. The positive control PRKCA1 NMD-sensitive transcript levels indicate the inhibition of NMD pathway occurred (Figure 33C). A tendency

towards higher level of E8b inclusion (Figure 33A) and total LSD1 expression (Figure 33B) can be appreciated. These preliminary results will be confirmed on a higher number of replicates. However, they support data obtained with CHX-treatment consolidating E8b role in regulating LSD1 transcript level through NMD degradation.

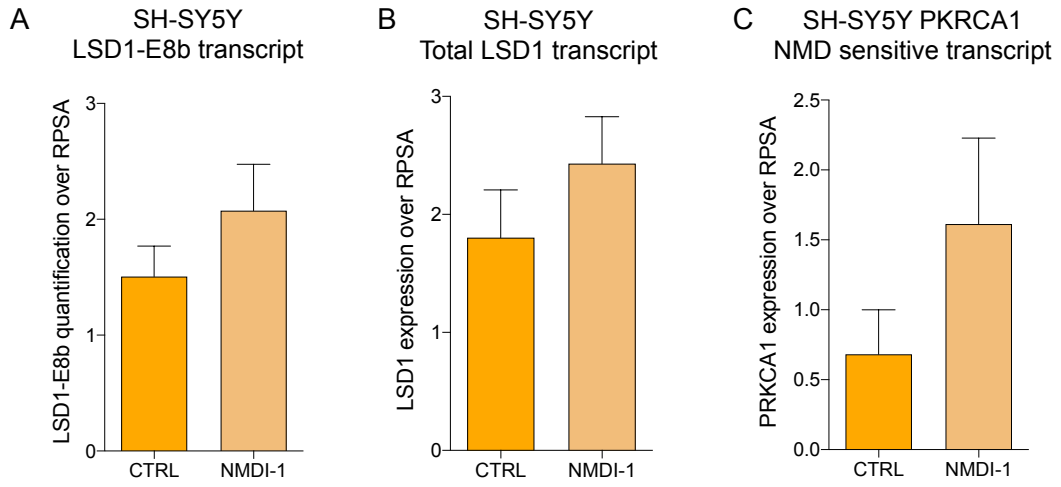

Figure 33. NMD inhibition with NMDI-1 further supports the hypothesis that E8b inclusion in mature transcript affects LSD1 transcript level by triggering NMD degradation. (A) E8b-containing LSD1 transcript quantification after 20 hours of 5μM NMDI-1 treatment in SH-SY5Y, normalized over RPSA. (B) Total LSD1 transcript level assessed by qRT-PCR and normalized over RPSA. (C) PRKCA1 was used as positive control for NMD inhibition. Data are presented as means ± SEM.

4.1.1.3.2 RBFOX1 regulates LSD1 transcript and protein levels through NMD by promoting E8b inclusion

Up to now, we demonstrated that exon E8b really exists in endogenous LSD1 mature transcripts and it is an anthropoid primates acquisition. Furthermore, we showed that human LSD1 mRNA is susceptible to NMD. Indeed, inhibition of this process with drugs acting through different mechanism, is able to increase overall LSD1 expression and exon E8b-including transcripts. It remained to demonstrate that LSD1 expression is directly regulated by RBFOX1 through the inclusion of exon E8b in endogenous LSD1 transcripts. To this aim, we exploited Tet-On system to generate a stable SH-SY5Y cell line that expresses RBFOX1 only in presence of doxycycline. Briefly, we firstly produced pTetOn stable SH-SY5Y clones and we chose the suitable ones for stable transfection with pTRE2hyg-HA-RBFOX1 (not shown). Then, we performed a stable transfection of the chosen SH-SY5Y pTetOn clones (SH-SY5Y TetOn) with pTRE2hyg-HA-RBFOX1. We used this SH-SY5Y inducible stable cell line that overexpresses RBFOX1 upon doxycycline treatment to gain more insights into the role of RBFOX1 in LSD1 levels regulation through E8b inclusion-triggered NMD.

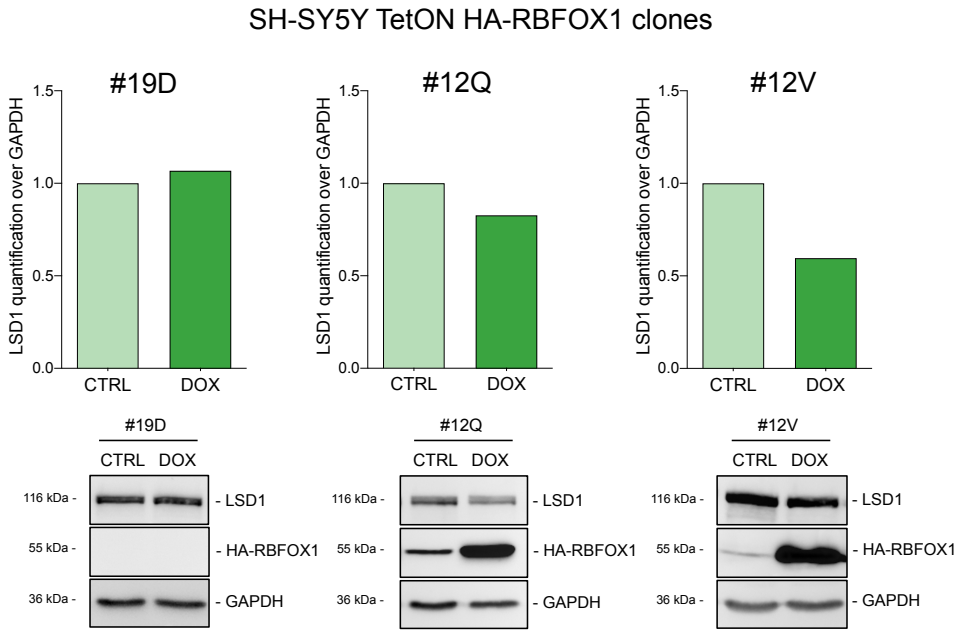

Figure 34. Western blot based screening of SH-SY5Y TetOn HA-RBFOX1 clones. Evaluation of HA-RBFOX1 expression after 24 hours of DOX induction assessed by western blot analyses on SH-SY5Y TetOn HA-RBFOX1 clones carrying DOX inducible HA-RBFOX1. Three representative clones are reported. RBFOX1 overexpression was detected using anti-HA antibody. LSD1 protein was visualized using a pan-isoform anti-LSD1 antibody and normalized over GAPDH. Gel images are shown under the graphs.

We screened SH-SY5Y pTetOn pTRE2hyg-HA-RBFOX1 clones (SH-SY5Y TetOn HA-RBFOX1) by western blot analysis, after 24 hours of 1μg/ml doxycycline (DOX) induction, looking for clones with low or absent basal expression, and a significant increase in RBFOX1 expression upon doxycycline stimulation. During clones screening by western blot we carried out an early analysis of LSD1 protein level and interestingly we noticed that the higher RBFOX1 induction the higher dowregulation effect on LSD1 was measured (Figure 34).

Subsequently, we chose the most promising SH-SY5Y TetOn HA-RBFOX1 clone and we carried out RNA and protein analyses. Specifically, we seeded 60% confluent cells in 6-well plates and the day after we induced RBFOX1 expression through 1μg/ml DOX treatment. 24 hours after RBFOX1 induction cells were harvested for RNA extraction.

Firstly, we verify that RBFOX1 overexpression actually results in changes in alternative splicing of some transcripts known to be target of RBFOX1 and RBFOX2 [177, 233]: Abl Interactor 1 (ABI1) and Nuclear Mitotic Apparatus protein 1 (NUMA1). We performed a RT-PCR on these target in DOX-treated samples compared to untreated ones. Figure 35 show that alternative splicing of both ABI1 and NUMA1 is affected by RBFOX1 increase.

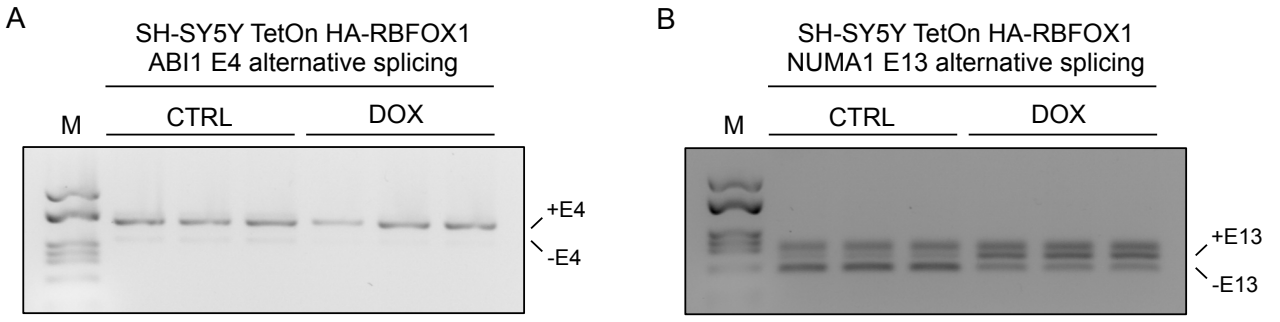

Figure 35. RBFOX1 overexpression results in changes in the alternative splicing of known RBFOX1/2 target transcripts. After 24-hour induction of RBFOX1 expression with 1ug/ml DOX in SH-SY5Y TetOn HA-RBFOX1 cells, we performed RT-PCR on RBFOX1/2 known target transcripts: (A) E4-lacking ABI1 transcript is not detectable upon RBFOX1 overexpression and (B) NUMA1 transcripts containing exon E13 increased after DOX-induced RBFOX1 overexpression.

Then, we analyzed E8b-inclusion and total LSD1 transcript levels, normalized over RPSA, by upstream E8b-specific RT-PCR and qRT-PCR, respectively, comparing DOX induced and basal samples (Figure 36). It is important to highlight that we did not expect a substantial increase in exon E8b inclusion upon RBFOX1 overexpression considering that even if exon E8b should be more included LSD1-8b and neuroLSD1-8b transcripts are rapidly degraded by NMD. Interestingly, when RBFOX1 is present thanks to DOX treatment we observed a slight increase in exon E8b-containing LSD1 transcripts (Figure 36A and 36B) and a significant reduction of total LSD1 transcripts level (Figure 36C) compared to controls. Note that total LSD1 transcript downregulation does not occur when DOX treatment is performed in SH-SY5Y TetOn clone used as negative control since it does not carry DOX-inducible HA-RBFOX1 (Figure 36D).

In order to assess if LSD1 transcript decrease induced by RBFOX1 overexpression could affect LSD1 protein levels we performed the same experiments analyzing proteins by western blot analysis. Western blot results are shown in Figure 37. Upon DOX treatment we could observe an increase in HA-RBFOX1 expression with a concomitant LSD1 protein downregulation in SH-SY5Y TetOn HA-RBFOX1 (Figure 37A). On the contrary, LSD1 protein level did not change in SH-SY5Y TetOn cells after DOX treatment compared to controls, coherently with no LSD1 transcript modulation (Figure 37B).

Taken together these results prove that the splicing factor RBFOX1 is directly involved in LSD1 transcript and protein levels regulation through exon E8b-induced NMD.

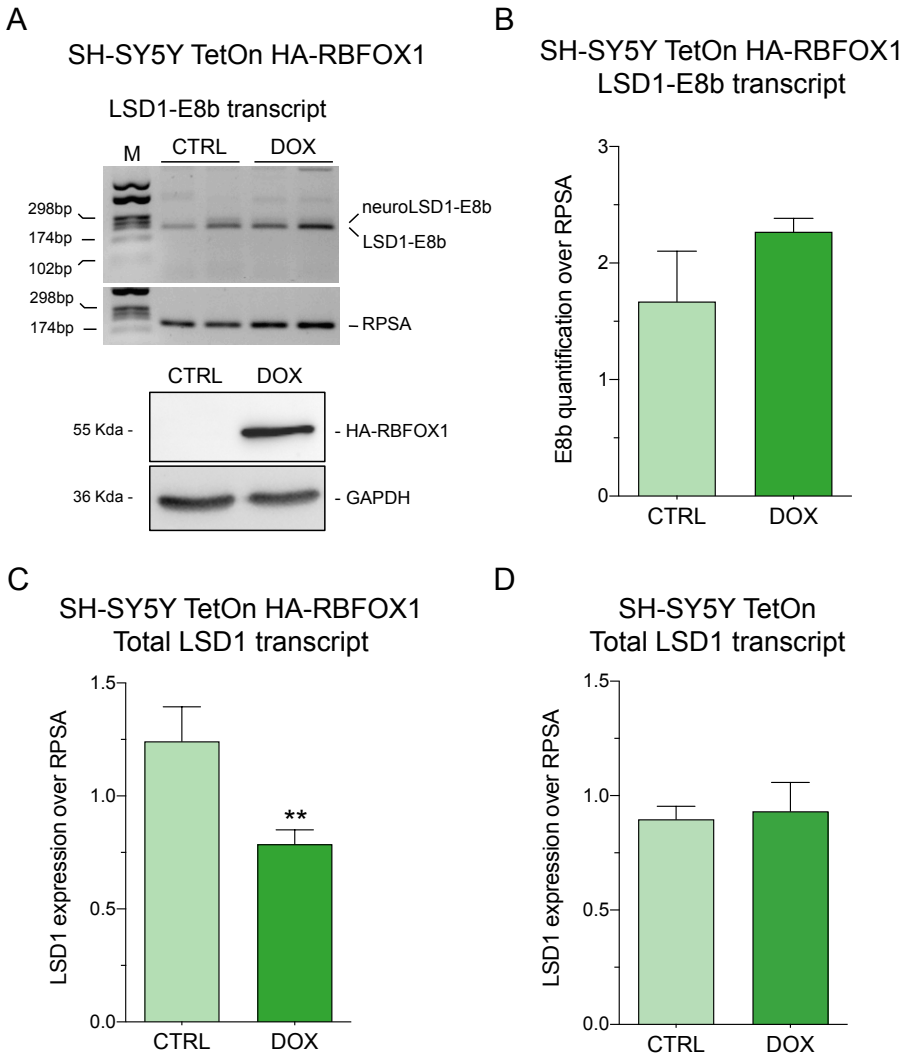

Figure 36. RBFOX1 negatively regulates LSD1 transcript levels by promoting E8b splicing into LSD1 mature transcripts. After 24-hour induction of RBFOX1 expression with 1ug/ml DOX in SH-SY5Y TetON and SH-SY5Y TetON HA-RBFOX1 cells, we performed (A) E8b-specific RT-PCR and (B) quantification over RPSA in SY5Y TetON HA-RBFOX1 cells treated with DOX compared to untreated samples. RBFOX1 overexpression in shown below agarose gel. LSD1 expression level, normalized over RPSA, was assessed by qRT-PCR performed on (C) SH-SY5Y TetON HA-RBFOX1 cells and (D) SH-SY5Y TetON cells, as negative control, comparing DOX-treated samples to untreated ones. Data are presented as means ± SEM. ** $p<0.01$, Student's *t* test.

Changes in expression of RBFOX1 that increase or decrease E8b splicing should modulate the amount of transcripts subject to NMD, thus altering LSD1 expression. In this perspective, we are planning to perform some experiments in order to verify if blocking RBFOX1 activity could lead to LSD1 modulation in a opposite direction to the one observed upon RBFOX1 overexpression. To do this we will exploit a decoy oligonucleotides-based strategy described in [234]. They designed decoy oligonucleotides that target different splicing factors, among them RBFOX1 and RBFOX2, consisting of several tandem repeats of the RNA motifs recognized by the target splicing factor. In this way, decoy oligonucleotides can specifically

bind to the RNA binding domain directly blocking splicing activity without interfering with other functions of the protein.

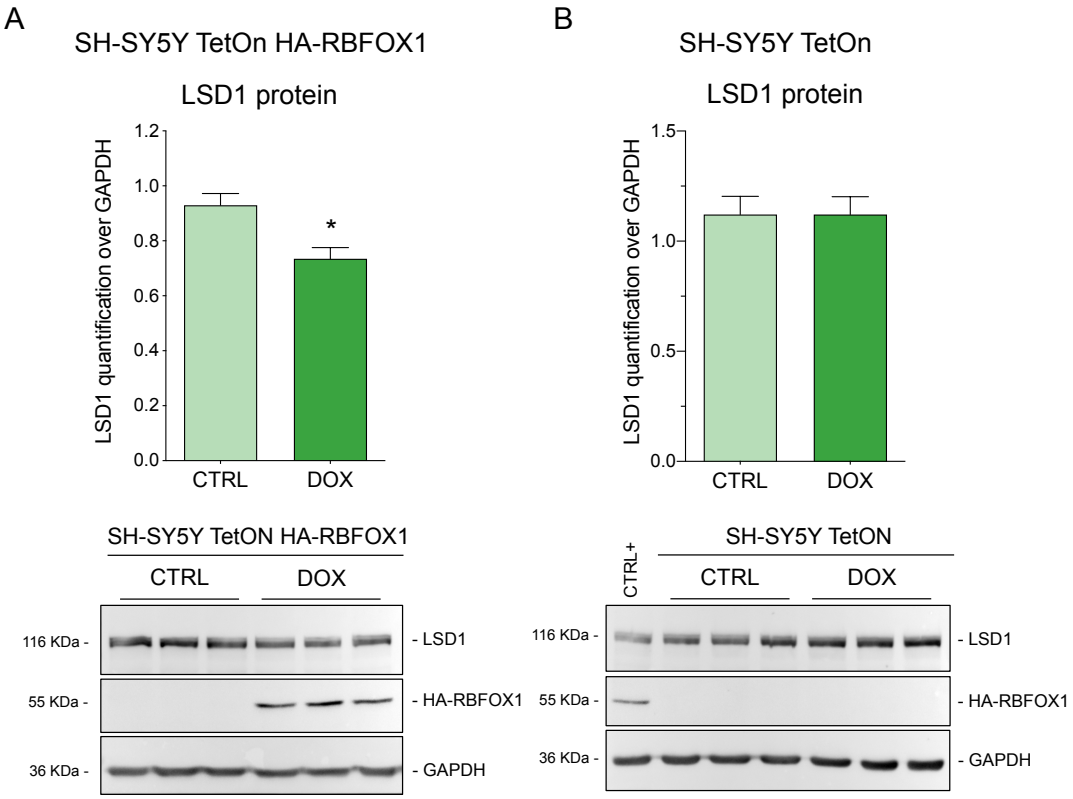

Figure 37. RBFOX1 overexpression leads to downregulation of total LSD1 protein levels. After 24-hour induction of RBFOX1 expression with 1ug/ml DOX, we performed western blot analysis on (A) SH-SY5Y TetOn HA-RBFOX1 and (B) SH-SY5Y TetOn cells, the latter as negative controls, to quantify LSD1 protein level. RBFOX1 overexpression was detected using anti-HA antibody. LSD1 protein was visualized using a pan-isoform anti-LSD1 antibody and normalized over GAPDH. Representative gel images are shown below each graph. Data are presented as means ± SEM. * $p<0.05$, Student's *t* test.

In collaboration with the laboratory of Professor Daniela Perrone of the University of Ferrara (Italy), we are producing the RBFOX1/2 decoy oligonucleotide and a scrambled one to use as control. The RBFOX1/2 decoy will be a 24-nt long RNA oligonucleotide composed of four tandem repeats of UGCAUG sequence with 2'OMe-phosphorothiotate backbone, in order to reduce the vulnerability to endonucleases. Scramble decoy will be 21-nt long with three tandem repeats of GCAAUCU sequence that does not resemble any of the known splicing factors motifs [235].

4.1.1.4. Exon E8b in neuronal context: an additional strategy mediated by RBFOX1 to finely tune LSD1/neuroLSD1 splicing ratio

We demonstrated that RBFOX1 is involved in the regulation of the overall amount of LSD1 transcript and protein, a regulatory mechanism with potential impacts in several neuronal but also non-neuronal contexts where RBFOX1 paralogs might contribute to regulate LSD1 expression outside the nervous system. However, in the brain LSD1 activity does not only depend on its overall expression, but also by the fine balance between its two isoforms, LSD1 and neuroLSD1. For this reason, it is now important to evaluate if RBFOX1 in neurons might also indirectly interfere with the isoform ratio. In the next chapters, I discuss four experimental evidences that together indicate how RBFOX1 is indeed able to affect LSD1 and neuroLSD1 ratio balance.

4.1.1.4.1 E8a and E8b, along with their splicing regulators nSR100 and RBFOX1, are similarly modulated during neuronal differentiation

We started E8b characterization in human neuronal context investigating exon E8b expression during neuronal development. Thanks to an extremely fruitful collaboration with Professor Luciano Conti and his laboratory, at University of Trento, we could rely on human induced pluripotent stem cells (iPSCs). The reasons why we chose human iPSCs model are manifold. First, E8b splicing is a phenomenon restricted to human and anthropoid primates. Second, compared to other in vitro models available, such as human immortalized cell lines, human iPSCs and iPSCs-derived neuronal cells are particularly advantageous, as they provide a more realistic picture of human cellular biology and processes. Finally, none of human neuronal-like immortalized cell line available in our laboratory expresses detectable levels of neuroLSD1.

Our collaborators provided us with RNA extracted from iPSCs and hiPSCs-derived cellular types representative of the process of differentiation in neuronal lineage, granting us an insight into LSD1 isoform expression alongside neuronal differentiation. More in detail, we analyzed pluripotent stem cells (iPSCs), neuronal progenitors (CxPs), glutamatergic neurons at two different differentiation stages, 30 (CxGLUT 30dd) and 60 (CxGLUT 60dd) days, GABAergic neurons (GABA) at 21 days of differentiation and motor neurons (MN).

We started measuring total LSD1 expression through qRT-PCR using pan-isoform primers annealing to E15 and E16. We also performed isoform-specific qRT-PCRs. We used a couple of primers able to specifically detect only neuroLSD1 transcript with forward primer annealing

to E8-E8a-E9 junctions and reverse one annealing to E9. To specifically amplify LSD1 transcripts that do not contain exon E8a we used the same reverse primer and a forward one annealing to E8-E9 junction. Ribosomal Protein Lateral Stalk Subunit P0 (RPLP0) was used as normalizer since its expression levels do not change alongside differentiation [236, 237]. Results are reported in Figure 38. Accordingly to literature [62, 238], LSD1 total transcript levels decrease alongside human iPSC neuronal differentiation (Figure 38A). Indeed, LSD1 is known to be an epigenetic regulator of gene expression in stem cells and a reduction of LSD1 transcript levels is observed during physiological differentiation to tissue-committed cells [239-241]. A similar trend can be found looking at LSD1 transcripts that do not contain exon E8a (LSD1 w/o E8a) (Figure 38B).

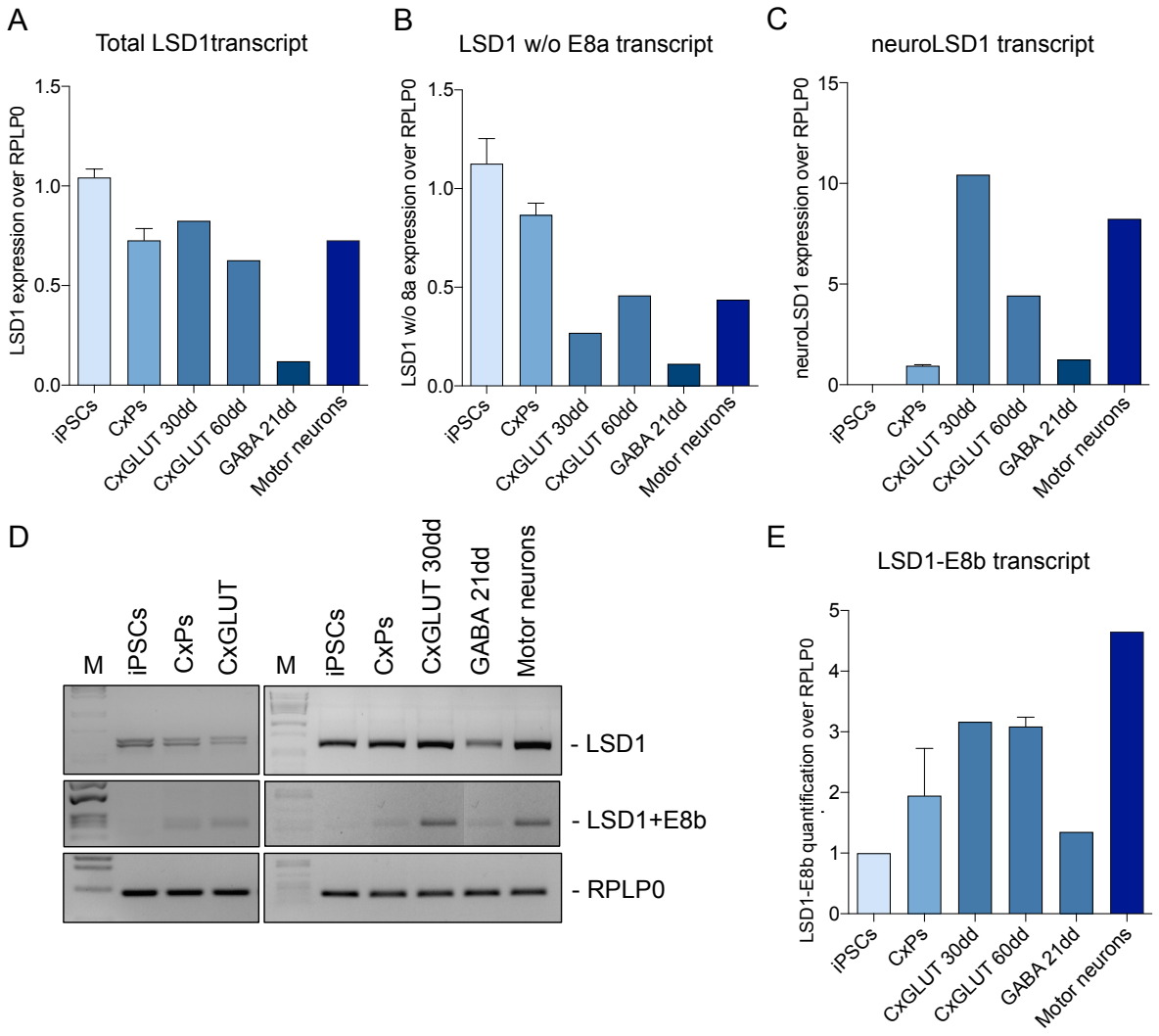

Figure 38. LSD1 isoforms are modulated during neuronal differentiation. qRT-PCR analysis in human iPSCs, CxPS, CxGLUT30, CxGLUT60, GABA and motor neurons on (A) total LSD1, performed with pan-isoform primers, (B) LSD1 isoform that does not contain exon E8a and (C) neuroLSD1 isoform performed using isoform-specific primers. (D) E8b-specific RT-PCR and quantification. The normalization was performed using RPLP0.

NeuroLSD1 transcript, containing exon E8a, follows an opposite trend: coherently with its neuro-specific expression and its essential role in neuronal maturation [91, 102], neuroLSD1 is not detectable in staminal context and its expression increases during neuronal differentiation (Figure 38C). NeuroLSD1 upregulation during neuronal differentiation was confirmed also by rqfRT-PCR (not shown). Afterward we analyzed LSD1-E8b transcripts expression through E8b-specific RT-PCR using RPLP0 as a normalization factor and total LSD1 as a positive control. Interestingly, exon E8b inclusion in LSD1 transcripts rises during differentiation (Figure 38D and 38E).

Taken together these preliminary results confirm some general assumptions regarding LSD1 and neuroLSD1 expression. Moreover, they indicate that exon E8b inclusion is dynamically modulated during neuronal differentiation following a trend similar to the one of exon E8a and suggest the existence of a link between the splicing of these two LSD1 alternative exons. Therefore, we decided to inspect the expression of splicing factors known to modulate LSD1 alternative splicing. We analyzed the transcript levels of nSR100 and NOVA1 as exon E8a positive regulators and RBFOX1 as LSD1 E8b-specific splicing factor. As expected, nSR100 (Figure 39A) and NOVA1 (Figure 39B) are overexpressed during neuronal differentiation, along with exon E8a inclusion rise. RBFOX1 (Figure 39C) follows an analogous trend, coherently with its role in neuronal maturation [185] and E8b increase during neuronal differentiation.

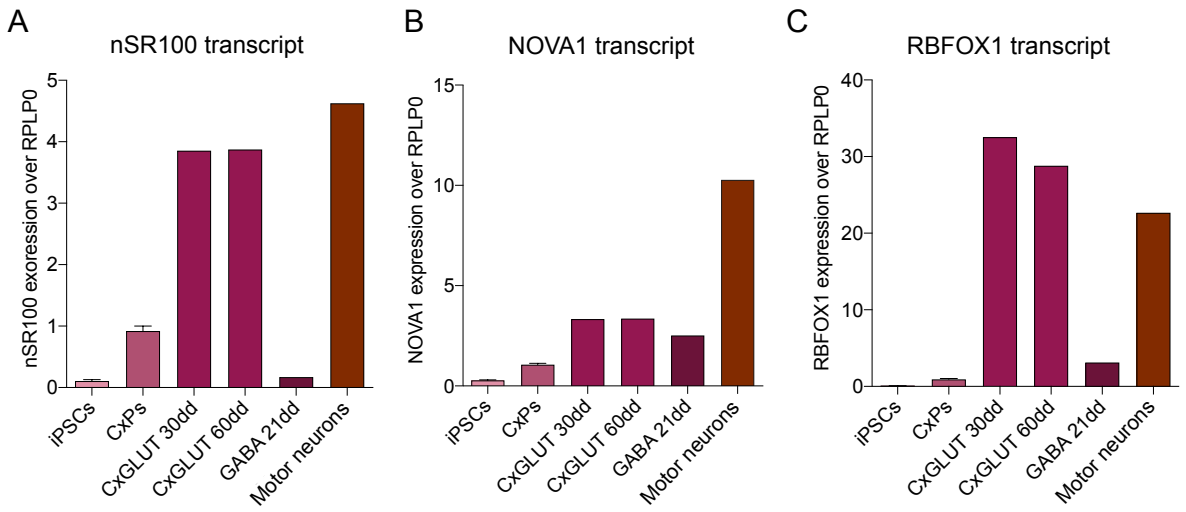

Figure 39. The expression of E8a splicing factors, nSR100 and NOVA1, and E8b-specific splicing factor RBFOX1 is modulated during neuronal differentiation. qRT-PCR analysis on (A) nSR100, (B) NOVA1 and (C) RbFOX1 in iPSCs, CxPS, CxGLUT30, CxGLUT60, GABA and motor neurons. RPLP0 was used to normalize transcript levels.

Interestingly, comparing different lineages of neuronal-commitment we noticed that LSD1 and neuroLSD1 system modulation was completely different in GABAergic neurons compared to glutamatergic and motor neurons. Indeed, what can be immediately observed is that LSD1 transcript amount is very low in GABAergic neurons compared to glutamatergic ones and motor neurons. In addition, in GABAergic-committed cells also neuroLSD1 transcripts amount is very low. Coherently with poor exon E8a inclusion, nSR100 is barely detectable in GABAergic neurons. Similarly, exon E8b inclusion in LSD1 transcripts that increases during glutamatergic and motor neuron differentiation remains almost stable in GABAergic one, according with RBFOX1 transcript levels modulation. Although very preliminary, these data are of particular relevance if we consider the different nature of GABAergic and glutamatergic neurons. It would be interesting to analyze also LSD1 protein level and chromatin status of LSD1-target IEGs to have more insights into this divergent trend of LSD1 expression between glutamatergic and GABAergic neurons, opening new possibilities for neuroLSD1 excitatory neurons-specific role.

4.1.1.4.2 In E8b-including LSD1 transcripts exon E8a frequency is higher compared to E8b-non-containing LSD1 transcripts

As discussed till now, inclusion of exon E8b can modulate overall LSD1 expression, in a neuronal but in principle also in a non-neuronal context. However in the brain, exon E8b inclusion could have an additional effect that is to change the LSD1/neuroLSD1 ratio. This can happen if E8b could be preferentially included in a specific LSD1 isoform, potentially impacting on LSD1/neuroLSD1 splicing ratio. Thus, we examined whether exon E8b is equally represented in exon E8a including (neuroLSD1) and excluding (LSD1) isoforms, or if it is preferentially included in one of the two LSD1 isoforms. In this second case, an uneven E8b inclusion in the two transcript families should modify not only overall LSD1 expression but also the fine balance between LSD1 and neuroLSD1. We reasoned that if E8b inclusion in LSD1 transcripts were totally independent upon E8a splicing, then E8a inclusion frequency should be the same in E8b-including and E8b-skipping LSD1 transcript populations.

To this aim, we quantitatively analyzed the minigene splicing experiments performed in SH-SY5Y cells (described in section 4.1.1.1), in which minigene MG2700 was transfected together with nSR100 and RBFOX1 expression plasmids (Figure 40A). As previously shown, upon nSR100 and RBFOX1 overexpression exon E8b appears and it is included alone (peak 3) or together with exon E8a (peak 4) in minigene transcripts. We examined E8a inclusion frequency in different minigene splicing isoform populations, those skipping exon E8b (MG

and MG-E8a, peaks 1 and 2) and those including exon E8b (MG-E8b and MG-E8a/E8b, peaks 3 and 4). If exon E8b splicing occurs at the same extent in minigene transcripts that contain or do not contain exon E8a, E8a inclusion frequency will be the same in these two transcript populations. Actually, E8a inclusion frequency is higher in E8b-containing transcripts compared to minigene products that do not contain E8b. Specifically, E8a is included in more than 31% of minigene splicing isoforms that include E8b (peak 4) and only 17% of minigene transcript without E8b (peak 2) (Figure 40B), indicating that at least in the minigene assay, the relative ratio between E8a-containing and non-containing isoforms is higher in E8b containing transcripts.

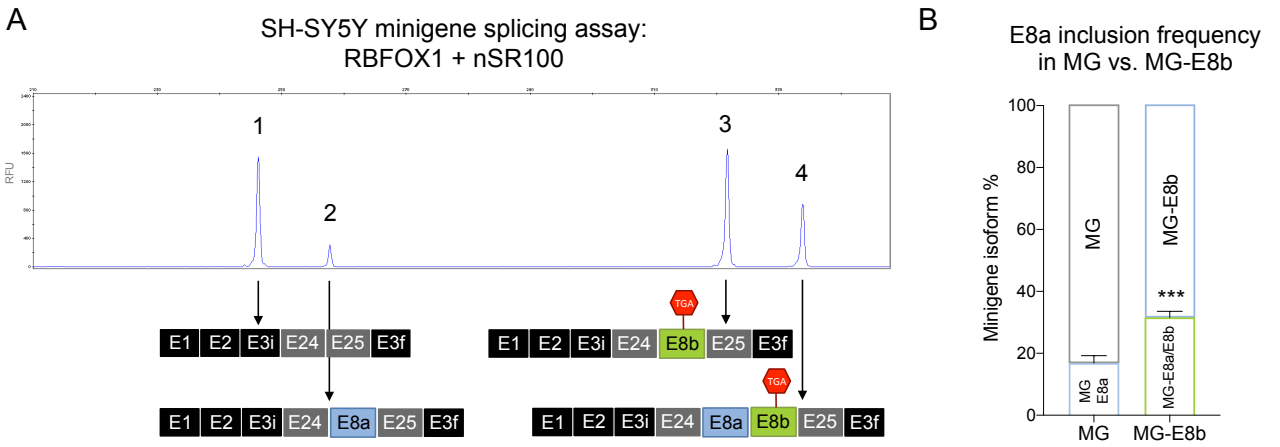

Figure 40. In MG splicing assays, exon E8b splicing is favored in E8a-containing transcripts. (A) GeneMapper capillary gel electrophoresis output of minigene rfqRT-PCR products showing minigene splicing assay performed in SH-SY5Y transfected with MG2700 together with nSR100 and RBFOX1. A schematic representation of minigine splicing products is reported below. (B) Relative amount of exon E8a-containing transcripts in MG2700 isoforms that contain (MG-E8b and MG-E8a/E8b, peaks 3 and 4) or do not contain (MG and MG-E8a, peaks 1 and 2) exon E8b upon nSR100 and RBFOX1 overexpression. Data are presented as means ± SEM. ***p<0.001, Student's *t* test.

On a physiological perspective, a possible implication of these results is that degradation of E8b-containing isoforms (not occurring in minigene-derived transcripts) should affect more E8a-containing LSD1 transcripts, preferentially degrading neuroLSD1 and increasing in vivo LSD1/neuroLSD1 ratio.

To demonstrate that this can occur also in vivo, in endogenous LSD1 transcripts, is more challenging, considering that exon E8b-including isoforms are present at very low levels in vivo as they are rapidly degraded by NMD. Hence, since we could not measure and compare E8a relative splicing frequency in E8b-containing and E8b-skipping LSD1 transcripts within the same rqfRT-PCR, a different strategy needed to be exploited.

We approached the problem performing two specific rqfRT-PCR, allowing the former (PCR1) a specific evaluation of E8b-non-containing isoforms and the latter (PCR2) a measure of E8b-containing transcripts:

- PCR1 was performed using E2-annealing fluorescinated forward primer and unmodified reverse one annealing to E9, allowing a specific evaluation of E8a inclusion frequency in E8b-non-containing LSD1 transcripts. In principle, such a PCR should also amplify the E8b-containing transcripts. However, this is not the case. Indeed, since LSD1-E8b mRNAs are selectively affected by NMD they fall under the resolution threshold of the PCR.
- PCR2 was performed using fluorochrome-conjugated forward primer annealing to exon E7 and unmodified reverse one annealing to E8b, allowing the identification of E8a inclusion frequency in E8b-containing LSD1 transcripts.

In other words, PCR1 permits the quantification of E8a inclusion frequency in LSD1 transcripts that are not subjected to NMD, while PCR2 measures E8a inclusion frequency in LSD1 transcripts that are susceptible to NMD. We reasoned that PCR1 analysis yields a picture of exon E8a distribution on LSD1 isoforms "after" NMD. On the contrary, PCR2 provides a picture "before" NMD. If E8a is included in LSD1 transcripts independently on E8b, then, E8a inclusion frequency in PCR1 and PCR2 should be identical. Vice versa, if exon E8a is differentially included in LSD1-E8b and E8b-non-containing LSD1 isoforms, the percentages should be different in the two PCRs.

We carried out PCR1 and PCR2 on RNA extracted from human post-mortem hippocampal samples (see section 4.2 for details about the collected samples) and from human post-mortem cerebellar samples, kindly donated by Professor Marco Venturin. We compared E8a inclusion frequency in total LSD1 transcripts (pale orange, PCR1) and in E8b-containing LSD1 isoforms (orange, PCR2). We observed that neuroLSD1 relative percentage is higher in E8b-including LSD1 transcripts ("before NMD") compared to those who do not ("after NMD"), both in human hippocampal and cerebellar samples. In detail, in the hippocampus E8a relative percentage is higher in E8b-containing LSD1 transcripts (43%, PCR2) compared to its inclusion in total LSD1 transcripts (26.1%, PCR1) (Figure 41A). Notably, also in the cerebellum E8a inclusion relative percentage in LSD1-E8b is higher (78.1%, PCR2) compared to that of total E8b-non-containing LSD1 transcripts (58.9%, PCR2) (Figure 41B). These results suggest that also in human-derived samples exon E8a and exon E8b splicing events are functionally correlated and, precisely, exon E8b inclusion is favored on transcripts in which also E8a is spliced.

All this said, we can conclude that RBFOX1-regulated exon E8b-induced NMD in the human brain represents a further molecular layer of LSD1/neuroLSD1 ratio regulation.

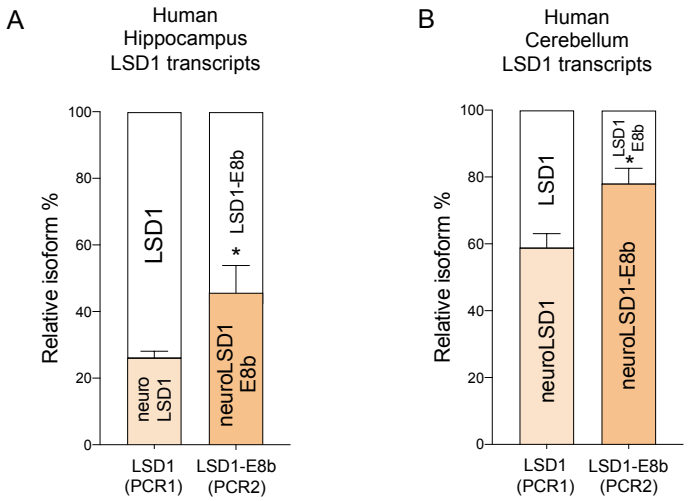

Figure 41. In human post-mortem specimen exon E8a frequency is higher in E8b-including LSD1 transcripts compared to non-E8b LSD1 isoforms. Relative quantification of exon E8a (neuroLSD1) inclusion in total LSD1 transcripts (LSD1, PCR1) and E8b-containing LSD1 transcripts (LSD1-E8b, PCR2) in (A) human hippocampus and (B) human cerebellum, assessed by rqfRT-PCR. Data are presented as means ± SEM. * $p<0.05$, Student's *t* test.

In order to prove the preferential degradation of neuroLSD1 by NMD we plan to assess whether NMD inhibition could modify LSD1/neuroLSD1 splicing ratio. Unfortunately, neither SH-SY5Y nor other neuronal-like cell line in our laboratory expresses neuroLSD1 isoform. As a result, we could not appreciate the proposed preferential effect of exon E8b-induced NMD on neuroLSD1 through CHX treatment. Thanks to the collaboration with Professor Luciano Conti and colleagues, at University of Trento, we will repeat the previously described NMD inhibition treatment on differentiated human neuronal precursor cells (hNPCs). Indeed, we have already assessed that differentiated hNPCs expresses significant levels of neuroLSD1 isoform, representing a powerful in vitro model to analyze E8a splicing modulation upon NMD inhibition. Considering that in minigene splicing assay and human post-mortem brain samples analysis E8b displays a preferential inclusion in neuroLSD1 isoform suggesting its preferential degradation, we expect to observe an increase in neuroLSD1 relative percentage after the inhibition of NMD, further corroborating our hypothesis.

We have previously proved that exon E8b inclusion leads to transcript degradation by NMD machinery (Figure 31) and this affects total LSD1 transcript level in vitro (Figure 32). By virtue of the results just presented, we can infer that E8b-induced degradation involves preferentially neuroLSD1 transcripts rather than LSD1, suggesting that E8b inclusion can ultimately affect LSD1/neuroLSD1 splicing ratio. In this perspective, physiological or

pathological changes in RBFOX1 levels or activity, affecting E8b splicing and modifying the proportion of transcripts subjected to degradation, might impact on LSD1/neuroLSD1 balance. Accordingly, the primate-restricted acquisition of exon E8b links the MDD-associated RBFOX1 gene to neuroLSD1 modulation providing a new regulatory mechanism for fine-tuning LSD1 and neuroLSD1 splicing ratio and strengthening neuroLSD1 role in stress susceptibility.

4.1.1.4.3 Acute Social Defeat Stress affects RBFOX1 splicing activity in the mouse hippocampus

This chapter aims at providing all the available experimental evidences supporting a role for RBFOX1 as a potential fine regulator of the ratio between LSD1 and neuroLSD1. In this regard, we here present an interesting piece of evidence showing concomitant stress-induced regulation of RBFOX1-FAPY/RBFOX1-TALVP splicing isoforms (nuclear, active as splicing factor, and cytosolic, acting as RNA binding factor RBFOX1 isoforms, respectively) and LSD1/neuroLSD1 in the mouse hippocampus.

We performed acute social defeat stress (ASDS) on two-month-old male wild-type mice. ASDS is a paradigm of physiological form of psychosocial stress, which comprises two main phases. In the first phase, the experimental mouse undergoes a direct and physical interaction with the aggressor CD1 mouse. During this phase, that lasts 5 minutes, aggressor mouse physically attacks the intruder. In the second phase the two mice are separated by a perforated Plexiglas divider and remain in visual and olfactory interaction allowing the psychosocial stress. After 2 or 7 hours of psychosocial stress we collected hippocampal samples that were processed for RNA extraction. We also collected hippocampal samples 24 hours after the cease of the 7-hour-long psychosocial stress phase during which defeated mice are allowed to recover in their home cage.

Cytosolic RBFOX1-TALVP isoform differs from the nuclear RBFOX1-FAPY one for the presence of the 53-bp long alternative exon E19 [175, 176]. Thus, we analyzed exon E19 RbFOX1 alternative splicing (Figure 42A) by standard RT-PCR using a couple of primers able to amplify both E19-containing and skipping RBFOX1 isoform. We quantified the relative amount of each splicing isoform using UVITEC Gel Documentation System Essential V6 (Cambridge). Remarkably, E19 splicing into RbFOX1 transcripts is modulated by ASDS in the hippocampus (Figure 42C). Specifically, upon 2 and 7 hours of ASDS RBFOX1 nuclear isoform relative frequency is significantly increased with respect to controls. Note that stress-induced RBFOX1 splicing modification is transient and nuclear/cytoplasmic isoform ratio is restored

24 hours after ASDS. We also performed rqfRT-PCR to evaluate LSD1 isoforms relative ratio. As expected, defeated mice undergo neuroLSD1 transient downregulation (data not shown), which we used as quality control of ASDS paradigm. Indeed, with superimposable kinetics environmental stress induces both a transient neuroLSD1 downregulation, and an increase in RBFOX1-FAPY, the active, nuclear isoform of RBFOX1 in turn involved in downstream splicing regulation. We reason that these data represent the first in vivo insight about consistency of stress-mediated RBFOX1-dependent LSD1/neuroLSD1 splicing regulation.

Considering that exon E8b-containing LSD1 transcripts are not present in mouse, neuroLSD1 downregulation in the mouse hippocampus could not be related to RBFOX1 modulation upon acute stress. However, thanks to disclosed E8b preferential inclusion in neuroLSD1 isoform, we think that this primate-restricted acquisition could link RBFOX1 to neuroLSD1 modulation in human and higher primates neurons as a further layer of homeostatic control.

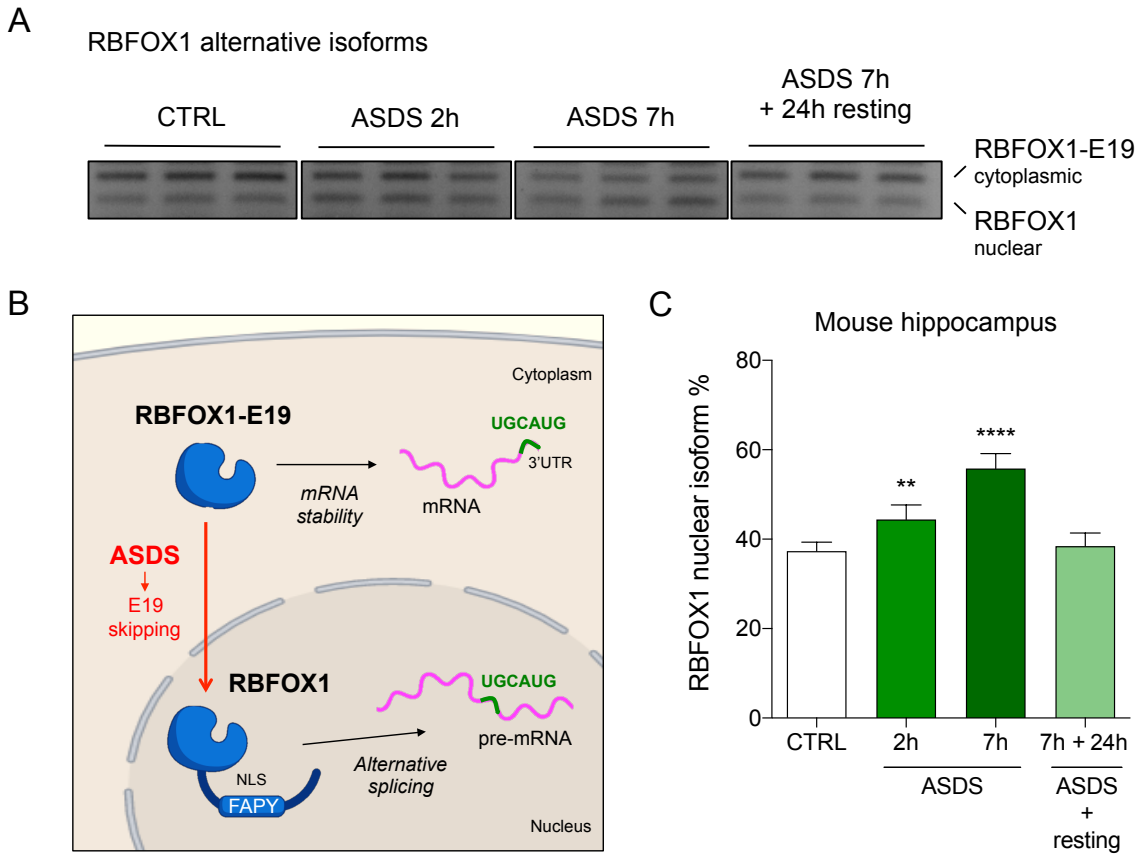

Figure 42. RBFOX1 nuclear and cytoplasmic splicing isoforms are modulated during ASDS in the mouse hippocampus. (A) Evaluation of RBFOX1 alternative splicing in the mouse hippocampus comparing defeated mice to controls. Nuclear (RBFOX1) and cytoplasmic (RBFOX1-E19) isoforms are indicated. (B) Schematic representation of ASDS-induced RBFOX1 isoforms modulation in the mouse hippocampus. (C) Quantification of the relative percentage of RBFOX1 nuclear isoform. Data are presented as means ± SEM. * compared to CTRL. **p<0.01, **** p<0.0001, one way Anova Tukey *post hoc* test.

4.1.2 Intronic Single Nucleotide Variants affect neuroLSD1 splicing modulation

In the human population, similar environmental challenges can elicit adaptive or maladaptive stress response in an individual-specific manner. Resilient individuals are able to cope with stressful situation maintaining normal psychophysical functioning. The same threatening situation can elicit maladaptive behavioral changes in susceptible individuals eventually leading to the onset stress-related neuropsychiatric disorders. Genetic predisposition plays a central role in the divergence point between engaging resiliency or vulnerability pathways in response to stress. In this regard, we hypothesized the genetic basis of stress resiliency or susceptibility could directly involve *LSD1* gene. Indeed, LSD1 alternative spliced isoforms layout could be genetically modulated by the presence of single nucleotide variants that contribute in fine-tuning E8a splicing process. Considering the neuroLSD1^{KO} mouse phenotype of low anxiety, the presence of SNPs associated with different frequencies of exon E8a inclusion might contribute to the generation of a wide spectrum of anxiety behaviors among human population. Moreover, LSD1 and neuroLSD1 modulation in response to stress as an adaptive mechanism of homeostatic stress response could be a nodal point in neurobiology of stress resiliency and the presence of LSD1 human genetic variants with a functional role in exon E8a splicing could concur to generate stress-response variability between individuals.

Nowadays, it is well known that Single Nucleotide Polymorphisms (SNPs) in regulatory regions of genes represent vulnerability factors for many complex diseases and these regulatory polymorphisms in conserved non-coding regions occur more frequently than in coding ones. Interestingly, the human LSD1 alignment across vertebrates by GenomeVista browser (http://pipeline.lbl.gov/cgi-bin/GenomeVista) shows that exon E8a sequence and its intronic regulatory elements are highly conserved in mammals (Figure 43). This high conservation degree of exon E8a surrounding introns raised the possibility that the genetic background could have a role in regulating exon E8a splicing.

Thus, we deepen the genetic characterization of exon E8a and its flanking introns in human *LSD1* gene in order to find single nucleotide variants with a functional role in neuroLSD1 alternative splicing regulation.

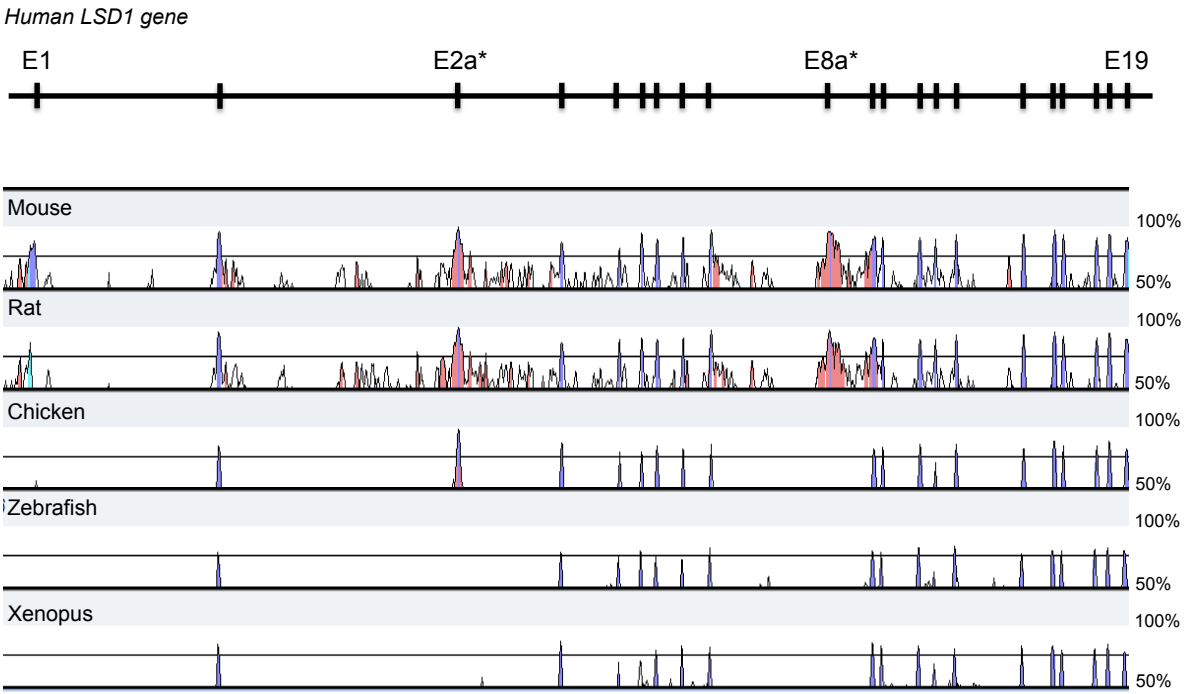

Figure 43. VISTA conservation graph for LSD1 gene. Human-vertebrates alignment of LSD1 gene from VISTA browser (http://pipeline.lbl.gov/cgi-bin/textBrowser2?act=summary&run=u171-ZBFCa5YJ&base=hg18); the "peaks and valleys" graphs show genomic coordinates on human chromosome on x-axis and conservation level among vertebrates on y-axis. Exons are shown in violet while highly conserved intronic regions are shown in pink. Alternatively spliced exons are marked with asterisk.

Taking advantage of UCSC Genome Browser, we found several single nucleotide polymorphisms in exon E8a flanking regions sequence. We selected the SNPs with the highest frequencies among the human population, located in the highly conserved intronic regions that surround exon E8a: rs2235549, rs778266261 and rs7512264, referred to hereafter as SNP 1, SNP 2 and SNP 3 (Figure 44). SNPs precise position, possible alleles and their frequencies in the human population are reported in Table 5. We decided to focus only on these three most frequent common SNPs in order to virtually divide all the human population in nine groups represented by the haplotypes deriving from the combination of minor and major alleles of these chosen SNPs. In collaboration with Professor Rosanna Asselta and colleagues, at Humanitas University, we calculated the frequencies of these selected SNPs in their Italian population cohort composed by 3284 subjects (Table 5) and they provided us the frequencies of each haplotype deriving from the combination of major and minor allele of these three SNPs (Table 6).

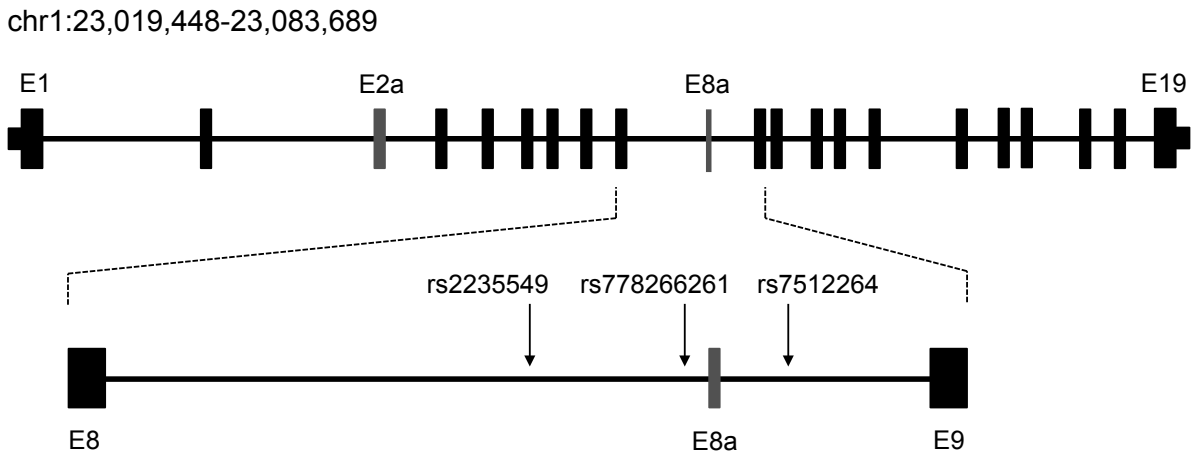

Figure 44. Three common SNPs identified in human exon E8a flanking introns. Schematic representation of human LSD1 genetic map (chr1:23,019,448-23,083,689) with blown up view of the analyzed region; the genomic localization of the three identified SNPs in exon E8a flanking introns is marked with an arrow.

Table 5. Main features of selected SNPs: Three common SNPs can be identified in human exon E8a flanking introns. The SNPs main features are reported. (MAF = minor allele frequency).

	SNP 1	SNP 2	SNP 3
dbSNP RefSNP ID	rs2235549	rs778266261	rs7512264
Position	chr1:23065282	chr1:23066010	chr1:23066503
Variation type	SNV	SNV	SNV
Gene : Consequence	KDM1A : intron variant	KDM1A : intron variant	KDM1A : intron variant
Variants	T/G	T/G	T/A
Ancestral allele	G	T	T
MAF	G = 0.32 (1000Genomes)	G < 0.01 (gnomAD)	A = 0.06 (1000Genomes)
Highest MAF	G = 0.49 (1000Genomes)	G = 0.01 (gnomAD)	A = 0.23 (1000Genomes)
MAF in Italians	G = 0.1935	G = 0.01	A < 0.01

Table 6. Possible haplotypes and their frequencies in Italians: the eight possible haplotypes deriving from combination of the SNPs under analysis with their frequencies in Italian population are reported. The name assigned to the four haplotypes that we analyzed is indicated in the last column.

Possible haplotypes (SNP1-SNP2-SNP3)	Frequency in Italians	Functional investigation	Assigned haplotype name
T - T - T	79.20 %	✔	HAPLO1
G - T - T	19.04%	✔	HAPLO2
T - G - T	1.20%	✔	HAPLO3
T - T - A	<1.00%	✔	HAPLO4
G - G - T	0%	✗	/
G - T - A	0%	✗	/
T - G - A	0%	✗	/
G - G - A	0%	✗	/

We inferred eight different haplotypes but only three of them where identified within the analyzed sample representing the Italian population. We named these haplotypes 1, 2 and 3: haplotype 1 carries the major allele of all three SNPs (T – T – T); haplotype 2 carries SNP1 minor allele and SNP2 and SNP3 major alleles (G – T – T); haplotype 3 carries SNP2 minor allele and SNP1 and SNP3 major alleles (T – G – T). Although not represented in the Italian population, we decided to include in our functional analysis a fourth haplotype, haplotype 4 which carries SNP1 and SNP2 major alleles and SNP3 minor allele (T – T – A), since it probably can be found in the human population.

To assess whether these four haplotypes are functionally different in terms of exon E8a splicing regulation, we performed functional studies exploiting the minigene report system. The 1393 nucleotide-long genomic region showed in Figure 45B was cloned in pBSplicing plasmid using NdeI restriction sites (Figure 45A). In this way, we generated a minigene containing exon E8a sequence and its flanking intronic regions (chr1:23,065,177-23,066,569) showing high degree of conservation among mammalian species and including the SNPs under analysis. We called it MG1300.

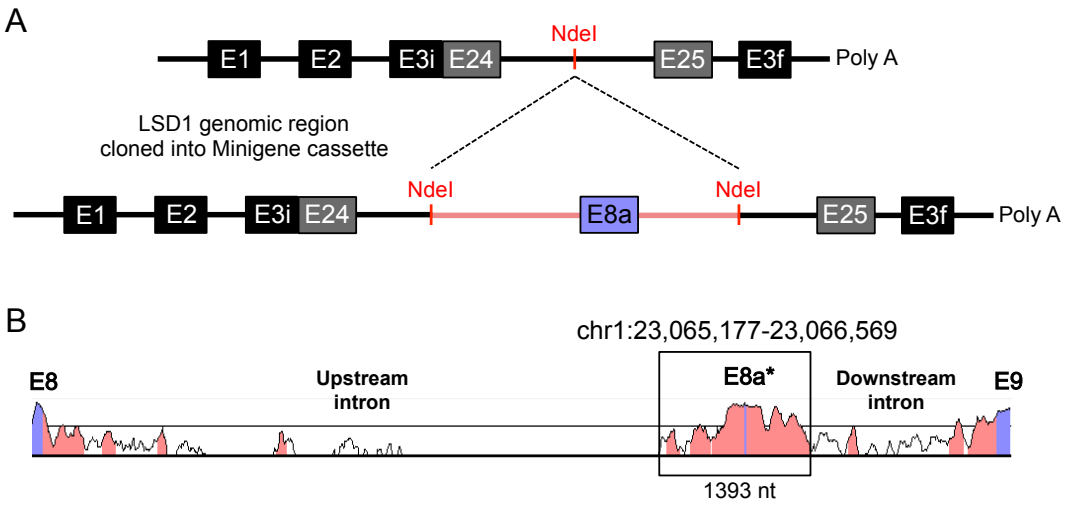

Figure 45. MG1300 generation. (A) Schematic representation of minigene-based strategy performed to test the effect of single nucleotide variants in exon E8a flanking introns on exon E8a splicing: LSD1 genomic region was cloned into pBSplicing plasmid using NdeI restriction sites; pBSplicing is composed of pBluescript II KS+ (not shown) and the minigene cassette with α-globin (in black) and fibronectin (in grey) exons. (B) VISTA conservation graph for human exon E8a flanking introns, showing high degree of conservation among mammalian species. The highly conserved LSD1 genomic region that was cloned into minigene cassette is indicated with a box (chr1:23,065,177-23,066,569).

Exon E8a intronic regions cloned into the minigene cassette were mutagenized in SNP1, SNP2 or SNP3 positions in order to obtain the four different minigenes carrying different alleles. We called them MG1300 HAPLO1, MG1300 HAPLO2, MG1300 HAPLO3 and MG1300 HAPLO4 (Figure 46).

The different minigens were transfected separately into Neuro2a neuroblastoma cell line and 24 hours after transfection RNA was extracted and reverse transcribed. Exon E8a inclusion percentage in chimeric minigene transcript was analyzed through rqfRT-PCR using primers that anneal to minigene exons. We considered MG1300 HAPLO1 as a reference construct for exon E8a inclusion frequency since it carries the major alleles of all three SNPs.

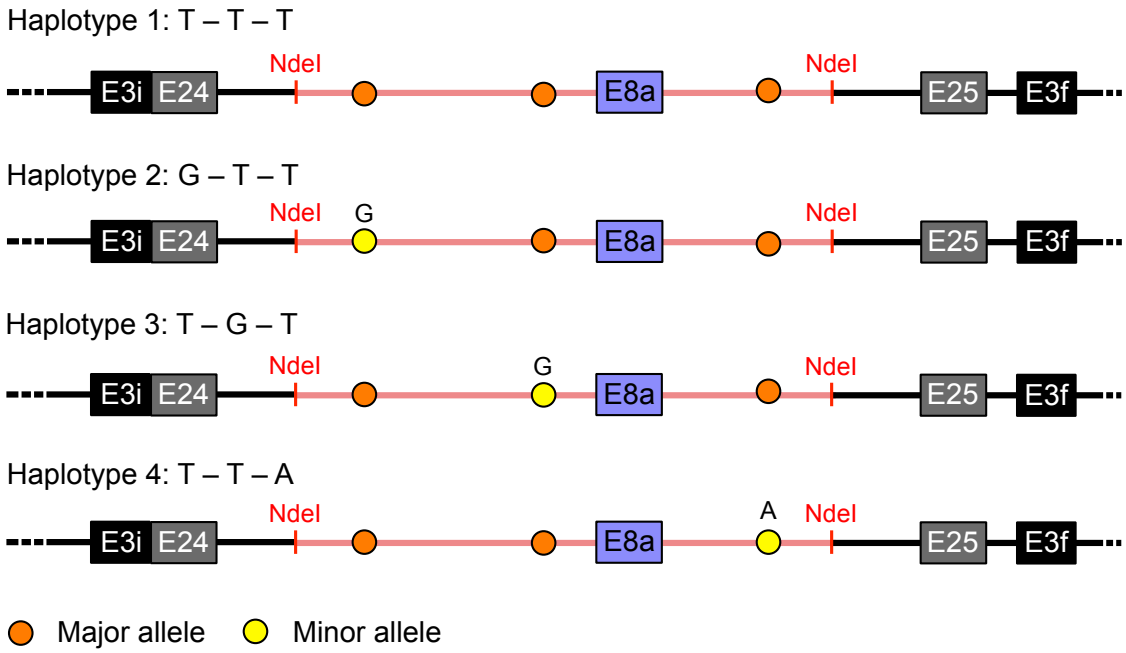

Figure 46. Minigene constructs generated to study the functional role of the selected SNPs. Schematic representation of the mutagenized MG1300 that recapitulate the four haplotypes under study.

Interestingly, the presence of the minor allele of SNP2 (rs778266261), carried by MG1300 HAPLO3, led to a small but significant reduction of exon E8a inclusion in minigene transcript compared to MG1300 HAPLO1. On the contrary, minor alleles of SNP1 (rs2235549) and SNP3 (rs7512264) did not affect exon E8a splicing (Figure 47). Interestingly, SNP2 maps 49 nucleotides upstream exon E8a sequence and the presence of its minor allele could alter the sequence of a splicing regulatory region. This result suggests that, at least in vitro, intronic variants can modify as *cis*-acting regulatory elements affecting neuroLSD1 splicing. We plan to confirm this result in a more neuronal-like setting where we expect a higher exon E8a inclusion and potentially we would observe a greater impact of haplotype 3 on exon E8a splicing. Moreover, since neuroLSD1 undergoes activity-dependent downregulation [103] we are planning to verify whether the presence of rs778266261 minor allele could affect not only exon E8a basal inclusion but also its modulation upon neuronal activation.

The identification of a SNP that affects exon E8a splicing in minigene system suggests that also in endogenous context this single nucleotide variation can modify basal or activity-dependent

LSD1/neuroLSD1 splicing ratio in the brain and may hence contribute in setting different level of stress-plasticity consolidation among the human population responsible for specific anxiety profile or stress responsiveness. In this perspective, the presence of this variant of exon E8a flanking intron in individuals suffering of major depression disorder (MDD) and post-traumatic stress disorder (PTSD) in a different frequency compared to a control cohort would corroborate the hypothesis of a LSD1-related genetic basis underlying an aberrant stress response, providing a possible functional biomarker for susceptibility or resiliency in human stress-related neuropsychiatric disorders.

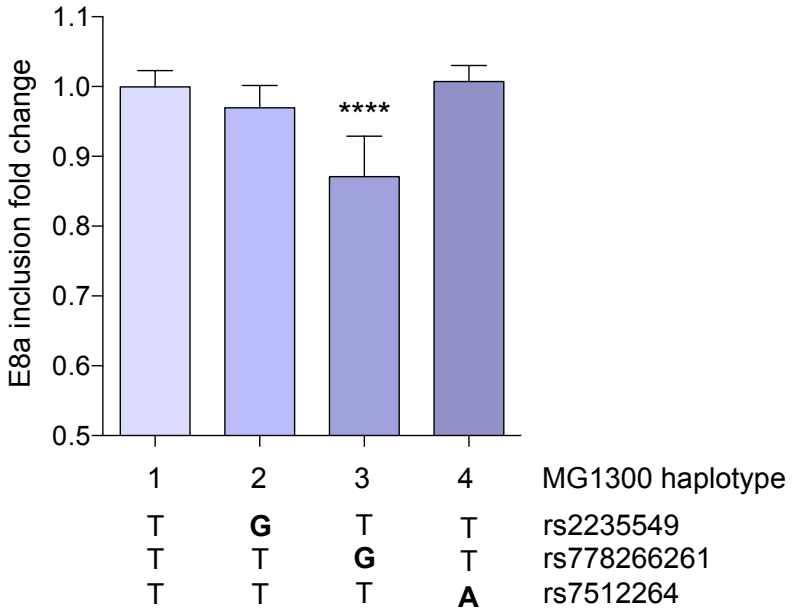

Figure 47. The minigene MG1300 HAPLO3, carrying minor allele of SNP rs778266261, shows a reduced exon E8a inclusion compared to other haplotypes. Alternative splicing of exon E8a from minigene chimeric transcript in shown in the figure. Minigenes carrying the indicated haplotypes were transfected into N2a cells and exon E8a inclusion percentage was measured through rqfRT-PCR. SNPs alleles are indicated; minor allele is in bold. Data are presented as mean ± SD (n=3 separate transfections, each performed in triplicates). ****p<0.0001, one-way ANOVA Tukey *post hoc* test.

4.2 HUMAN POST-MORTEM SAMPLES TO HIGHLIGHT DYNAMIC LSD1/neuroLSD1 RATIO MODULATION IN HUMANS

The molecular characterization of LSD1 and neuroLSD1 functions within neuronal activation and stress response has been investigated mainly in neuronal primary cultures and in the mouse brain [42-44, 91, 102, 103, 109]. In vitro and in vivo models allowed us to characterize the dynamic modulation of LSD1/neuroLSD1 ratio upon stressful stimuli and to propose that it might be functional to a homeostatic process aimed at protecting neurons from potential glutamate-induced toxicity and associated behavioral negative effects [103, 109]. However, up to now, there were neither evidences of LSD1/neuroLSD1 relevance in the human brain nor evidences of its possible alteration in physiological or pathological conditions.

The characterization of LSD1 and neuroLSD1 transcriptional profile in human post-mortem brain samples represents a unique opportunity to implicate these LSD1 isoforms in human brain physiology. We therefore extended our study analyzing human hippocampal post-mortem brain specimens in two different conditions: i) physiological brain aging comparing young individuals to the elderly, and ii) psychiatric drift, including suicidal death compared to age and gender-matched healthy individuals.

In this regard, we recently obtained ethic committee approval to collect and analyze specimens from post-mortem human hippocampus in order to characterize LSD1 physiological and possibly pathological relevance in the human brain (University of Milan Ethic Committee protocol n. 40-18 and Territorial Ethic Committee AUSLRE protocol n. 2019/0004645). With the help of Dr. Maria Paola Bonasoni, a pathologist at Arcispedale Santa Maria Nuova in Reggio Emilia, we collected hippocampal specimens from post-mortem human brain deriving from female and male individuals of different ages and from individuals who underwent suicidal death. This psychiatric-relevant behavior is indeed often associated with depression earlier in life [242], representing a good proxy to study LSD1 and neuroLSD1 relevance in traumatic stress susceptibility. Moreover, we were able to perform a molecular characterization of LSD1 and neuroLSD1 in normal aging brains thanks to Professor Marco Venturin, who kindly provided us with some human hippocampal specimens from the elderly, obtained from MRC London Neurodegenerative Diseases Brain Bank, South West Dementia Brain Bank and Newcastle Brain Tissue Resource, deriving also from very old individuals (≥ 80-year-old). It is important to highlight that all healthy control samples did not have a history of psychiatric diseases.

Table 7. Post-mortem hippocampal healthy donor samples information. Information about gender, age (years), origin, cause of death, agonal state (1-3), post-mortem delay (hours) and RNA integrity number are reported for each sample. Age group is indicated. M = male; F = female; PMD = post-mortem delay; RIN = RNA integrity number; MRC Brain Bank = MRC London Neurodegenerative Diseases Brain Bank; SWDBB = South West Dementia Brain Bank; NBTR = Newcastle Brain Tissue Resource.

Age group	ID	Gender	Age (years)	Origin	Cause of death	Agonal state (1-3)	PMD (hours)	RIN
20-39y	hHIPPO C18	M	21	Dedicated study	Work accident	1	75	/
	hHIPPO C2	M	25	Dedicated study	Intoxication	3	44	5.9
	hHIPPO C20	M	35	Dedicated study	Car accident	1	50	4.8
	hHIPPO C12	M	39	Dedicated study	Hypersensitivity reaction	3	50	5.9
40-59y	hHIPPO C9	M	44	Dedicated study	Ischemic heart disease	1	30	5.5
	hHIPPO C21	M	47	Dedicated study	Overdose	3	50	4.7
	hHIPPO C14	M	49	Dedicated study	Ischemic heart disease	1	68	5.9
	hHIPPO C17	M	50	Dedicated study	Ischemic heart disease	1	60	7.5
	hHIPPO C4	F	53	Dedicated study	Sepsis	3	28	6.2
	hHIPPO C19	M	54	Dedicated study	Arrhythmia	2	30	5.3
	hHIPPO C11	M	54	Dedicated study	Ischemic heart disease	1	30	6.6
	hHIPPO C13	F	56	Dedicated study	Car accident	1	27	6.0
	hHIPPO C6	M	59	Dedicated study	Ischemic heart disease	1	24	/
60-79y	hHIPPO C22	F	60	Dedicated study	Ischemic heart disease	1	80	5.9
	hHIPPO C7	M	66	Dedicated study	Ischemic heart disease	1	26	5.4
	hHIPPO C3	F	70	Dedicated study	Chronic obstructive pulmonary disease	3	40	5.4
	hHIPPO C8	F	71	Dedicated study	Pulmonary embolism	3	70	/
	hHIPPO C10	M	71	Dedicated study	Ischemic heart disease	1	24	6.5
	hHIPPO C25	M	73	MRC Brain Bank	Cancer	3	23	/
	hHIPPO C26	M	74	MRC Brain Bank	Natural death	2	22,5	5.1
	hHIPPO C1	F	77	Dedicated study	Car accident	1	72	/
	hHIPPO C29	M	77	MRC Brain Bank	Cancer	3	1	/
	hHIPPO C27	M	78	MRC Brain Bank	Infection	3	24	4.6
≥80y	hHIPPO C23	M	80	MRC Brain Bank	Natural death	2	11	4.8
	hHIPPO C28	M	82	MRC Brain Bank	Cancer	3	24	/
	hHIPPO C16	F	85	SWDBB	Ischemic enterocolitis	2	14	4.8
	hHIPPO C30	M	87	NBTR	Renal failure	2	8	/
	hHIPPO C24	F	92	MRC Brain Bank	Natural death	2	9	5
	hHIPPO C31	F	94	NBTR	Ischemic heart disease	1	15	/
	hHIPPO C15	M	96	SWDBB	Bronchopneumonia	3	21	5.5

To date, we collected 9 female and 21 male hippocampal samples from 21- to 96-year-old subjects and 7 samples from individuals who committed suicide with ages ranging from 22 to 90 years old. Sex, age, cause of death and post-mortem delay (PMD) were available for each donor. We also evaluated the agonal state of the donors because it is known that pre-mortem events impact on extracted RNA quality by affecting brain acidosis [216-219]. We scored agonal state on the basis of the cause of death, using a three-point scale classification adapted from [220]. Extracted RNA quality was assessed measuring RNA integrity number (RIN),

which set between 4.6 and 7.5 a range declared elsewhere [243] as sufficient for the purpose of our analyses. In Table 7 and 8 information about hippocampal samples and donors are reported.

Table 8. Information about post-mortem hippocampal samples derived from suicide victims. Information about gender, age (years), origin, cause of death, agonal state (1-3), post-mortem delay (hours) and RNA integrity number are reported for each sample. M = male; F = female; PMD = post-mortem delay; RIN = RNA integrity number.

ID	Gender	Age (years)	Origin	Cause of death	Agonal state (1-3)	PMD (hours)	RIN
hHIPPO S1	F	22	Dedicated study	Suicide	2	56	/
hHIPPO S5	M	28	Dedicated study	Suicide	2	80	6.0
hHIPPO S7	M	41	Dedicated study	Suicide	2	70	6.5
hHIPPO S8	F	44	Dedicated study	Suicide	2	71	5.0
hHIPPO S2	F	51	Dedicated study	Suicide	2	42	4.6
hHIPPO S3	F	59	Dedicated study	Suicide	2	55	4.7
hHIPPO S4	F	90	Dedicated study	Suicide	2	80	5.9

4.2.1 LSD1 and neuroLSD1 are modulated during aging

Aging of the human society represents a challenging consequence of increased well-being that started within the 20th century and continues strait on the 21st. Indeed, inexorable growth of the older age groups overloads the healthcare systems, posing interesting challenges as how to ameliorate working abilities, physiological functioning and independency of the elderly. Age-associated cognitive and executive decline represents therefore an increasing clinical issue, warranting new molecular studies aimed at improving health in older adults. Normal brain aging process is associated with physiological changes and neurological conditions, among which hippocampal, temporal and frontal lobe atrophy [244]. One of all, age-associated reductions in gray matter have been shown to negatively impact cognitive functions [245]. In line, the most common deficit among elderly is memory decline and related cognitive impairment [246]. The neurobiological bases of age-associated memory deficits include epigenetic changes that are able to modulate the responsiveness of neuroplasticity-related IEGs, thoroughly limiting the ability of the aged brain to preserve plasticity [247]. LSD1 and its dominant negative splicing isoform neuroLSD1 are recruited on IEGs promoters by the Serum Response Factor (SRF) transcription factor, contributing in setting the chromatin state of this plasticity-related genes [44, 101], whose activity-evoked transcription is reduced during aging. Direct evidence supporting the idea that LSD1 and

neuroLSD1 regulate the transcriptional substrates of memory and cognition came from the observation that neuroLSD1^{KO} mice show an impaired memory in the Novel Object Recognition test [42, 103]. This is why we hypothesized a functional relevance for LSD1 and neuroLSD1 in age-related physiological decline. The first transcription factor described to tether LSD1 at the level of target genes promoter was RE1-Silencing Transcription factor (REST). Relevantly, an increased expression of this transcriptional repressor has been recently associated to a protective role in the human aging brain, increasing neuronal survival through the repression of genes involved in cell death pathways and genes associated with Alzheimer Disease and dementia [248]. These results pointed to an important role of REST repressive function (largely accounting on corepressors among which LSD1) more than on REST overexpression *per se* in healthy neuronal preservation. Last but not least, in aged mouse brain, increased LSD1 and decreased neuroLSD1 relative mRNA levels were detected [42].

Given this evidence, we decided to investigate LSD1 and neuroLSD1 modulation in human brain aging. We performed molecular analyses on RNA extracted from post-mortem hippocampal samples described above in order to assess a possible LSD1/neuroLSD1. Data collected from qRT-PCR performed on these samples showed that LSD1 expression slightly decreases along with aging (Figure 48A). Since this qRT-PCR was performed with pan-isoform primers annealing to exon E15 and E16, we performed a neuroLSD1-specific qRT-PCR using a forward primer annealing to exon E8-E8a-E9 junction and a reverse primer annealing to E9. This experiment remarkably confirmed that neuroLSD1 is present in the human hippocampus. Moreover, it showed a marked neuroLSD1 downregulation during aging (Figure 48B). We indeed noticed that neuroLSD1 transcripts reached almost undetectable levels in the elderly (≥ 80-year-old age group). Therefore, we decided to verify if LSD1/neuroLSD1 splicing ratio would be maintained during brain aging. We performed rqfRT-PCR and we observed that in post-mortem human hippocampal samples neuroLSD1 relative expression percentage decreases along with aging (Figure 48C). Although our collected samples were not balanced for gender, we did not observe differences comparing males and females (Figure 49).

Considering that the pro-repressive LSD1 isoform is virtually the only one present in aged human hippocampus, these results suggest that LSD1 increases its repressive activity during human brain aging through a splicing based mechanism.

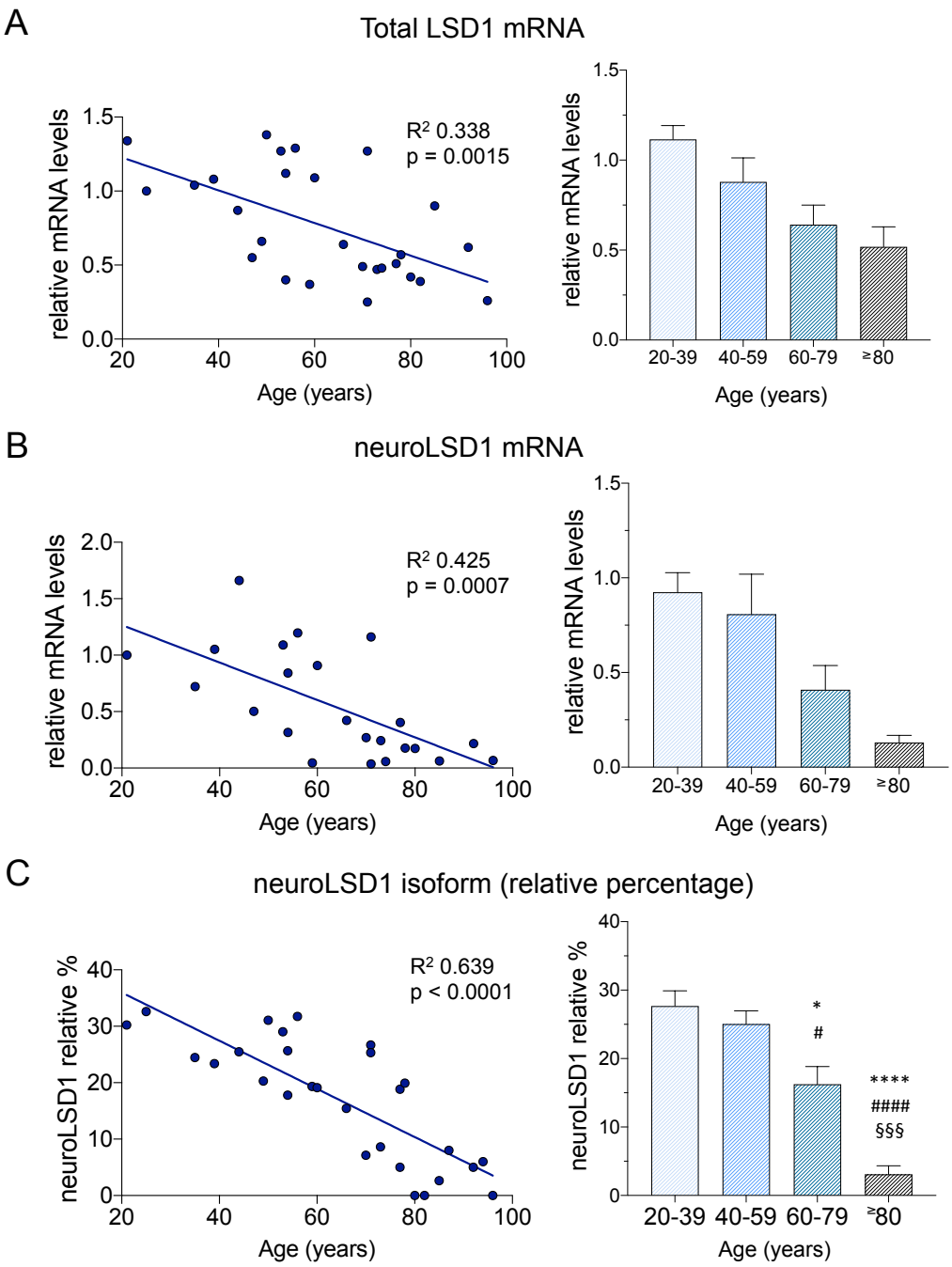

Figure 48. Along with aging, increased LSD1 and decreased neuroLSD1 relative ratio is observed in the human hippocampus. (A) Linear regression analysis of LSD1 expression and age, assessed by qRT-PCR using pan-isoform primers, on the left. On the right, same data are shown clustered in age groups. (B) On the left, linear regression analysis of neuroLSD1 expression and age, evaluated with qRT-PCR using isoform-specific primers. On the right, data are shown clustered in age ranges. Transcripts expression was normalized over RPL13. (C) Linear regression analysis of neuroLSD1 relative percentage, assessed by rqfRT-PCR, along with aging, on the left. On the right, data are clustered in age groups. Data are presented as means ± SEM. * Refers to 20-39y group. *p<0.01, ***p<0.0001, one-way ANOVA Tukey *post hoc* test.

These are the first data collected from human samples and are described in a submitted article [103] corroborating the proposed hypothesis according to which glutamate-mediated neuroLSD1 downregulation is a negative feedback mechanism aimed at restraining neuronal

excitatory responses in the hippocampus, participating to stress termination and to the buffering of memory consolidation.

Further analyses are needed to investigate whether LSD1 increase and concomitant neuroLSD1 decrease during brain aging could be protective or detrimental.

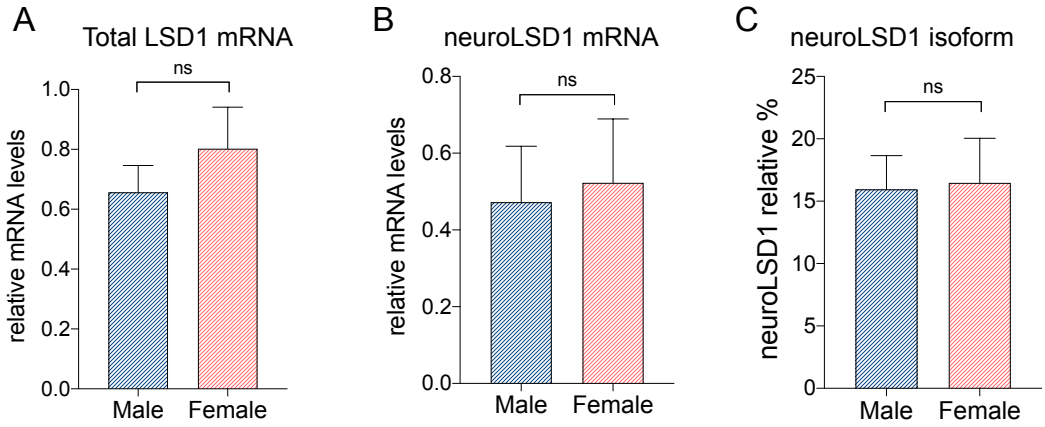

Figure 49. LSD1 and neuroLSD1 expression did not show a gender effect in the analyzed human post-mortem hippocampal samples. LSD1 (A) and neuroLSD1 (B) expression, assessed by qRT-PCR, comparing males and females. (C) NeuroLSD1 relative percentage assessed by rqfRT-PCR comparing males and females. All male and all female samples were pool together in the analysis of gender-effect. Data are presented as means ± SEM.

4.2.2 Increased neuroLSD1 levels could be correlated with neuropsychiatric-relevant behavior

In vitro and in vivo experiments performed in our lab [44, 103, 109] suggest LSD1 and neuroLSD1 splicing modulation, shifting LSD1 isoforms splicing balance towards a more repressive layout, as a homeostatic mechanism aimed at limiting the toxic effect of stress. Accordingly, an aberrant regulation of this stress-response buffering mechanism could concur to stress-vulnerability.

In order to better investigate LSD1 and neuroLSD1 relevance in the onset of neuropsychiatric disorders in humans, we collected hippocampal specimens from suicide individuals and controls through a multicentric study coordinated by Dr. Maria Paola Bonasoni that involves the Forensic Medicine Unit of Arcispedale Santa Maria Nuova ASMN/IRCCS in Reggio Emilia, University of Parma and University of Ancona (Italy).

The particular choice of suicidal victims as neuropsychiatric patients has to be related to multiple reasons. First of all, the mortality risk for suicide is strongly associated to neuropsychiatric disorders. Indeed, incidence of suicide in depressed people is several times higher than in the general population and more than 50% of all people who die by suicide meet criteria for major depressive disorder (MDD) [242]. Although not all suicide individuals

match the criteria for MDD, 90% of the remaining suicides have a neuropsychiatric disorder of a different nature, such as bipolar disorder and schizophrenia [249]. Moreover, suicidal behavior can be interpreted as a typical vulnerability-related behavior [249]. Given that we proposed that an aberrant stress-induced LSD1 and neuroLSD1 splicing modulation entails the loss of a homeostatic mechanism underlying stress-vulnerability, our choice of suicides hippocampal samples to evaluate LSD1 role in stress-induced neuropsychiatric disorder, among which MDD, might therefore be appropriate. Last but not least, another reason is mainly related to post-mortem brain availability. As a matter of fact, suicide victims' parents and Public Prosecutors frequently ask legal autopsies increasing the availability of these samples.

Until now, we gathered 7 post-mortem human hippocampal samples deriving from individuals who undertook suicidal choice and we carried out rqfRT-PCR on RNA extracted from these samples. We analyzed data plotting controls and suicide neuroLSD1 relative percentage along with aging (Figure 50A). As described previously, a significant inverse correlation between neuroLSD1 levels and age could be detected. Conversely, in suicidal samples this correlation seemed to be loss and we measured higher neuroLSD1 relative percentage compared to controls. Since specimens belong to patients whose ages are mainly clustered among 45 and 60 years old, we focused on this age range (Figure 50B). Interestingly, in suicidal samples higher levels of neuroLSD1 can be scored in the adulthood. However, considering that our samples were not balanced for gender, indeed 5 out of 7 samples belong to female subjects, a female gender-specific analysis needed to be done. Similarly, we observed higher levels of neuroLSD1 relative percentage also comparing 5 suicidal women to 7 control ones (Figure 50C).

These are the first data obtained on human samples deriving from neuropsychiatrc patients and suggest that specific LSD1/neuroLSD1 ratio alteration in the human hippocampus correlates with psychiatric-relevant behavior often associated with depression early in life, pointing out an aberrant LSD1/neuroLSD1 splicing ratio as a possible signature of psychiatric disorders in the human hippocampus.

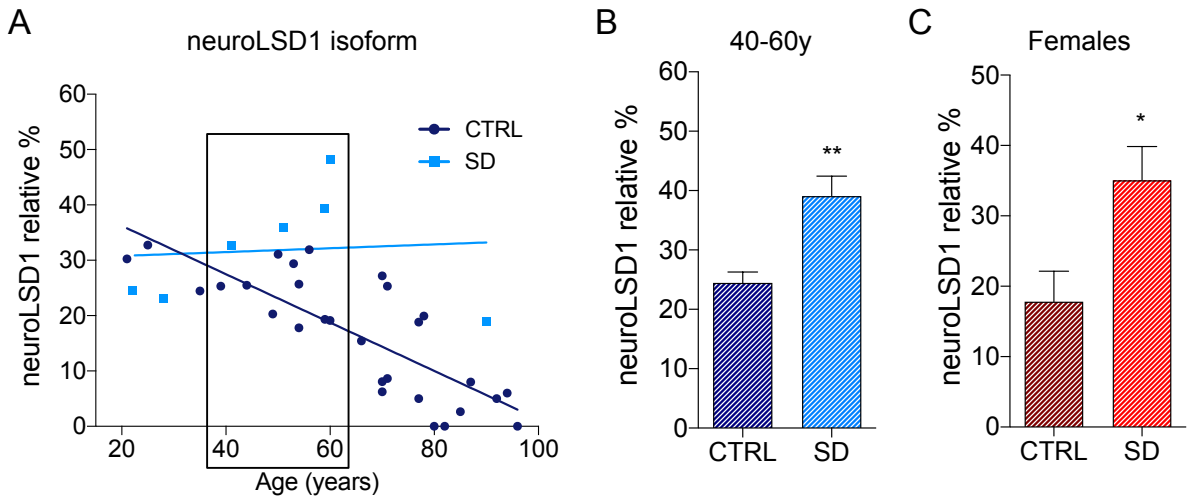

Figure 50. In the hippocampus, increased neuroLSD1 splicing can be scored in individuals who undertook suicidal choice. (A) Linear regression analysis of neuroLSD1 splicing and age, comparing suicidal individuals (SD in light blue) to control ones (CTRL in blue). (B) NeuroLSD1 relative percentage in the adulthood comparing suicide and control. Samples included in this analysis are highlighted with a square in the linear regression. (C) Female-restricted neuroLSD1 relative percentage evaluation in suicidal subjects (SD) and controls (CTRL). Data are presented as means ± SEM. *p<0.01, **p<0.001, Student's t test.

As suggested above, an aberrant LSD1/neuroLSD1 isoform ratio might be related to specific genetic conditions, for instance mutations in *RBFOX1* gene, or the presence of a "vulnerable" *LSD1* allele, or several other genetic factors. However, and independently from a specific genetic setting, it is interesting to explore the possibility that the splicing mechanism regulating LSD1/neuroLSD1 homeostatic stress response, might per se loose the ability to respond after several stress sessions. Indeed, the engagement of adaptive responses that occurs upon acute stress is often disrupted after chronic stress [101, 109]. To this aim, we performed a chronic social defeat protocol, to evaluate if the plastic neuroLSD1 splicing downregulation that in general occurs in the 85% of the analyzed mice (Figure 51C) was maintained after 10 sections of social defeat stress.

We performed a chronic social defeat stress (CSDS). Once a day for 10 days two-month-old male mice were defeated in a direct interaction with a CD1 aggressor mouse for 5 minutes and then kept in visual and olfactory interaction during the 7-hour-long psychosocial stress phase. Intruder mice are not subjected with a continuous 24/24 hours stress for 10 days but returns to their home cages, far from the stressor CD1 mouse, every evening to recover. This resting phase allowed LSD1/neuroLSD1 splicing ratio to return to control levels (Figure 51A). We carried out the evaluation of LSD1 splicing isoforms in the mouse hippocampus after the resting phase of the 9th stress session and after the stress on 10th day. We observed that LSD1/neuroLSD1 rescue occurred also during the resting phase of 9th stress session. However, the neuroLSD1 downregulation that we observe after 10 days of CSDS was

noticeably smaller compared to the one that occurred during the first stress session (ASDS) (Figure 51D) as we have already published in [109]. What is more important is that following ten daily subsequent social defeats, the percentage of mice that are still able to downregulate neuroLSD1 the last day considerably decreases with only 57% of responders and 43% of non-responders (Figure 51E and 51F).

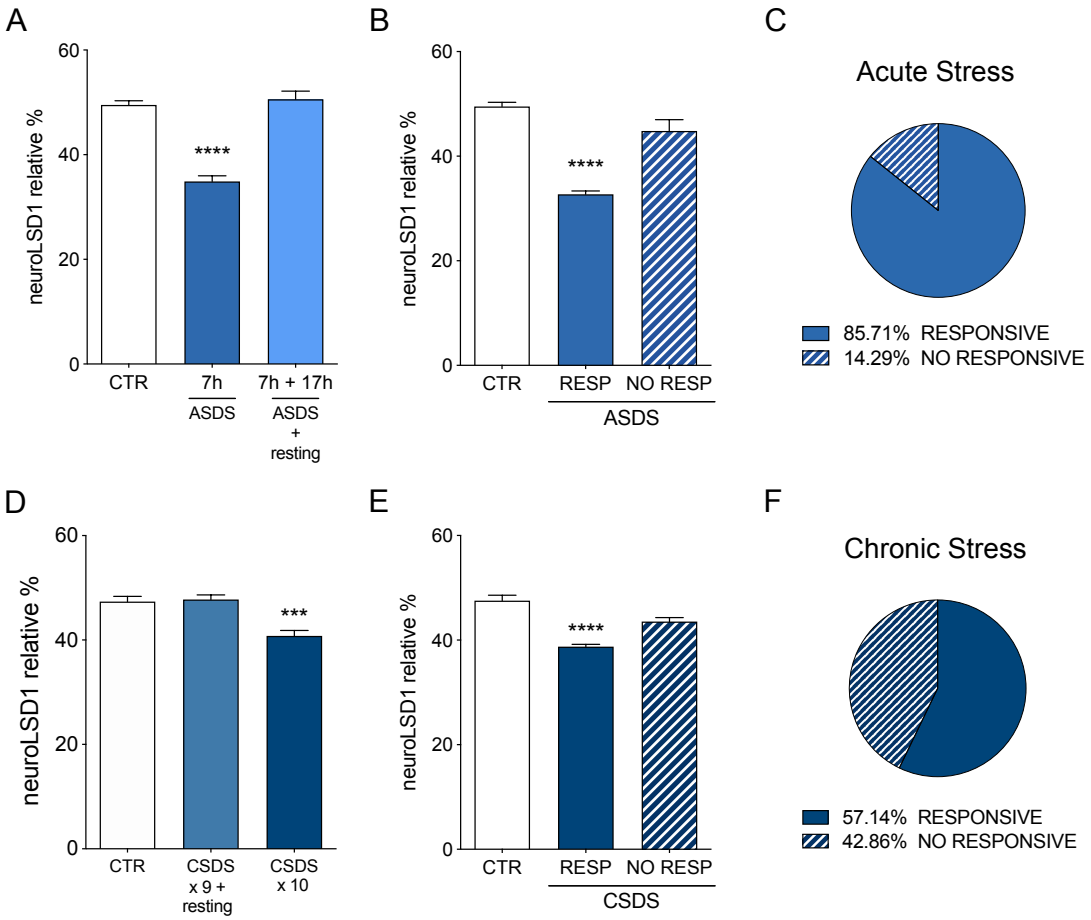

Figure 51. Chronic psychosocial stress hampers in a subset of mice (non responders) the ability to downregulate neuroLSD1 in the hippocampus. (A) NeuroLSD1 relative percentage upon ASDS comparing defeated mice after 7-hour-long psychosocial stress (ASDS 7h) and after the recovery phase (ASDS 7h + resting) to control mice (CTRL). (B) NeuroLSD1 relative percentage upon ASDS comparing responder (RESP) and non-responder (NO RESP) defeated mice after 7-hour-long psychosocial stress to control mice (CTRL). (C) Percentage of responder mice upon ASDS. (D) NeuroLSD1 relative percentage upon CSDS comparing defeated mice after nine-day stress who underwent recovery (CSDS x 9 + resting) and after the 10th 7-hour-long psychosocial stress (CSDS x 10) to control mice (CTRL). (E) NeuroLSD1 relative percentage upon CSDS comparing responder (RESP) and non-responder (NO RESP) defeated mice to control mice (CTRL). (F) Percentage of responder mice upon CSDS. The evaluation of neuroLSD1 relative percentage was assessed by rqfRT-PCR. Data are presented as means ± SEM. * referred to controls. *** $p<0.001$, **** $p<0.0001$, one-way ANOVA Tukey's post hoc test.

These data indicate that stress reiteration is able to hamper in a discrete subset of mice the ability to shift LSD1 and neuroLSD1 splicing towards an adaptive homeostatic balance. We hypothesized that the desensitization of this splicing based physiological protective mechanism of stress response could contribute to the divergence point between engaging resiliency or vulnerability pathways. This hypothesis will be evaluated performing a Social

Interaction Test (SIT) to distinguish between resilient and susceptible mice after CSDS, and is currently under investigation. This experiment will allow us verify if the neuroLSD1 splicing repression process that normally occurs in naïve mice in response to stress, is a protective mechanism required for an healthy stress response and if its corruption might be a pathogenic mechanism involved in the onset of stress-related psychiatric disorders.

5 DISCUSSION AND CONCLUSION

5.1 LSD1-associated genetic bases of stress-related neuropsychiatric disorders

According to our results a picture emerges in which the splicing factor RBFOX1, representing one of the few genetic loci strongly associated to Major Depressive Disorder (MDD), is engaged as a higher primate-specific strategy to finely tune LSD1/neuroLSD1 splicing ratio, possibly modifying LSD1-driven response to stress.

We discovered that RBFOX1 positively regulates the alternative splicing of a new LSD1 cryptic exon, that we named exon E8b because of its position within *LSD1* gene, both in minigene-derived products and in endogenous LSD1 transcripts. A relevant aspect that characterizes exon E8b is its higher primate-restricted splicing, due to E8b 5' splice site conservation. E8b-containing LSD1 transcripts are ubiquitously expressed in human tissues, according to the fact that the activity of RBFOX proteins, which specifically bind the same (U)GCAUG element, is ubiquitously represented in all human tissues. Exon E8b inclusion, due to the presence of an in-frame premature stop codon at its 5' end, provides LSD1 with a new regulatory mechanism based on transcripts degradation through nonsense-mediated decay (NMD). Exploiting a stable cell line carrying inducible RBFOX1 expression, we showed that an increase in RBFOX1 levels is indeed able to reduce LSD1 transcript and protein levels. We further demonstrated that in neuronal tissues E8b is included both in E8a-containing and E8a-skipping LSD1 isoforms. Remarkably, E8b is preferentially included in neuroLSD1 transcripts, likely affecting LSD1/neuroLSD1 splicing ratio through the preferential degradation of neuroLSD1 isoform. Together, this data point to a new primate-restricted additional level of regulation exerted by RBFOX1 dedicated not only to total LSD1 levels control in non-neuronal tissues, but also to the regulation of LSD1/neuroLSD1 ratio in neurons. We previously showed that correct tuning of LSD1/neuroLSD1 ratio in the hippocampus is crucial to guarantee homeostatic adaptive plasticity in response to environmental stimuli, possibly in the frame of a stress-resiliency instrumental pathway. In this regard, we must highlight that RBFOX1 activity is itself modulated in a homeostatic fashion in response to neuronal activation [190] via a splicing dependent mechanism aimed at restoring resting level neuronal excitability. Interestingly, upon a stressful challenge, RBFOX1 shuts down CRH levels to terminate HPA axis activation in the mouse hypothalamus, extending its homeostatic function to the proper regulation of stress response in the mammalian brain [195]. Within this work, we observed that the same splicing-based modulation occurs also in the mouse hippocampus in response

to acute psychosocial stress, suggesting a brain area-integrated role for RBFOX1 in the homeostatic modulation of stress response. Taken together, these results led us hypothesizing that another mechanism through which RBFOX1 participates in stress response might be related to its regulatory role on neuroLSD1. Further studies will be aimed at dissecting RBFOX1 functional role in regulating LSD1 levels and neuroLSD1 splicing ratio both in physiological and pathological human conditions.

LSD1 involvement in non-neurological diseases seems to strengthen the link between RBFOX1 and LSD1 expression. LSD1 is highly expressed in ovarian cancer and its overexpression correlates with an aggressive transcriptomic signature observed in ovarian tumors associated with poor prognosis [250, 251]. It is interesting that in these aggressive cancers RBFOX2 undergoes downregulation [204]. Considering that E8b expression is enriched in human ovarian tissue, one of the mechanisms involved in LSD1 regulation in ovarian cancer could be based on RBFOX2-mediated exon E8b inclusion in LSD1 mature transcripts.

Within these years I discovered that LSD1 and neuroLSD1 are post-transcriptional targets of RBFOX1, which has been genetically associated to MDD through a genome-wide association study involving an unprecedented number of depressed individuals [203]. Consistently, RBFOX1-mediated LSD1 and neuroLSD1 modulation could play an important role in engaging resilient or susceptible phenotypes in response to traumatic events in terms of protecting, or favouring, the onset of stress-related neuropsychiatric drift. Remarkably, another genetic source of stress resiliency or vulnerability could involve *LSD1* gene also independently on its functional interactions with RBFOX1. In this regard, we demonstrated that LSD1 and neuroLSD1 alternative splicing mechanisms is regulated by regulatory intronic single nucleotide variants. We disclosed that a single SNP within exon E8a flanking introns is able *per se* to affect E8a splicing process. In particular the presence of minor allele of SNP rs778266261, which is present in almost 1.5% of individuals in the Italian population, is associated to a reduced inclusion of exon E8a in minigene-derived splicing products in basal condition. These data suggest that this single nucleotide variation could modify basal or activity-dependent LSD1/neuroLSD1 splicing ratio in the human brain hence potentially contributing in setting different levels of stress-plasticity consolidation among the human population, impinging the *quality* of traumatic memories. Concordantly, *LSD1* variants that generate different levels of neuroLSD1 isoform might be involved in setting stress-response interindividual variability impacting anxiety profile. It will be interesting to explore a possible

association of SNP rs778266261 or other *LSD1* polymorphisms with stress-resilient or -vulnerable phenotypes. In this perspective, a genetic case-control study aimed at scoring the frequency of LSD1 genetic variants in individuals suffering of major depressive disorder (MDD), post-traumatic stress disorder (PTSD) or other stress-related neuropsychiatric diseases, would corroborate the hypothesis of a *LSD1*-related genetic predisposition underlying aberrant stress response or providing possible genetic biomarkers for susceptibility or resiliency in humans.

5.2 LSD1/neuroLSD1 ratio is dynamically modulated in physiological and pathological conditions in humans

We performed a characterization of LSD1 and neuroLSD1 transcriptional profile on human post-mortem brain samples, which allowed us to unambiguously demonstrate that the regulation of LSD1/neuroLSD1 balance is finely tuned also in the human brain. We discovered that LSD1/neuroLSD1 modulation is somehow implicated in the process of brain aging as well as in stress-related disorders also in humans.

Our observations suggest that in the hippocampus LSD1 increases its repressive activity during aging in humans, through a splicing-based mechanism that shifts the isoforms balance towards a reduction in neuroLSD1 expression. This age-related increase of LSD1 levels could take part in preventing neuronal overstimulation and death. This hypothesis is based on a solid literature in which the transcription factor REST is described as a prominent neuroprotective factor during aging, and overexpressed in centenarians' brain [248, 252]. Transcriptional repressor REST adopts LSD1/CoREST/HDAC2, as co-repressive molecular tool. This evidence, in association with increased LSD1 activity in the old brain, suggests a cooperative partnership warranting further investigations. On the other side, since neuroLSD1 has an important role in the regulation of IEGs as a gate-like function in memory formation, the resulting neuroLSD1 progressive hippocampal unavailability during aging will likely contribute to negatively impact brain plasticity, concurring to age-related decline of cognitive processes. In other words, the neuroprotective contribution of LSD1 to REST repressive activity, might exert a neuroplastic cost, entailing a concomitant negative effect on SRF-mediated transcriptional modulation of learning and memory consolidation. Thus, LSD1 and neuroLSD1 modulation concurs to the establishment of a fine equilibrium between neuroprotection and neuroplasticity, two antagonistic processes that have to be optimally balanced for a healthy aging. In this conceptual frame, an aberrant regulation of

LSD1/neuroLSD1 splicing process, unbalancing the system towards one extreme or the other, might actually concur to age-related neuropsychiatric disorders, or represent a possible molecular substrate for age-related metabolic and inflammatory pathologies cumulatively referred to as frailty.

Interestingly, preliminary data obtained from post-mortem human hippocampal samples deriving from individuals who underwent suicidal death show that LSD1/neuroLSD1 relative ratio is decreased in all age ranges and the correlation between neuroLSD1 downregulation and aging is partially lost. In other words, we observed an alteration of LSD1/neuroLSD1 ratio towards increased levels of neuroLSD1 splicing associated to a condition, the suicidal choice, which quintessentially suggests a psychiatric-relevant interruption of the instinctive ontological conservation, not to mention the tragically-diffused comorbidity between neuropsychiatric disorders and suicide all over the world. Further studies are needed to investigate whether an higher neuroLSD1 expression in the human hippocampus could represent a genetic drive favoring the suicidal state of mind or whether the onset of neuropsychiatric disorders in humans is possibly fostered as a result of maladaptive responses to repeated or severe stressful events in susceptible individuals. In other words, understanding whether neuroLSD1 increase in the human hippocampus is a cause or a consequence of neuropsychiatric disorders. In any case, these data pinpoint the aberrant LSD1/neuroLSD1 splicing ratio as a possible signature of psychiatric disorders in the human hippocampus.

As a matter of fact, compared to that induced by a single acute stressful, *chronic* psychosocial stress less efficiently elicits neuroLSD1 homeostatic downregulation in the mouse hippocampus [109]. Relevantly, we observed that stress reiteration prevents, in a defined percentage of mice, the ability to shift LSD1 and neuroLSD1 splicing towards the adaptive homeostatic balance. This led us hypothesizing that the *desensitization* of LSD1/neuroLSD1 splicing-based physiological protective mechanism of stress response could contribute to the divergence point between engaging resiliency or vulnerability pathways.

5.3 An evolutionary perspective

Nowadays, it is commonly accepted that changes in regulatory mechanisms play an important role in speciation and adaptation. Among them, alternative splicing is considered a powerful mechanism underlying proteomic and transcriptomic changes, contributing in giving rise to phenotypic differences among vertebrates [149]. In the brain, alternative splicing represents

a plausible means for combined gene expression and protein function regulation allowing a fine control of fundamental neuronal processes [151, 152, 253] and concurring to the establishment of complex brain functions, such as cognitive and emotional information processing [155, 156]. From an evolutionary point of view, alternative splicing contributes to increase organisms' complexity in terms of brain performances, providing the organisms with improved abilities to adapt to an ever-changing environment, especially in primates and humans [149].

LSD1 gene particularly reflects these evidences. The neurospecific alternatively spliced exon E8a appeared in mammals generating the dominant negative isoform neuroLSD1 [91]. The regulation of neuroLSD1 expression represents a mammalian-specific mechanism to increase the layers of LSD1 repressive activity tuning at the level of its plasticity-related target genes [91]. In the mammalian brain, LSD1 not only represents a transducer of environmental stimuli, but, thanks to neuroLSD1, it also acquires the role of epigenetic modifier of homeostatic control of stress-response aimed at limiting the toxic effect of stress and promoting adaptation also at the behavioral level [44, 103, 109]. Accordingly, dysregulation of LSD1-driven stress-coping strategy, a condition that we observed upon chronic psychosocial stress, could concur to stress-vulnerability. In line, an aberrant LSD1/neuroLSD1 balance can be associated to a stress-related psychiatric relevant behavior (suicidal death). Moreover, LSD1/neuroLSD1 splicing ratio can be genetically determined by the presence of single nucleotide regulatory variants, possibly contributing to the implementation of different stereotypic adaptive behaviors among the population, entailing different shades of bravery and prudence, which increases mammalian ability to adapt to the environment in the frame of a population-related resiliency. In this context, resilience or susceptibility to stress might be also related to genetically modified LSD1/neuroLSD1 ratios, predisposing to or protecting against stress disorders.

Furthermore, we demonstrated that a novel LSD1 alternative splicing event takes place being restricted to higher primates, leading to the inclusion of the "poison" exon E8b, increasing the overall complexity and tunability of the system. We can assume that during evolution a single base mutation, implementing exon E8b acceptor site, appeared in a higher primate ancestor to whom it provided evolutionary advantage. RBFOX1, by virtue of its regulatory role toward E8b inclusion in LSD1 transcripts, is engaged as a new possible regulator of LSD1-driven homeostatic stress-response, enriching the modulation of LSD1/neuroLSD1 ratio with an additional molecular switch. Thus, E8b splicing likely entails an advantage, possibly contributing to improve adaptation concurring to increase the complexity of cognitive and

social abilities in higher primates. On the other hand, we must consider that the same changes allowing emergent complexity also represent a novel vulnerability harbor multiplying susceptibility substrates for neuropsychiatric disorder. It is not a coincidence, hence, that RBFOX1 has recently been listed among the few genetic loci strongly associated to major depressive disorder (MDD) [203].

How can we explain the fact that natural selection leads not only to advantages but also to system vulnerability? A possible answer to this question may be the more complex is the system, the easier is to negatively interfering with it.

However, we cannot overlook the fact that individuals, whose vulnerability is higher compared to the rest of the population, often display forms of geniality or peculiar creativity. In line, schizophrenia is likely to be influenced by various balancing advantages such as creativity [254]. An interesting consideration stems from the example of *Neuregulin 1* gene (*NRG1*). The same biologically relevant polymorphism in *NRG1* promoter, shown to be related to psychosis risk [255], has been also associated with extreme creativity in people with high intellectual achievement [256]. It seems that genetic variations related to mental disorders are maintained in the populations because they may have a positive impact on psychological functions. This suggests that complex skills and oversensitivity, which could result in pathological conditions, may go hand in hand. Thus, can we infer that mental illness is the price we have to pay for our extremely complex and adaptable nervous system?

Other authors, however, propose a rather different, yet equally provocative answer. They observed that evolution selects individuals that are likely to be successful in generating offspring, rather than being characterized by high levels of health and happiness. As a result, aspects that we are used to label as negative, such as mental illness, may have been selected because they can give, under certain conditions, advantages to the human species [257].

Whatever the answer, there must be an evolutionary reason for psychiatric disorders. To appropriate and slightly paraphrase the title of a recent novel by Randolph M. Nesse [258], there must be some “good reasons for bad feelings”.

6. REFERENCES

1. de Kloet, E.R. et al. (2005) Stress, genes and the mechanism of programming the brain for later life. Neurosci Biobehav Rev 29 (2), 271-81.

2. Gold, P.W. (2015) The organization of the stress system and its dysregulation in depressive illness. Mol Psychiatry 20 (1), 32-47.

3. Joëls, M. and Baram, T.Z. (2009) The neuro-symphony of stress. Nat Rev Neurosci 10 (6), 459-66.

4. de Kloet, E.R. et al. (2005) Stress and the brain: from adaptation to disease. Nat Rev Neurosci 6 (6), 463-75.

5. McEwen, B.S. (2007) Physiology and neurobiology of stress and adaptation: central role of the brain. Physiol Rev 87 (3), 873-904.

6. McEwen, B.S. (2000) Allostasis and allostatic load: implications for neuropsychopharmacology. Neuropsychopharmacology 22 (2), 108-24.

7. Simpson, J.R. et al. (2001) Emotion-induced changes in human medial prefrontal cortex: II. During anticipatory anxiety. Proc Natl Acad Sci U S A 98 (2), 688-93.

8. Drevets, W.C. et al. (2008) The subgenual anterior cingulate cortex in mood disorders. CNS Spectr 13 (8), 663-81.

9. Price, J.L. and Drevets, W.C. (2012) Neural circuits underlying the pathophysiology of mood disorders. Trends Cogn Sci 16 (1), 61-71.

10. Purves, D. et al., N*euroscience*, Oxford University Press, 2007.

11. Sapolsky, R.M. et al. (2000) How do glucocorticoids influence stress responses? Integrating permissive, suppressive, stimulatory, and preparative actions. Endocr Rev 21 (1), 55-89.

12. Jankord, R. and Herman, J.P. (2008) Limbic regulation of hypothalamo-pituitary-adrenocortical function during acute and chronic stress. Ann N Y Acad Sci 1148, 64-73.

13. Kim, J.J. and Diamond, D.M. (2002) The stressed hippocampus, synaptic plasticity and lost memories. Nat Rev Neurosci 3 (6), 453-62.

14. Italia, M. et al. (2020) Rationale, Relevance, and Limits of Stress-Induced Psychopathology in Rodents as Models for Psychiatry Research: An Introductory Overview. Int J Mol Sci 21 (20).

15. Sun, H. et al. (2013) Epigenetics of the depressed brain: role of histone acetylation and methylation. Neuropsychopharmacology 38 (1), 124-37.

16. Rusconi, F. and Battaglioli, E. (2018) Acute Stress-Induced Epigenetic Modulations and Their Potential Protective Role Toward Depression. Front Mol Neurosci 11, 184.

17. McEwen, B.S. (2003) Mood disorders and allostatic load. Biol Psychiatry 54 (3), 200-7.

18. McEwen, B.S. et al. (2012) Stress and anxiety: structural plasticity and epigenetic regulation as a consequence of stress. Neuropharmacology 62 (1), 3-12.

19. Bagot, R.C. et al. (2014) Epigenetic signaling in psychiatric disorders: stress and depression. Dialogues Clin Neurosci 16 (3), 281-95.

20. Golden, S.A. et al. (2011) A standardized protocol for repeated social defeat stress in mice. Nat Protoc 6 (8), 1183-91.

21. Sanacora, G. et al. (2012) Towards a glutamate hypothesis of depression: an emerging frontier of neuropsychopharmacology for mood disorders. Neuropharmacology 62 (1), 63-77.

22. Chattarji, S. et al. (2015) Neighborhood matters: divergent patterns of stress-induced plasticity across the brain. Nat Neurosci 18 (10), 1364-75.

23. Joëls, M. et al. (2007) Chronic stress: implications for neuronal morphology, function and neurogenesis. Front Neuroendocrinol 28 (2-3), 72-96.

24. Golden, S.A. et al. (2013) Epigenetic regulation of RAC1 induces synaptic remodeling in stress disorders and depression. Nat Med 19 (3), 337-44.

25. McEwen, B.S. et al. (2015) Recognizing Resilience: Learning from the Effects of Stress on the Brain. Neurobiol Stress 1, 1-11.

26. McEwen, B.S. et al. (2016) Stress Effects on Neuronal Structure: Hippocampus, Amygdala, and Prefrontal Cortex. Neuropsychopharmacology 41 (1), 3-23.

27. Squire, L.R. and Zola-Morgan, S. (1991) The medial temporal lobe memory system. Science 253 (5026), 1380-6.

28. Martin, S.J. et al. (2000) Synaptic plasticity and memory: an evaluation of the hypothesis. Annu Rev Neurosci 23, 649-711.

29. Christian, K.M. et al. (2011) Chronic stress-induced hippocampal dendritic retraction requires CA3 NMDA receptors. Neuroscience 174, 26-36.

30. Cook, S.C. and Wellman, C.L. (2004) Chronic stress alters dendritic morphology in rat medial prefrontal cortex. J Neurobiol 60 (2), 236-48.

31. Goldwater, D.S. et al. (2009) Structural and functional alterations to rat medial prefrontal cortex following chronic restraint stress and recovery. Neuroscience 164 (2), 798-808.

32. Arnsten, A.F. (2015) Stress weakens prefrontal networks: molecular insults to higher cognition. Nat Neurosci 18 (10), 1376-85.

33. Mitra, R. et al. (2005) Stress duration modulates the spatiotemporal patterns of spine formation in the basolateral amygdala. Proc Natl Acad Sci U S A 102 (26), 9371-6.

34. Roozendaal, B. et al. (2009) Stress, memory and the amygdala. Nat Rev Neurosci 10 (6), 423-33.

35. Weaver, I.C. et al. (2004) Early environmental regulation of hippocampal glucocorticoid receptor gene expression: characterization of intracellular mediators and potential genomic target sites. Ann N Y Acad Sci 1024, 182-212.

36. Provençal, N. and Binder, E.B. (2015) The effects of early life stress on the epigenome: From the womb to adulthood and even before. Exp Neurol 268, 10-20.

37. Hunter, R.G. et al. (2009) Regulation of hippocampal H3 histone methylation by acute and chronic stress. Proc Natl Acad Sci U S A 106 (49), 20912-7.

38. Hunter, R.G. et al. (2012) Acute stress and hippocampal histone H3 lysine 9 trimethylation, a retrotransposon silencing response. Proc Natl Acad Sci U S A 109 (43), 17657-62.

39. Gupta, S. et al. (2010) Histone methylation regulates memory formation. J Neurosci 30 (10), 3589-99.

40. Saunderson, E.A. et al. (2016) Stress-induced gene expression and behavior are controlled by DNA methylation and methyl donor availability in the dentate gyrus. Proc Natl Acad Sci U S A 113 (17), 4830-5.

41. Shi, Y. et al. (2004) Histone demethylation mediated by the nuclear amine oxidase homolog LSD1. Cell 119 (7), 941-53.

42. Wang, J. et al. (2015) LSD1n is an H4K20 demethylase regulating memory formation via transcriptional elongation control. Nat Neurosci 18 (9), 1256-64.

43. Rusconi, F. et al. (2014) LSD1 Neurospecific Alternative Splicing Controls Neuronal Excitability in Mouse Models of Epilepsy. Cereb Cortex.

44. Rusconi, F. et al. (2016) LSD1 modulates stress-evoked transcription of immediate early genes and emotional behavior. Proc Natl Acad Sci U S A 113 (13), 3651-6.

45. Bagot, R.C. et al. (2015) Ventral hippocampal afferents to the nucleus accumbens regulate susceptibility to depression. Nat Commun 6, 7062.

46. Dallman, J.E. et al. (2004) A conserved role but different partners for the transcriptional corepressor CoREST in fly and mammalian nervous system formation. J Neurosci 24 (32), 7186-93.

47. Lakowski, B. et al. (2006) CoREST-like complexes regulate chromatin modification and neuronal gene expression. J Mol Neurosci 29 (3), 227-39.

48. Gemelli, T. et al. (2006) Postnatal loss of methyl-CpG binding protein 2 in the forebrain is sufficient to mediate behavioral aspects of Rett syndrome in mice. Biol Psychiatry 59 (5), 468-76.

49. Forneris, F. et al. (2005) Histone demethylation catalysed by LSD1 is a flavin-dependent oxidative process. FEBS Lett 579 (10), 2203-7.

50. Chen, Y. et al. (2006) Crystal structure of human histone lysine-specific demethylase 1 (LSD1). Proc Natl Acad Sci U S A 103 (38), 13956-61.

51. Aravind, L. and Iyer, L.M. (2002) The SWIRM domain: a conserved module found in chromosomal proteins points to novel chromatin-modifying activities. Genome Biol 3 (8), RESEARCH0039.

52. Rusconi, F. et al. (2017) NeuroLSD1: Splicing-Generated Epigenetic Enhancer of Neuroplasticity. Trends Neurosci 40 (1), 28-38.

53. Forneris, F. et al. (2008) LSD1: oxidative chemistry for multifaceted functions in chromatin regulation. Trends Biochem Sci 33 (4), 181-9.

54. Ballas, N. et al. (2001) Regulation of neuronal traits by a novel transcriptional complex. Neuron 31 (3), 353-65.

55. Struhl, K. (1998) Histone acetylation and transcriptional regulatory mechanisms. Genes Dev 12 (5), 599-606.

56. Bernstein, B.E. et al. (2005) Genomic maps and comparative analysis of histone modifications in human and mouse. Cell 120 (2), 169-81.

57. Lee, M.G. et al. (2005) An essential role for CoREST in nucleosomal histone 3 lysine 4 demethylation. Nature 437 (7057), 432-5.

58. Yang, M. et al. (2006) Structural basis for CoREST-dependent demethylation of nucleosomes by the human LSD1 histone demethylase. Mol Cell 23 (3), 377-87.

59. Battaglioli, E. et al. (2002) REST repression of neuronal genes requires components of the hSWI.SNF complex. J Biol Chem 277 (43), 41038-45.

60. Ballas, N. et al. (2005) REST and its corepressors mediate plasticity of neuronal gene chromatin throughout neurogenesis. Cell 121 (4), 645-657.

61. Sun, G. et al. (2010) Histone demethylase LSD1 regulates neural stem cell proliferation. Mol Cell Biol 30 (8), 1997-2005.

62. Sáez, J.E. et al. (2015) Decreased Expression of CoREST1 and CoREST2 Together with LSD1 and HDAC1/2 during Neuronal Differentiation. PLoS One 10 (6), e0131760.

63. Ballas, N. and Mandel, G. (2005) The many faces of REST oversee epigenetic programming of neuronal genes. Curr Opin Neurobiol 15 (5), 500-6.

64. Maiques-Diaz, A. and Somervaille, T.C. (2016) LSD1: biologic roles and therapeutic targeting. Epigenomics 8 (8), 1103-16.

65. Bhan, A. and Mandal, S.S. (2015) LncRNA HOTAIR: A master regulator of chromatin dynamics and cancer. Biochim Biophys Acta 1856 (1), 151-64.

66. Porro, A. et al. (2014) TERRA-reinforced association of LSD1 with MRE11 promotes processing of uncapped telomeres. Cell Rep 6 (4), 765-76.

67. Huang, J. et al. (2007) p53 is regulated by the lysine demethylase LSD1. Nature 449 (7158), 105-8.

68. Kontaki, H. and Talianidis, I. (2010) Lysine methylation regulates E2F1-induced cell death. Mol Cell 39 (1), 152-60.

69. Cho, H.S. et al. (2011) Demethylation of RB regulator MYPT1 by histone demethylase LSD1 promotes cell cycle progression in cancer cells. Cancer Res 71 (3), 655-60.

70. Bao, L. et al. (2018) Methylation of hypoxia-inducible factor (HIF)-1α by G9a/GLP inhibits HIF-1 transcriptional activity and cell migration. Nucleic Acids Res 46 (13), 6576-6591.

71. Metzger, E. et al. (2005) LSD1 demethylates repressive histone marks to promote androgen-receptor-dependent transcription. Nature 437 (7057), 436-9.

72. Nair, S.S. et al. (2010) PELP1 is a reader of histone H3 methylation that facilitates oestrogen receptor-alpha target gene activation by regulating lysine demethylase 1 specificity. EMBO Rep 11 (6), 438-44.

73. Kerenyi, M.A. et al. (2013) Histone demethylase Lsd1 represses hematopoietic stem and progenitor cell signatures during blood cell maturation. Elife 2, e00633.

74. Wang, J. et al. (2007) Opposing LSD1 complexes function in developmental gene activation and repression programmes. Nature 446 (7138), 882-7.

75. Kim, J. et al. (2015) LSD1 is essential for oocyte meiotic progression by regulating CDC25B expression in mice. Nat Commun 6, 10116.

76. Nam, H.J. et al. (2014) Phosphorylation of LSD1 by PKCα is crucial for circadian rhythmicity and phase resetting. Mol Cell 53 (5), 791-805.

77. Mosammaparast, N. et al. (2013) The histone demethylase LSD1/KDM1A promotes the DNA damage response. J Cell Biol 203 (3), 457-70.

78. Macfarlan, T.S. et al. (2011) Endogenous retroviruses and neighboring genes are coordinately repressed by LSD1/KDM1A. Genes Dev 25 (6), 594-607.

79. Hino, S. et al. (2012) FAD-dependent lysine-specific demethylase-1 regulates cellular energy expenditure. Nat Commun 3, 758.

80. Wang, J. et al. (2009) The lysine demethylase LSD1 (KDM1) is required for maintenance of global DNA methylation. Nat Genet 41 (1), 125-9.

81. Foster, C.T. et al. (2010) Lysine-specific demethylase 1 regulates the embryonic transcriptome and CoREST stability. Mol Cell Biol 30 (20), 4851-63.

82. Adamo, A. et al. (2011) LSD1 and pluripotency: a new player in the network. Cell Cycle 10 (19), 3215-6.

83. Hayami, S. et al. (2011) Overexpression of LSD1 contributes to human carcinogenesis through chromatin regulation in various cancers. Int J Cancer 128 (3), 574-86.

84. Majello, B. et al. (2019) Expanding the Role of the Histone Lysine-Specific Demethylase LSD1 in Cancer. Cancers (Basel) 11 (3).

85. Callegari, K. et al. (2018) Pharmacological inhibition of LSD1 activity blocks REST-dependent medulloblastoma cell migration. Cell Commun Signal 16 (1), 60.

86. Xu, S. et al. (2018) Optimization of 5-arylidene barbiturates as potent, selective, reversible LSD1 inhibitors for the treatment of acute promyelocytic leukemia. Bioorg Med Chem 26 (17), 4871-4880.

87. Macheleidt, I.F. et al. (2018) Preclinical studies reveal that LSD1 inhibition results in tumor growth arrest in lung adenocarcinoma independently of driver mutations. Mol Oncol 12 (11), 1965-1979.

88. Li, L. et al. (2019) Identification of selective and reversible LSD1 inhibitors with anti-metastasis activity by high-throughput docking. Bioorg Med Chem Lett 29 (4), 544-548.

89. Qin, Y. et al. (2019) Inhibition of histone lysine-specific demethylase 1 elicits breast tumor immunity and enhances antitumor efficacy of immune checkpoint blockade. Oncogene 38 (3), 390-405.

90. Soldi, R. et al. (2020) The novel reversible LSD1 inhibitor SP-2577 promotes anti-tumor immunity in SWItch/Sucrose-NonFermentable (SWI/SNF) complex mutated ovarian cancer. PLoS One 15 (7), e0235705.

91. Zibetti, C. et al. (2010) Alternative splicing of the histone demethylase LSD1/KDM1 contributes to the modulation of neurite morphogenesis in the mammalian nervous system. J Neurosci 30 (7), 2521-32.

92. Toffolo, E. et al. (2014) Phosphorylation of neuronal Lysine-Specific Demethylase 1LSD1/KDM1A impairs transcriptional repression by regulating interaction with CoREST and histone deacetylases HDAC1/2. J Neurochem 128 (5), 603-16.

93. Lee, M.G. et al. (2006) Functional interplay between histone demethylase and deacetylase enzymes. Mol Cell Biol 26 (17), 6395-402.

94. Etkin, A. et al. (2006) A role in learning for SRF: deletion in the adult forebrain disrupts LTD and the formation of an immediate memory of a novel context. Neuron 50 (1), 127-43.

95. Knöll, B. and Nordheim, A. (2009) Functional versatility of transcription factors in the nervous system: the SRF paradigm. Trends Neurosci 32 (8), 432-42.

96. Kim, T.K. et al. (2010) Widespread transcription at neuronal activity-regulated enhancers. Nature 465 (7295), 182-7.

97. West, A.E. and Greenberg, M.E. (2011) Neuronal activity-regulated gene transcription in synapse development and cognitive function. Cold Spring Harb Perspect Biol 3 (6).

98. Madabhushi, R. et al. (2015) Activity-Induced DNA Breaks Govern the Expression of Neuronal Early-Response Genes. Cell 161 (7), 1592-605.

99. Minatohara, K. et al. (2015) Role of Immediate-Early Genes in Synaptic Plasticity and Neuronal Ensembles Underlying the Memory Trace. Front Mol Neurosci 8, 78.

100. Belaguli, N.S. et al. (1999) Dominant negative murine serum response factor: alternative splicing within the activation domain inhibits transactivation of serum response factor binding targets. Mol Cell Biol 19 (7), 4582-91.

101. Gerosa, L. et al. (2019) SRF and SRFΔ5 Splicing Isoform Recruit Corepressor LSD1/KDM1A Modifying Structural Neuroplasticity and Environmental Stress Response. Mol Neurobiol.

102. Laurent, B. et al. (2015) A Specific LSD1/KDM1A Isoform Regulates Neuronal Differentiation through H3K9 Demethylation. Mol Cell 57 (6), 957-70.

103. Longaretti A et al., LSD1, an environment and aging-sensitive negative modulator of the glutamatergic synapse, Accepted at Neurobiology of Stress, 2020.

104. Quesnel-Vallières, M. et al. (2016) Misregulation of an Activity-Dependent Splicing Network as a Common Mechanism Underlying Autism Spectrum Disorders. Mol Cell 64 (6), 1023-1034.

105. Eom, T. et al. (2013) NOVA-dependent regulation of cryptic NMD exons controls synaptic protein levels after seizure. Elife 2, e00178.

106. Morena, M. et al. (2016) Neurobiological Interactions Between Stress and the Endocannabinoid System. Neuropsychopharmacology 41 (1), 80-102.

107. deRoon-Cassini, T.A. et al. (2020) Meet Your Stress Management Professionals: The Endocannabinoids. Trends Mol Med.

108. Rusconi, F. et al. (2020) Endocannabinoid-Epigenetic Cross-Talk: A Bridge toward Stress Coping. Int J Mol Sci 21 (17).

109. Longaretti, A. et al. (2020) Termination of acute stress response by the endocannabinoid system is regulated through LSD1-mediated transcriptional repression of 2-AG hydrolases ABHD6 and MAGL. J Neurochem, e15000.

110. Lutz, B. et al. (2015) The endocannabinoid system in guarding against fear, anxiety and stress. Nat Rev Neurosci 16 (12), 705-18.

111. Samocha, K.E. et al. (2014) A framework for the interpretation of de novo mutation in human disease. Nat Genet 46 (9), 944-50.

112. Rauch, A. et al. (2012) Range of genetic mutations associated with severe non-syndromic sporadic intellectual disability: an exome sequencing study. Lancet 380 (9854), 1674-82.

113. Tunovic, S. et al. (2014) De novo ANKRD11 and KDM1A gene mutations in a male with features of KBG syndrome and Kabuki syndrome. Am J Med Genet A 164A (7), 1744-9.

114. Chong, J.X. et al. (2016) Gene discovery for Mendelian conditions via social networking: de novo variants in KDM1A cause developmental delay and distinctive facial features. Genet Med 18 (8), 788-95.

115. Pilotto, S. et al. (2016) LSD1/KDM1A mutations associated to a newly described form of intellectual disability impair demethylase activity and binding to transcription factors. Hum Mol Genet.

116. Kopelman, N.M. et al. (2005) Alternative splicing and gene duplication are inversely correlated evolutionary mechanisms. Nat Genet 37 (6), 588-9.

117. Parmley, J.L. et al. (2007) Splicing and the evolution of proteins in mammals. PLoS Biol 5 (2), e14.

118. Pan, Q. et al. (2008) Deep surveying of alternative splicing complexity in the human transcriptome by high-throughput sequencing. Nat Genet 40 (12), 1413-5.

119. Chaudhary, S. et al. (2019) Alternative Splicing and Protein Diversity: Plants Versus Animals. Front Plant Sci 10, 708.

120. Irimia, M. and Blencowe, B.J. (2012) Alternative splicing: decoding an expansive regulatory layer. Curr Opin Cell Biol 24 (3), 323-32.

121. Wang, Y. et al. (2015) Mechanism of alternative splicing and its regulation. Biomed Rep 3 (2), 152-158.

122. Hallegger, M. et al. (2010) Alternative splicing: global insights. FEBS J 277 (4), 856-66.

123. Black, D.L. (2000) Protein diversity from alternative splicing: a challenge for bioinformatics and post-genome biology. Cell 103 (3), 367-70.

124. Graveley, B.R. (2001) Alternative splicing: increasing diversity in the proteomic world. Trends Genet 17 (2), 100-7.

125. Matlin, A.J. et al. (2005) Understanding alternative splicing: towards a cellular code. Nat Rev Mol Cell Biol 6 (5), 386-98.

126. Kalsotra, A. and Cooper, T.A. (2011) Functional consequences of developmentally regulated alternative splicing. Nat Rev Genet 12 (10), 715-29.

127. Cieply, B. and Carstens, R.P. (2015) Functional roles of alternative splicing factors in human disease. Wiley Interdiscip Rev RNA 6 (3), 311-26.

128. Pickrell, J.K. et al. (2010) Noisy splicing drives mRNA isoform diversity in human cells. PLoS Genet 6 (12), e1001236.

129. Leoni, G. et al. (2011) Coding potential of the products of alternative splicing in human. Genome Biol 12 (1), R9.

130. Lejeune, F. et al. (2004) eIF4G is required for the pioneer round of translation in mammalian cells. Nat Struct Mol Biol 11 (10), 992-1000.

131. Maquat, L.E. (2004) Nonsense-mediated mRNA decay: splicing, translation and mRNP dynamics. Nat Rev Mol Cell Biol 5 (2), 89-99.

132. Losson, R. and Lacroute, F. (1979) Interference of nonsense mutations with eukaryotic messenger RNA stability. Proc Natl Acad Sci U S A 76 (10), 5134-7.

133. Lykke-Andersen, S. and Jensen, T.H. (2015) Nonsense-mediated mRNA decay: an intricate machinery that shapes transcriptomes. Nat Rev Mol Cell Biol 16 (11), 665-77.

134. Ni, J.Z. et al. (2007) Ultraconserved elements are associated with homeostatic control of splicing regulators by alternative splicing and nonsense-mediated decay. Genes Dev 21 (6), 708-18.

135. Green, R.E. et al. (2003) Widespread predicted nonsense-mediated mRNA decay of alternatively-spliced transcripts of human normal and disease genes. Bioinformatics 19 Suppl 1, i118-21.

136. Lewis, B.P. et al. (2003) Evidence for the widespread coupling of alternative splicing and nonsense-mediated mRNA decay in humans. Proc Natl Acad Sci U S A 100 (1), 189-92.

137. Mudge, J.M. et al. (2013) Functional transcriptomics in the post-ENCODE era. Genome Res 23 (12), 1961-73.

138. Lareau, L.F. and Brenner, S.E. (2015) Regulation of splicing factors by alternative splicing and NMD is conserved between kingdoms yet evolutionarily flexible. Mol Biol Evol 32 (4), 1072-9.

139. Lareau, L.F. et al. (2007) The coupling of alternative splicing and nonsense-mediated mRNA decay. Adv Exp Med Biol 623, 190-211.

140. Müller-McNicoll, M. et al. (2019) Auto-regulatory feedback by RNA-binding proteins. J Mol Cell Biol 11 (10), 930-939.

141. Jaffrey, S.R. and Wilkinson, M.F. (2018) Nonsense-mediated RNA decay in the brain: emerging modulator of neural development and disease. Nat Rev Neurosci 19 (12), 715-728.

142. Ohnishi, T. et al. (2003) Phosphorylation of hUPF1 induces formation of mRNA surveillance complexes containing hSMG-5 and hSMG-7. Mol Cell 12 (5), 1187-200.

143. Xu, X. et al. (2013) Exome sequencing identifies UPF3B as the causative gene for a Chinese non-syndrome mental retardation pedigree. Clin Genet 83 (6), 560-4.

144. Tarpey, P.S. et al. (2007) Mutations in UPF3B, a member of the nonsense-mediated mRNA decay complex, cause syndromic and nonsyndromic mental retardation. Nat Genet 39 (9), 1127-33.

145. Nguyen, L.S. et al. (2012) Transcriptome profiling of UPF3B/NMD-deficient lymphoblastoid cells from patients with various forms of intellectual disability. Mol Psychiatry 17 (11), 1103-15.

146. F., L. et al., UPF3B Gene and Nonsense-Mediated mRNA Decay in Autism Spectrum Disorders., Springer, Comprehensive Guide to Autism, 2014.

147. Addington, A.M. et al. (2011) A novel frameshift mutation in UPF3B identified in brothers affected with childhood onset schizophrenia and autism spectrum disorders. Mol Psychiatry 16 (3), 238-9.

148. Gulsuner, S. et al. (2013) Spatial and temporal mapping of de novo mutations in schizophrenia to a fetal prefrontal cortical network. Cell 154 (3), 518-29.

149. Barbosa-Morais, N.L. et al. (2012) The evolutionary landscape of alternative splicing in vertebrate species. Science 338 (6114), 1587-93.

150. Merkin, J. et al. (2012) Evolutionary dynamics of gene and isoform regulation in Mammalian tissues. Science 338 (6114), 1593-9.

151. Lipscombe, D. (2005) Neuronal proteins custom designed by alternative splicing. Curr Opin Neurobiol 15 (3), 358-63.

152. Licatalosi, D.D. and Darnell, R.B. (2006) Splicing regulation in neurologic disease. Neuron 52 (1), 93-101.

153. Zhang, M. et al. (2019) Axonogenesis Is Coordinated by Neuron-Specific Alternative Splicing Programming and Splicing Regulator PTBP2. Neuron 101 (4), 690-706.e10.

154. Zheng, S. (2020) Alternative splicing programming of axon formation. Wiley Interdiscip Rev RNA 11 (4), e1585.

155. Raj, B. and Blencowe, B.J. (2015) Alternative Splicing in the Mammalian Nervous System: Recent Insights into Mechanisms and Functional Roles. Neuron 87 (1), 14-27.

156. Grabowski, P.J. and Black, D.L. (2001) Alternative RNA splicing in the nervous system. Prog Neurobiol 65 (3), 289-308.

157. Irimia, M. et al. (2014) A highly conserved program of neuronal microexons is misregulated in autistic brains. Cell 159 (7), 1511-23.

158. Yang, L. and Chen, L.L. (2014) Microexons go big. Cell 159 (7), 1488-9.

159. Torres-Méndez, A. et al. (2019) A novel protein domain in an ancestral splicing factor drove the evolution of neural microexons. Nat Ecol Evol 3 (4), 691-701.

160. Braunschweig, U. et al. (2013) Dynamic integration of splicing within gene regulatory pathways. Cell 152 (6), 1252-69.

161. Hsiao, Y.H. et al. (2016) Alternative splicing modulated by genetic variants demonstrates accelerated evolution regulated by highly conserved proteins. Genome Res 26 (4), 440-50.

162. Anna, A. and Monika, G. (2018) Splicing mutations in human genetic disorders: examples, detection, and confirmation. J Appl Genet 59 (3), 253-268.

163. Lewandowska, M.A. (2013) The missing puzzle piece: splicing mutations. Int J Clin Exp Pathol 6 (12), 2675-82.

164. Dörk, T. et al. (1993) Four novel cystic fibrosis mutations in splice junction sequences affecting the CFTR nucleotide binding folds. Genomics 15 (3), 688-91.

165. Gao, K. et al. (2008) Human branch point consensus sequence is yUnAy. Nucleic Acids Res 36 (7), 2257-67.

166. Di Leo, E. et al. (2004) A point mutation in the lariat branch point of intron 6 of NPC1 as the cause of abnormal pre-mRNA splicing in Niemann-Pick type C disease. Hum Mutat 24 (5), 440.

167. Maslen, C. et al. (1997) A rare branch-point mutation is associated with missplicing of fibrillin-2 in a large family with congenital contractural arachnodactyly. Am J Hum Genet 60 (6), 1389-98.

168. Carboni, N. et al. (2011) Aberrant splicing in the LMNA gene caused by a novel mutation on the polypyrimidine tract of intron 5. Muscle Nerve 43 (5), 688-93.

169. Vaz-Drago, R. et al. (2017) Deep intronic mutations and human disease. Hum Genet 136 (9), 1093-1111.

170. Sanz, D.J. et al. (2017) Cas9/gRNA targeted excision of cystic fibrosis-causing deep-intronic splicing mutations restores normal splicing of CFTR mRNA. PLoS One 12 (9), e0184009.

171. Park, E. et al. (2018) The Expanding Landscape of Alternative Splicing Variation in Human Populations. Am J Hum Genet 102 (1), 11-26.

172. Kuroyanagi, H. (2009) Fox-1 family of RNA-binding proteins. Cell Mol Life Sci 66 (24), 3895-907.

173. Kabat, J.L. et al. (2006) Intronic alternative splicing regulators identified by comparative genomics in nematodes. PLoS Comput Biol 2 (7), e86.

174. Jin, Y. et al. (2003) A vertebrate RNA-binding protein Fox-1 regulates tissue-specific splicing via the pentanucleotide GCAUG. EMBO J 22 (4), 905-12.

175. Underwood, J.G. et al. (2005) Homologues of the Caenorhabditis elegans Fox-1 protein are neuronal splicing regulators in mammals. Mol Cell Biol 25 (22), 10005-16.

176. Nakahata, S. and Kawamoto, S. (2005) Tissue-dependent isoforms of mammalian Fox-1 homologs are associated with tissue-specific splicing activities. Nucleic Acids Res 33 (7), 2078-89.

177. Zhang, C. et al. (2008) Defining the regulatory network of the tissue-specific splicing factors Fox-1 and Fox-2. Genes Dev 22 (18), 2550-63.

178. Damianov, A. and Black, D.L. (2010) Autoregulation of Fox protein expression to produce dominant negative splicing factors. RNA 16 (2), 405-16.

179. Conboy, J.G. (2017) Developmental regulation of RNA processing by Rbfox proteins. Wiley Interdiscip Rev RNA 8 (2).

180. Casanovas, S. et al. (2020) Rbfox1 Is Expressed in the Mouse Brain in the Form of Multiple Transcript Variants and Contains Functional E Boxes in Its Alternative Promoters. Front Mol Neurosci 13, 66.

181. Dredge, B.K. and Jensen, K.B. (2011) NeuN/Rbfox3 nuclear and cytoplasmic isoforms differentially regulate alternative splicing and nonsense-mediated decay of Rbfox2. PLoS One 6 (6), e21585.

182. Gehman, L.T. et al. (2011) The splicing regulator Rbfox1 (A2BP1) controls neuronal excitation in the mammalian brain. Nat Genet 43 (7), 706-11.

183. Gehman, L.T. et al. (2012) The splicing regulator Rbfox2 is required for both cerebellar development and mature motor function. Genes Dev 26 (5), 445-60.

184. Lovci, M.T. et al. (2013) Rbfox proteins regulate alternative mRNA splicing through evolutionarily conserved RNA bridges. Nat Struct Mol Biol 20 (12), 1434-42.

185. Fogel, B.L. et al. (2012) RBFOX1 regulates both splicing and transcriptional networks in human neuronal development. Hum Mol Genet 21 (19), 4171-86.

186. Weyn-Vanhentenryck, S.M. et al. (2014) HITS-CLIP and integrative modeling define the Rbfox splicing-regulatory network linked to brain development and autism. Cell Rep 6 (6), 1139-1152.

187. Li, Y.I. et al. (2015) RBFOX and PTBP1 proteins regulate the alternative splicing of micro-exons in human brain transcripts. Genome Res 25 (1), 1-13.

188. Lee, J.A. et al. (2016) Cytoplasmic Rbfox1 Regulates the Expression of Synaptic and Autism-Related Genes. Neuron 89 (1), 113-28.

189. Hamada, N. et al. (2016) Essential role of the nuclear isoform of RBFOX1, a candidate gene for autism spectrum disorders, in the brain development. Sci Rep 6, 30805.

190. Lee, J.A. et al. (2009) An inducible change in Fox-1/A2BP1 splicing modulates the alternative splicing of downstream neuronal target exons. Genes Dev 23 (19), 2284-93.

191. Li, Q. et al. (2007) Neuronal regulation of alternative pre-mRNA splicing. Nat Rev Neurosci 8 (11), 819-31.

192. McKee, A.E. et al. (2007) Exon expression profiling reveals stimulus-mediated exon use in neural cells. Genome Biol 8 (8), R159.

193. Sengar, A.S. et al. (2019) Control of Long-Term Synaptic Potentiation and Learning by Alternative Splicing of the NMDA Receptor Subunit GluN1. Cell Rep 29 (13), 4285-4294.e5.

194. Voineagu, I. et al. (2011) Transcriptomic analysis of autistic brain reveals convergent molecular pathology. Nature 474 (7351), 380-4.

195. Amir-Zilberstein, L. et al. (2012) Homeodomain protein otp and activity-dependent splicing modulate neuronal adaptation to stress. Neuron 73 (2), 279-91.

196. Agarwal, A. et al. (2005) Pituitary adenylate cyclase-activating polypeptide (PACAP) mimics neuroendocrine and behavioral manifestations of stress: Evidence for PKA-mediated expression of the corticotropin-releasing hormone (CRH) gene. Brain Res Mol Brain Res 138 (1), 45-57.

197. Stroth, N. and Eiden, L.E. (2010) Stress hormone synthesis in mouse hypothalamus and adrenal gland triggered by restraint is dependent on pituitary adenylate cyclase-activating polypeptide signaling. Neuroscience 165 (4), 1025-30.

198. Brunson, K.L. et al. (2001) Neurobiology of the stress response early in life: evolution of a concept and the role of corticotropin releasing hormone. Mol Psychiatry 6 (6), 647-56.

199. Liu, Y. et al. (2008) Cyclic adenosine 3',5'-monophosphate responsive element binding protein phosphorylation is required but not sufficient for activation of corticotropin-releasing hormone transcription. Endocrinology 149 (7), 3512-20.

200. Bhalla, K. et al. (2004) The de novo chromosome 16 translocations of two patients with abnormal phenotypes (mental retardation and epilepsy) disrupt the A2BP1 gene. J Hum Genet 49 (6), 308-311.

201. Elia, J. et al. (2010) Rare structural variants found in attention-deficit hyperactivity disorder are preferentially associated with neurodevelopmental genes. Mol Psychiatry 15 (6), 637-46.

202. Hamshere, M.L. et al. (2009) Mood-incongruent psychosis in bipolar disorder: conditional linkage analysis shows genome-wide suggestive linkage at 1q32.3, 7p13 and 20q13.31. Bipolar Disord 11 (6), 610-20.

203. Wray, N.R. et al. (2018) Genome-wide association analyses identify 44 risk variants and refine the genetic architecture of major depression. Nat Genet 50 (5), 668-681.

204. Venables, J.P. et al. (2009) Cancer-associated regulation of alternative splicing. Nat Struct Mol Biol 16 (6), 670-6.

205. Lapuk, A. et al. (2010) Exon-level microarray analyses identify alternative splicing programs in breast cancer. Mol Cancer Res 8 (7), 961-74.

206. Shapiro, I.M. et al. (2011) An EMT-driven alternative splicing program occurs in human breast cancer and modulates cellular phenotype. PLoS Genet 7 (8), e1002218.

207. C, B. et al., The RNA-binding protein Rbfox2: an essential regulator of EMT-driven alternative splicing and a mediator of cellular invasion, *Oncogene*, 2014, pp. 1082–1092.

208. El Marabti, E. and Younis, I. (2018) The Cancer Spliceome: Reprograming of Alternative Splicing in Cancer. Front Mol Biosci 5, 80.

209. Linde, L. et al. (2007) Nonsense-mediated mRNA decay affects nonsense transcript levels and governs response of cystic fibrosis patients to gentamicin. J Clin Invest 117 (3), 683-92.

210. Sanchez, G. et al. (2016) A novel role for CARM1 in promoting nonsense-mediated mRNA decay: potential implications for spinal muscular atrophy. Nucleic Acids Res 44 (6), 2661-76.

211. Cardamone, G. et al. (2017) The Characterization of GSDMB Splicing and Backsplicing Profiles Identifies Novel Isoforms and a Circular RNA That Are Dysregulated in Multiple Sclerosis. Int J Mol Sci 18 (3).

212. Durand, S. et al. (2007) Inhibition of nonsense-mediated mRNA decay (NMD) by a new chemical molecule reveals the dynamic of NMD factors in P-bodies. J Cell Biol 178 (7), 1145-60.

213. Keeling, K.M. et al. (2013) Attenuation of nonsense-mediated mRNA decay enhances in vivo nonsense suppression. PLoS One 8 (4), e60478.

214. Pfaffl, M.W. et al. (2004) Determination of stable housekeeping genes, differentially regulated target genes and sample integrity: BestKeeper--Excel-based tool using pair-wise correlations. Biotechnol Lett 26 (6), 509-15.

215. Baralle, D. and Baralle, M. (2005) Splicing in action: assessing disease causing sequence changes. J Med Genet 42 (10), 737-48.

216. Preece, P. and Cairns, N.J. (2003) Quantifying mRNA in postmortem human brain: influence of gender, age at death, postmortem interval, brain pH, agonal state and inter-lobe mRNA variance. Brain Res Mol Brain Res 118 (1-2), 60-71.

217. Tomita, H. et al. (2004) Effect of agonal and postmortem factors on gene expression profile: quality control in microarray analyses of postmortem human brain. Biol Psychiatry 55 (4), 346-52.

218. Durrenberger, P.F. et al. (2010) Effects of antemortem and postmortem variables on human brain mRNA quality: a BrainNet Europe study. J Neuropathol Exp Neurol 69 (1), 70-81.

219. Mizee, M.R. et al. (2017) Isolation of primary microglia from the human post-mortem brain: effects of ante- and post-mortem variables. Acta Neuropathol Commun 5 (1), 16.

220. Monoranu, C.M. et al. (2009) pH measurement as quality control on human post mortem brain tissue: a study of the BrainNet Europe consortium. Neuropathol Appl Neurobiol 35 (3), 329-337.

221. Nagy, C. et al. (2015) Effects of postmortem interval on biomolecule integrity in the brain. J Neuropathol Exp Neurol 74 (5), 459-69.

222. Caspi, A. and Moffitt, T.E. (2006) Gene-environment interactions in psychiatry: joining forces with neuroscience. Nat Rev Neurosci 7 (7), 583-90.

223. Sullivan, P.F. et al. (2018) Psychiatric Genomics: An Update and an Agenda. Am J Psychiatry 175 (1), 15-27.

224. Zhang, C. et al. (2010) Integrative modeling defines the Nova splicing-regulatory network and its combinatorial controls. Science 329 (5990), 439-43.

225. Holbrook, J.A. et al. (2004) Nonsense-mediated decay approaches the clinic. Nat Genet 36 (8), 801-8.

226. Pervouchine, D. et al. (2019) Integrative transcriptomic analysis suggests new autoregulatory splicing events coupled with nonsense-mediated mRNA decay. Nucleic Acids Res 47 (10), 5293-5306.

227. Li, Z. et al. (2017) Inhibition of nonsense-mediated RNA decay by ER stress. RNA 23 (3), 378-394.

228. Page, M.F. et al. (1999) SMG-2 is a phosphorylated protein required for mRNA surveillance in Caenorhabditis elegans and related to Upf1p of yeast. Mol Cell Biol 19 (9), 5943-51.

229. Yamashita, A. et al. (2001) Human SMG-1, a novel phosphatidylinositol 3-kinase-related protein kinase, associates with components of the mRNA surveillance complex and is involved in the regulation of nonsense-mediated mRNA decay. Genes Dev 15 (17), 2215-28.

230. Grimson, A. et al. (2004) SMG-1 is a phosphatidylinositol kinase-related protein kinase required for nonsense-mediated mRNA Decay in Caenorhabditis elegans. Mol Cell Biol 24 (17), 7483-90.

231. Chiu, S.Y. et al. (2003) Characterization of human Smg5/7a: a protein with similarities to Caenorhabditis elegans SMG5 and SMG7 that functions in the dephosphorylation of Upf1. RNA 9 (1), 77-87.

232. Luo, Y. et al. (2018) P-Bodies: Composition, Properties, and Functions. Biochemistry 57 (17), 2424-2431.

233. Yeo, G.W. et al. (2009) An RNA code for the FOX2 splicing regulator revealed by mapping RNA-protein interactions in stem cells. Nat Struct Mol Biol 16 (2), 130-7.

234. Denichenko, P. et al. (2019) Specific inhibition of splicing factor activity by decoy RNA oligonucleotides. Nat Commun 10 (1), 1590.

235. Cartegni, L. et al. (2003) ESEfinder: A web resource to identify exonic splicing enhancers. Nucleic Acids Res 31 (13), 3568-71.

236. Pollini, D. et al. (2018) Generation and characterization of a human iPSC line from an ALS patient carrying the Q66K-MATR3 mutation. Stem Cell Res 33, 146-150.

237. Augustyniak, J. et al. (2019) Reference Gene Validation via RT-qPCR for Human iPSC-Derived Neural Stem Cells and Neural Progenitors. Mol Neurobiol 56 (10), 6820-6832.

238. Hirano, K. and Namihira, M. (2016) LSD1 Mediates Neuronal Differentiation of Human Fetal Neural Stem Cells by Controlling the Expression of a Novel Target Gene, HEYL. Stem Cells 34 (7), 1872-82.

239. Yao, B. and Jin, P. (2014) Unlocking epigenetic codes in neurogenesis. Genes Dev 28 (12), 1253-71.

240. Zhu, D. et al. (2014) Lysine-specific demethylase 1 regulates differentiation onset and migration of trophoblast stem cells. Nat Commun 5, 3174.

241. Kosan, C. and Godmann, M. (2016) Genetic and Epigenetic Mechanisms That Maintain Hematopoietic Stem Cell Function. Stem Cells Int 2016, 5178965.

242. Cavanagh, J.T. et al. (2003) Psychological autopsy studies of suicide: a systematic review. Psychol Med 33 (3), 395-405.

243. Le François, B. et al. (2018) A Novel Alternative Splicing Mechanism That Enhances Human 5-HT1A Receptor RNA Stability Is Altered in Major Depression. J Neurosci 38 (38), 8200-8210.

244. Scahill, R.I. et al. (2003) A longitudinal study of brain volume changes in normal aging using serial registered magnetic resonance imaging. Arch Neurol 60 (7), 989-94.

245. Zimmerman, M.E. et al. (2006) The relationship between frontal gray matter volume and cognition varies across the healthy adult lifespan. Am J Geriatr Psychiatry 14 (10), 823-33.

246. Ferris, S.H. and Kluger, A., Commentary on age-associated memory impairment, age-related cognitive decline and mild cognitive impairment, Aging, Neuropsychology, and Cognition, 1996, pp. 148-153.

247. Penner, M.R. et al. (2010) An epigenetic hypothesis of aging-related cognitive dysfunction. Front Aging Neurosci 2, 9.

248. Lu, T. et al. (2014) REST and stress resistance in ageing and Alzheimer's disease. Nature 507 (7493), 448-54.

249. Hawton, K. and van Heeringen, K. (2009) Suicide. Lancet 373 (9672), 1372-81.

250. Konovalov, S. and Garcia-Bassets, I. (2013) Analysis of the levels of lysine-specific demethylase 1 (LSD1) mRNA in human ovarian tumors and the effects of chemical LSD1 inhibitors in ovarian cancer cell lines. J Ovarian Res 6 (1), 75.

251. Chen, C. et al. (2015) Expression of Lysine-specific demethylase 1 in human epithelial ovarian cancer. J Ovarian Res 8, 28.

252. Zullo, J.M. et al. (2019) Regulation of lifespan by neural excitation and REST. Nature 574 (7778), 359-364.

253. Ule, J. and Darnell, R.B. (2006) RNA binding proteins and the regulation of neuronal synaptic plasticity. Curr Opin Neurobiol 16 (1), 102-10.

254. Seldon, H.L. (2007) Extended neocortical maturation time encompasses speciation, fatty acid and lateralization theories of the evolution of schizophrenia and creativity. Med Hypotheses 69 (5), 1085-9.

255. Kéri, S. et al. (2009) Effects of a neuregulin 1 variant on conversion to schizophrenia and schizophreniform disorder in people at high risk for psychosis. Mol Psychiatry 14 (2), 118-9.

256. Kéri, S. (2009) Genes for psychosis and creativity: a promoter polymorphism of the neuregulin 1 gene is related to creativity in people with high intellectual achievement. Psychol Sci 20 (9), 1070-3.

257. Nesse, R.M. and Williams, G.C., Why We Get Sick: The New Science of Darwinian Medicine, Vintage, 1996.

258. Nesse, R.M., Good Reasons for Bad Feelings: Insights from the Frontier of Evolutionary Psychiatry, Dutton, 2019.